Texas A&M University

Department of

OCEANOGRAPHY

ON STEADY, WIND-DRIVEN OCEAN CURRENTS IN A STRATIFIED MODEL OF TWO MOVING LAYERS

Worth D. Nowlin, Jr.

Office of Naval Research
Contract Nonr 2119 (04)

Project 286-1
Reference 65-32T

November 1965

Research Conducted through the
Texas A & M Research Foundation
COLLEGE STATION, TEXAS

The Texas A&M University

Department of Oceanography

College Station, Texas

Research conducted through the
TEXAS A&M RESEARCH FOUNDATION

ON STEADY, WIND-DRIVEN OCEAN CURRENTS IN A STRATIFIED MODEL OF TWO MOVING LAYERS

by

Worth D. Nowlin, Jr.

I wish to express my appreciation to Professor R. O. Reid for the suggestions, assistance and criticisms offered during the course of work on this report. With the exception of computer time provided by the Texas A&M University, this work was sponsored by the Office of Naval Research, Contract Nonr 2119(04).

Office of Naval Research Contract Nonr 2119 (04)

A&M Project 286-1

REFERENCE 65-32T

November 1965

BLANK PAGE

ABSTRACT

Considered are steady, wind-driven currents in a two-layer model ocean, confined within a rectangular basin with a horizontal sea bed. The horizontal velocities are assumed independent of elevation within each layer of this finite difference approximation to the continuously stratified real ocean.

Neglecting nonlinear field accelerations, a frictional model for the entire basin is formulated which allows for vertical, but not horizontal, transfer of horizontal momentum due to turbulence. The exchange of horizontal momentum between layers and to the sea bed is provided through the assumption of interlayer and bottom stresses, which are assumed proportional to the vertical contrast of horizontal velocity across the appropriate interface. The constants of proportionality, which are estimated from considerations of the observed circulation, play decisive roles in controlling the circulation patterns within each layer and the internal dissipation of energy from the steady organized flow. The solution, obtained for a purely zonal wind stress which varies latitudinally as a cosine, depicts an anticyclonic circulation within the lower layer which is intensified more to the west than is the anticyclonic gyre within the upper layer. Numerical calculations were performed for a range of physical parameters. Within the oceanic interior, the resulting equatorward volume transport within the upper layer increases as a linear function of distance from the eastern basin boundary when measured along the latitude of maximum wind stress curl. At the same latitude the equatorward transport within the lower layer, although less than its upper layer counterpart, increases approximately as the second power of the distance from the eastern boundary. Moreover, the poleward flowing western boundary current is confined within a narrower region in the lower than in the upper layer. One effect of this differential intensification is to produce within the lower layer a relatively strong, narrow equatorward flow underlying the eastern portion of the upper layer boundary current.

As an alternate solution within the formation and growth region of western boundary currents, a system of steady inertial boundary currents for two moving layers is developed. Within each layer the potential vorticity, conserved along streamtubes, is non-uniform across the

stream, being expressed as a linear function of the appropriate volume transport streamfunction. Approximate solutions are obtained by employing perturbations on the basic state given at the eastern edge of the current regime by the interior solutions to the frictional model. Two methods of analysis appear equally successful in obtaining solutions: one employs layer thickness perturbations and requires numerical techniques to satisfy the nonlinear conditions at the western boundary; the other employs perturbations of the streamfunctions and linearized western boundary conditions, leading to a solution without requiring numerical techniques.

The boundary currents and interior flow predicted by several frictional cases are presented. For one frictional interior solution, the corresponding inertial boundary currents, as predicted by both analyses are presented.

TABLE OF CONTENTS

LIST OF TABLES

BLANK PAGE

LIST OF SYMBOLS

A_0, A_1, A_2	$cm^2 sec^{-1}$	Constants defined by equations (73)
a_j	cm^{-1}	Double-valued reciprocal width scale defined by equations (46)
B	cm	$(\rho H + \rho' H')/\rho'$, effective overall water depth
B_I	cm	Value of B within interior region at eastern edge of western boundary region
B_0, B_1, B_2	$cm^2 sec^{-1}$	Constants defined by equations (73)
b	cm	Meridional dimension of ocean basin as used in Chapter IV; effective water depth anomaly $(B-B_I)$ as used in Chapter V
c_j	cm^{-1}	Double-valued reciprocal width scale defined by equations (46)
D	cm	$Z_2 - Z_1$
d_o		H_o/H_o'
E_j	cm	Double-valued parameter given by equations (113) and (114)
e		Base of natural logarithms
F	$gm\ cm^{-1} sec^{-2}$	Maximum value of zonal wind stress as used in Chapter IV
F_0, F_1, F_2		Dimensional coefficients in expansion of $F(\Psi)$ with dimensions defined by equations (91)
$F(\Psi)$	$cm^2 sec^{-2}$	J expressed as function of Ψ only, defined by equations (85) as used in Chapter V
f	sec^{-1}	Coriolis parameter

f_o	sec^{-1}	Coriolis parameter evaluated at southern boundary of the basin, i.e., at $y = 0$
$G(\Psi')$	cm^2sec^{-2}	J' expressed as function of Ψ' only, defined by equations (85)
G_0, G_1, G_2		Dimensional coefficients in expansion of $G(\Psi')$ with dimensions defined by equations (91)
g	$cm\ sec^{-2}$	Gravity
g'	$cm\ sec^{-2}$	γg, reduced gravity
H, H'	cm	Thicknesses of upper and lower layer, respectively
H_I, H_I'	cm	Values of upper and lower layer thicknesses within interior of ocean basin at eastern edge of western boundary current regime
H_o, H_o'	cm	Mean upper and lower layer thicknesses, respectively, over horizontal extent of ocean basin
h	cm	Anomaly of upper layer thickness: $(H-H_o)$ as used in Chapter IV; $(H-H_I^o)$ as used in Chapter V
h'	cm	Anomaly of lower layer thickness: $(H'-H_o')$ as used in Chapter IV; $(H'-H_I^{o\prime})$ as used in Chapter V
$\hat{i}$		Unit vector in positive x-direction
J, J'	cm^2sec^{-2}	Mechanical energy densities within upper and lower layer, respectively, of inertial model; defined by equations (83)
j		Subscript with values 1 or 2: denotes evaluation for α_1 or α_2 in Chapter IV; denotes evaluation for ϵ_1 or ϵ_2 in Chapter V

$\hat{j}$		Unit vector in positive y-direction
K,K′	$cm^2 sec^{-1}$	Kinematically expressed coefficients of eddy viscosity within upper and lower layers, respectively.
$\hat{k}$		Unit vector in positive z-direction
M	$cm^3 sec^{-2}$	Constant defined by equation (49)
M_y	$gm\ cm^{-1} sec^{-1}$	Northward directed component of mass transport per unit width
m_j	cm^{-1}	Double-valued reciprocal width scale defined by equations (112)
N	$cm^2 sec^{-2}$	Constant defined by equation (75)
$\hat{n}$		Horizontal unit vector perpendicular to and directed to left of $\hat{q}$
p,p′	$gm\ cm^{-1} sec^{-2}$	Pressure in upper and lower layers, respectively
p*	$gm\ cm^{-1} sec^{-2}$	Pressure in hypothetical fluid layer
p_a	$gm\ cm^{-1} sec^{-2}$	Sea-level atmospheric pressure
Q	$cm^2 sec^{-1}$	$[U^2 + V^2]^{1/2}$
Q′	$cm^2 sec^{-1}$	$[(U')^2 + (V')^2]^{1/2}$
$\hat{Q}$	$cm^2 sec^{-1}$	$\hat{i}\ U + \hat{j}\ V$
$\hat{Q}'$	$cm^2 sec^{-1}$	$\hat{i}\ U' + \hat{j}\ V'$
q	$cm\ sec^{-1}$	$[u^2 + v^2]^{1/2}$
q′	$cm\ sec^{-1}$	$[(u')^2 + (v')^2]^{1/2}$
$\hat{q}$	$cm\ sec^{-1}$	$\hat{i}\ u + \hat{j}\ v$, horizontal fluid velocity in upper layer
$\hat{q}'$	$cm\ sec^{-1}$	$\hat{i}\ u' + \hat{j}\ v'$, horizontal fluid velocity in lower layer
q_o,q_o'	$cm\ sec^{-1}$	q(o,y) and q′(o,y), respectively

q_I, q_I'	cm sec^{-1}	Interior values of q and q′, respectively, at eastern edge of western boundary region
R_o	cm	Average value of earth's radius at latitude ϕ_o
R_j		Double-valued dimensionless constant defined by equations (46)
r		Dimensionless constant defined by equation (47)
S		Dimensionless constant defined by equation (103)
$\hat{T}$	$cm^2 sec^{-2}$	$\hat{\tau}/\rho$
T_x, T_y	$cm^2 sec^{-2}$	x- and y-directed components of surface stress normalized by density of upper layer
U	$cm^2 sec^{-1}$	uH
U′	$cm^2 sec^{-1}$	u′H′
u,u′	cm sec^{-1}	x-directed velocity components in upper and lower layers, respectively
u*	cm sec^{-1}	x-directed velocity in a hypothetical fluid layer
V	$cm^2 sec^{-1}$	vH
V′	$cm^2 sec^{-1}$	v′H′
v,v′	cm sec^{-1}	y-directed velocity components in upper and lower layers, respectively
v*	cm sec^{-1}	y-directed velocity in a hypothetical fluid layer
W_j	$cm^2 sec^{-2}$	Double-valued constant defined by equation (56)
w	cm	Zonal dimension of ocean basin

x	cm	Horizontal coordinate, increasing eastward
x_o	cm	Arbitrary reference value of x-coordinate for evaluation of the line integral in equation (52)
y	cm	Horizontal coordinate, increasing northward
y_o	cm	Arbitrary reference value of y-coordinate for evaluation of line integral in equation (52)
Z_1, Z_2	cm	Elevations, relative to z = 0, of upper and lower interfaces bounding a hypothetical fluid layer
z	cm	Vertical coordinate, increasing upward

Greek Symbols

α_j		Double-valued separation constant given by equations (40)
β	$sec^{-1}cm^{-1}$	Space rate of change of Coriolis parameter with y-directed distance
Γ_j	sec	Double-valued separation constant given by equations (41)
γ		$(\rho'-\rho)/\rho'$, density contrast
δ_j		Double-valued separation constant given by equations (102)
ϵ_j		Double-valued separation constant given by equations (101)
ζ, ζ'	sec^{-1}	Vertical components of relative vorticity within upper and lower layer, respectively

$\circledast_j$	cm	Double-valued variable defined by $(1 + \epsilon_j)b + \epsilon_j \gamma h$, equations (98)
λ_1	cm	$1/c_1$, an effective width scale
λ_2	cm	$1/c_2$, an effective width scale
ρ, ρ'	gm cm^{-3}	Fluid densities within upper and lower layers, respectively
$\rho_{s,t,o}$	gm cm^{-3}	Fluid density at in situ temperature and salinity but at sea level atmospheric pressure
ρ^*	gm cm^{-3}	Fluid density in hypothetical layer
σ	sec^{-1}	Interlayer frictional coefficient
σ'	sec^{-1}	Bottom frictional coefficient
σ_t	gm cm^{-3}	$(\rho_{s,t,o}-1) \times 10^3$
τ_x, τ_y	gm $cm^{-1}sec^{-2}$	x- and y-directed components of applied surface wind stress.
τ_x^B, τ_y^B	gm $cm^{-1}sec^{-2}$	x- and y-directed components of stress applied by lower fluid on bottom
τ_x^I, τ_y^I	gm $cm^{-1}sec^{-2}$	x- and y-directed components of stress applied by upper fluid on lower fluid
τ_{x_1}, τ_{x_2}	gm $cm^{-1}sec^{-2}$	x-directed components of shear stress applied by fluid above the Z_1, Z_2 surface on the fluid below this surface
τ_{y_1}, τ_{y_2}	gm $cm^{-1}sec^{-2}$	y-directed components of shear stress applied by fluid above the Z_1, Z_2 surface on the fluid below this surface
$\hat{\tau}$	gm $cm^{-1}sec^{-2}$	$\hat{i}\,\tau_x + \hat{j}\,\tau_y$

$\hat{\tau}^B$	$gm\ cm^{-1}sec^{-2}$	$\hat{i}\ \tau_x^B + \hat{j}\ \tau_y^B$
$\hat{\tau}^I$	$gm\ cm^{-1}sec^{-2}$	$\hat{i}\ \tau_x^I + \hat{j}\ \tau_y^I$
Φ_j	cm^3sec^{-1}	Double-valued variable defined by $\Psi + \alpha_j\Psi'$, equations (38)
ϕ		Latitude
ϕ_o		Latitude of southern boundary of basin
Ψ, Ψ'	cm^3sec^{-1}	Volume transport streamfunctions for upper and lower layers, respectively
Ω	sec^{-1}	Earth's angular speed of rotation
ω_j	cm^2sec^{-2}	Double-valued function of layer thickness defined by equation (51)

BLANK PAGE

C H A P T E R I

INTRODUCTION

In this dissertation are presented the results of an analysis of steady, wind-driven currents in a (stably stratified) two-layer ocean. This system is characterized by two moving layers. It is confined within a rectangular basin on a β-plane, which is a mathematical abstraction representing low and middle latitude regions of the earth as explained in Chapter II.

Two distinct mathematical problems are considered. The first deals with a steady frictional model of the entire basin. The second problem concerns inertial currents formed in the lower latitudes of the western boundary region. This inertial current system provides an alternative to the frictional current system as the solution in the lower boundary region.

The two-layer frictional model with stable density stratification is admittedly a rough approximation to the real ocean, in which density varies continuously with elevation. The purpose in pursuing the analysis for a discontinuously stratified model (finite difference approximation) is to obtain an approximation to the vertical, as well as the horizontal, variations in the mean horizontal velocity field. For this analysis the horizontal

transfer of horizontal momentum due to turbulence has been neglected. A unique steady-state solution, with western boundary currents, is admitted by allowing vertical exchange of horizontal momentum. The horizontal velocities are assumed independent of elevation within each layer, and vertically integrated forms of the mass and momentum conservation relations are employed. Transfer of momentum between layers, internal dissipation of energy from the steady organized flow and momentum transfer to the sea bed are accomplished through the assumption of interlayer and bottom stresses. These stresses are assumed proportional to the vertical contrast of horizontal velocity across the interfaces. As expected, the constants of proportionality, the effective frictional coefficients, play a major role in controlling the degree of westward intensification of circulation patterns in both upper and lower layers. Since these coefficients are unknown, the numerical results are necessarily somewhat speculative. However, apparently reasonable values for these friction coefficients can be estimated from physical consideration of the North Atlantic circulation.

A purely zonal wind stress which varies latitudinally as a cosine is chosen in order to simply represent that portion of the north Atlantic lying between the latitudes of maximum wind stresses in the Westerly and the Trade

Wind belts. The constants and parameters physically characterizing the model are chosen in an attempt to represent the North Atlantic as a two-layer ocean. The sea bed is assumed horizontal. The lateral boundaries are taken as streamsurfaces.

A system of inertial boundary currents at lower latitudes compatible with the interior* solutions to the frictional model is developed. This second analysis deals with the formation and growth regions of steady currents in which the nonlinear field accelerations play a principal role. External driving forces and all turbulent exchange of horizontal momentum are neglected. The potential vorticity is consequently conserved along streamtubes delineated by vertical and horizontal streamsurfaces. The potential vorticity within each layer is expressed as a first order approximation to a series expansion in terms of the appropriate transport streamfunction. The formulation is as a perturbation problem in terms of the differences between the local layer thicknesses and the layer thicknesses found at the same latitude in the interior region. The basic meridional variations in layer thicknesses and other boundary conditions employed at the eastern edge

---

*In the sense used here, interior denotes that region of the ocean basin removed from the western boundary currents. Further discussion is given on page 7.

of the current regime are obtained from the interior solution to the frictional model. The southern and western basin boundaries are taken as a single vertical streamsurface.

C H A P T E R I I

RELATION TO PREVIOUS STUDIES

The study of steady, wind-driven ocean currents contributes to but one facet of the problem of understanding the circulation within the world's oceans. Actually, because of the coupling between the atmosphere and the seas, the study of motions within these two fluid layers should be considered simultaneously. This leads, of course, to an extremely complex problem. For the description of large-scale motions within these two fluids, practicality dictates that the coupling between these layers be effected by imposing appropriate boundary conditions at the air-sea interface. The resulting ocean circulation problem, even for time-independent motion within a basin of simple geometry, is of sufficient difficulty to warrant (at the present time) a further, somewhat arbitrary, division into wind-driven and thermohaline circulation modes. For the study of wind-driven modes, only horizontal momentum is considered to be transferred across the air-sea interface. The thermohaline models are based on the assumption of no wind stress but allow for prescribed distributions of temperature and/or salinity at the sea surface in order to represent energy and/or mass exchanges. It should be

noted that these two modes of circulation are nonlinearly coupled (Stommel and Webster, 1962) so that the complete solution is not to be expected from a simple combination of the results of two such theories. Nevertheless, as based on comparisons of transports predicted by wind-driven and thermohaline models with those observed in the oceans, the general circulation is principally wind-driven (Stommel and Arons, 1960; Wyrtki, 1961). The study of such models is therefore of considerable interest.

Since very little free communication is provided via the Arctic Mediterranean Sea between the waters of the Atlantic and Pacific Oceans, both oceans can be considered as north-south channels closed to the north. The South Pacific, South Atlantic and Indian Oceans are interconnected only by the Antarctic Circumpolar Current, which flows eastward around the Antarctic Continent. The major wind regimes over the oceans are zonal belts. Moreover, the zonal components of mean wind direction are more or less symmetrical about the intertropical convergence zones, the meteorological equator, which occurs slightly to the north of the geographical equator in the Atlantic and Pacific Oceans and is associated with the zonal flowing equatorial current systems. Because of this north-south symmetry the world's ice-free oceans can be divided into

five basins: North Atlantic, South Atlantic, North Pacific, South Pacific and Indian.

Over each of these basins the dominant winds are easterly in the region just equatorward of the Doldrums and westerly in middle latitudes. Associated with these winds, the major oceanic gyre is anticyclonic within each basin. Therefore, most models of wind-driven ocean circulation have been devised for a rectangular basin with appropriate wind distribution. Such a model, with minor changes, serves equally well to describe any one of the five aforementioned basins.

The circulation within such a basin, e.g., the North Atlantic, is observed to be quite asymmetrical, being intensified to the west. The meridional strip in which intense boundary currents are observed is referred to as the western boundary region. The remainder of the basin is commonly known as the "interior" or interior region.

As the rule, the upper and intermediate depth waters of the oceans are observed to be stably stratified, even if allowance is made for the expected density increase with depth due to the compressibility of sea water. This stability tends to inhibit the development of vertical motions. Usually, therefore, the hydrostatic approximation is invoked and the equations expressing conservation of mass and horizontal momentum are employed in vertically

integrated form when dealing with steady, wind-driven currents (Fofonoff, 1962). This approach is justified under the assumption that current speeds decrease greatly with increasing depth over the upper portion of the water column; for, in this case, the resulting mathematical problem can be formulated in terms of a streamfunction and thus used to discuss the major fraction of the volume or mass transport.

In applying such a vertically integrated approach to the interior region, Sverdrup (1947) assumed a balance between Coriolis forces, pressure gradient forces and vertical stresses. Taking the stress and pressure gradients to be zero at great depth, he obtained as the correct interior solution the vorticity* equation

$$\beta M_y = \frac{\partial \tau_y}{\partial x} - \frac{\partial \tau_x}{\partial y} ,$$

where τ_x and τ_y are eastward and northward components of surface wind stress, M_y is the northward directed component of mass transport per unit width and β is the derivative of the Coriolis parameter with respect to northward coordinate. Stommel (1965) showed this solution to

*Although commonly referred to as a vorticity equation because of its form, the more general equation, of which this is a special case, is actually the differential equation for the transport streamfunction. It is obtained by cross-differentiation of the vertically integrated horizontal momentum equations.

be "the condition under which the divergence of the Ekman wind drift, produced by the wind, is compensated for by the divergence of the geostrophic flow."

It is seen that the interior flow is purely zonal only for latitudes at which the curl of the applied wind stress vanishes (Munk, 1950). Therefore, such latitudes can conveniently be chosen as the latitudinal boundaries of the ocean basin, for such boundaries are then stream-surfaces. Moreover, the flow regimes within adjacent basins can be joined by requiring continuity of the wind stress curl along the boundaries. For a zonal wind stress of simple harmonic form, the transport is zonal at the latitudes of maximum eastward and westward stresses, while the flow must evidence an equatorward component at all intermediate latitudes. Such a streamline pattern is pictured in Figure 1. Indeed the approximate solution for the interior region of the upper layer in the present frictional model is just such a Sverdrup solution.

Clearly, the Sverdrup solution is not applicable to the entire basin. Provision must be allowed for a poleward return flow and for energy dissipation, if a steady state solution for the whole basin, satisfying the conservation of mass, is to be obtained. In addition, a vorticity balance must be maintained, if absolute angular momentum is to be conserved. Munk (1950) was the first

to demonstrate that these requirements can be met by the addition to the model of a western boundary current, effectively applied as a lateral boundary condition to the interior region.

The first steady, wind-driven model for the entire basin was that of Stommel (1948). For this model of a homogeneous ocean of uniform undisturbed depth, Stommel added to the Sverdrup balance of forces a bottom stress proportional to the horizontal velocity. This allowed energy dissipation and admitted a solution which predicted an intense poleward flowing boundary current in the western boundary region. The greatest value of Stommel's work was in demonstrating that the westward intensification is due to the variation of the Coriolis parameter with latitude. This can best be examined in terms of the vorticity of a fluid column moved from one latitude to another on the earth, during which move the absolute angular momentum in conserved. In addition to the vertical component of vorticity of the earth, such a fluid column has a vertical component of relative vorticity equal to the magnitude of the curl of the local horizontal velocity vector. Now, if the column is to conserve vorticity while moving northward in the Northern Hemisphere, it must gain negative (clockwise) relative vorticity in order to compensate for the fact that it is moving into a region of

greater planetary vorticity. Consideration of the velocity gradients in the western boundary current shows that a fluid column moving northward gains this needed negative relative vorticity within the current.

The frictional model presented in this paper (referred to as Model I) is essentially an extension of the work of Stommel (1948) to a two-layer, stably stratified system. Within each layer the density is assumed uniform and the horizontal velocities independent of elevation, as in Stommel's model. However, Model I provides a finite difference, first approximation to an ocean with continuous depth variations of density and velocity. The fluid of the lower layer is assumed to be in motion, and a bottom stress proportional to the lower layer velocity provides frictional dissipation. An interesting feature of Model I is the internal frictional dissipation provided by the interlayer stress necessary to transfer momentum to the lower layer. This stress is assumed proportional to the horizontal velocity contrast between layers.

Analytical models treating the western boundary region of a steady, wind-driven ocean can be divided into two classes, linear and nonlinear, depending on whether or not the nonlinear field accelerations are neglected in the momentum equations. To date no analytical solutions have been reported for a model of the entire basin employing

both frictional terms and nonlinear accelerations, but numerical solutions for such a model have been obtained with the aid of computers by Bryan (1963). Although solutions for the entire basin can be predicted from the linear theories, the linear models generally suffer from the use of arbitrary coefficients of eddy viscosity necessary to represent the turbulent exchange of momentum.

Model I, being such a frictional model, is no exception, and the results predicted therefrom may be considered to be of a speculative nature. In fact, two somewhat arbitrary friction coefficients must be selected for this model: one for the bottom stress and one for the interlayer stress. Even so, it is felt that if a choice must be made between vertical or horizontal frictional stresses, the former choice offers the potential advantage that, if the analysis could later be extended to a model with a non-horizontal sea bed and/or more layers, the ensuing results would more realistically depict the ocean.

For comparison, the model of Munk (1950) must be mentioned. Lateral friction is included in this linear model. The equations of motion are vertically integrated, and the motion at great depths is assumed negligible--thus no bottom friction. This approach leads to a fourth order vorticity equation and therefore is more involved mathematically than either Stommel's model or Model I, both of

which yeid second order vorticity equations. However, the solution predicts not only a western boundary current, with zero velocities at the meridional boundaries, but also an offshore countercurrent. This latter feature is rather significant in that such a current is indeed observed offshore from the Gulf Stream. As with all frictional models, Munk's results suffer because of the manner in which turbulent momentum exchange is represented. The characteristic width scale of his western boundary current depends directly on the cube root of the value chosen for the coefficient of eddy viscosity. The chosen value predicts a stream 200 km wide, much wider than the observed Gulf Stream. However, if the value of this coefficient is chosen small enough to predict a realistic stream width, the nonlinear terms are large enough, as compared with the frictional terms, that they can no longer reasonably be neglected (Stommel, 1965).

The use of such arbitrary coefficients is unnecessary in the nonlinear theories, since frictional terms are neglected. On the other hand, since no provision is made for energy dissipation, these theories are applicable only to the low latitude (formation and growth) region of the boundary current.

Another disadvantage of nonlinear models, and of linear models without lateral friction as well, is that

the velocities at the meridional boundaries are not zero. In fact, the maximum velocities predicted with such models are found at the western boundary. Therefore, the western boundary of such models should probably be interpreted as the center of the boundary current. This comment applies to Model I and to the inertial model presented in this paper (Model II). A more nearly complete picture might be obtained by adding to such models a current regime in which lateral friction is important in order to represent the region between the high speed core and the western coast. This problem has recently been discussed by Stewart (1965).

The first inertial theories for the boundary current were developed, at the suggestion of Stommel, independently and almost simultaneously by Charney (1955) and Morgan (1956). By detailed examination of the equations of motion, Morgan was able to infer that frictional terms are not necessarily of importance in achieving a steady, wind-driven regime. Assuming an interior solution, he developed compatible inertial current regimes both for the homogeneous model and for a two-layer baroclinic model, in which the lower layer is a rest. Charney's model, also for a baroclinic system, was developed with the intention of matching as closely as possible, within the framework of such a two-layer system, the actual flow conditions in the formation and growth region of the Gulf Stream. In

these, and other, inertial models of the boundary region, the potential vorticity, defined as the absolute vorticity divided by the layer thickness, is conserved along stream-tubes. The potential vorticity along the eastern edge of the boundary region is specified by the interior flow regime chosen.

Blanford (1964, 1965) extended the work of Morgan and Charney along two avenues. He developed inertial theories for: (i) a stably stratified three-layer model in which the lower layer is at rest but both upper layers are in motion; and (ii) a stably stratified two-layer model in which both layers are in motion. In order to obtain analytical solutions for the first model, the potential vorticity was assumed uniform within each moving layer. Analytical solutions were obtained for the second model under this same assumption, and it is probably for this reason that the predicted results seem physically unrealistic. In the case of non-uniform potential vorticity, only numerical solutions were obtained. In each case, Blanford found it necessary to use numerical techniques in order to satisfy the western boundary conditions.

The present Model II, for a stably stratified system of two moving layers, allows for non-uniform potential vorticity within each layer. Since this model is not limited to uniform potential vorticity, more freedom is

allowed in the choice of an interior flow regime. Solutions to the present model are obtained through the use of perturbation techniques rather than by the numerical solution of the differential equations. Two perturbation analyses are presented. In one case, numerical techniques are necessary to satisfy the western boundary conditions, as with Blanford's analyses; in the second case, the boundary conditions are applied in linearized forms and numerical procedures are not necessary to their application. No other analytical solutions for the case of multiple layers with non-uniform potential vorticity are known to have been reported.

C H A P T E R I I I

FORMULATION OF THE TWO-LAYER SYSTEM

A. Assumptions and Restrictions

Consider a two-layer system in which the fluid densities within the upper and lower layers are denoted by ρ and ρ' respectively.* In general, the variables associated with the lower layer are denoted by primes.

The principal assumptions employed in the development are that:

(A) The motion is steady;

(B) No exchange of mass occurs between layers, and the densities ρ and ρ' are assumed constant and uniform;

(C) The vertical distribution of pressure is given by the hydrostatic relation;

(D) The model ocean is situated on a β-plane;

(E) The sea bed is horizontal;

(F) The fluid is bounded by rigid, vertical boundaries which form a rectangle;

(G) The horizontal exchange of horizontal momentum is neglected;

---

*The definitions and c.g.s. units of all symbols used in the body of the text are presented in the List of Symbols preceeding Chapter I.

(H) The only external force acting is that due to a steady wind stress distribution acting on the free surface; and

(I) The horizontal velocity components within each layer are assumed independent of elevation.

Assumption (A) implies that the model can be used to predict only the circulation associated with the hypothetical mean wind stress distribution chosen. Moreover, with the stipulation (B), that there is no mixing between layers, the assumption of steady state provides that the interfaces be streamsurfaces.

Assumption (C) states that the pressure difference between any two elevations can be determined from a knowledge of the density field between these two elevations. This balance of vertical forces, which neglects vertical accelerations, is a very good approximation for steady state, large-scale oceanic phenomena.

Let x, y and z be position coordinates in a coordinate system fixed to the earth. Assume that the earth's gravity vector is everywhere normal to planes z=constant. Let z be measured positive upward from the sea bed, and let x and y increase eastward and northward, respectively. Let f denote the Coriolis parameter, $2\Omega \sin \phi$, with Ω the earth's angular speed of rotation and ϕ the latitude. If f is expanded as a series in

powers of y about $y=0$, a linear approximation yields

$$f = f_o + \beta y ,$$

with ϕ_o and R_o the latitude and earth's radius at $y=0$, $f_o = 2\Omega \sin \phi_o$ and $\beta = 2\Omega \frac{\cos \phi_o}{R_o}$. The foregoing sphere-to-plane transformation, and the stipulation that f varies only as a linear function of y, with $\beta = \frac{df}{dy}$, constitute what is commonly referred to as a β-plane approximation. For details of the approximations and restrictions involved in performing such transformations on the equations of motion, the reader is referred to the work of Veronis (1963a, 1963b). In representing geophysical flow regimes with large ratios of meridional to vertical scale, Veronis has shown the β-plane approximation to be valid for the region between somewhat less than 10^o latitude and mid-latitudes. For such flow regimes, moreover, the locally horizontal components of the earth's vorticity can be neglected.

Any influence of bathymetry on the flow is ruled out by assumption (E). This would be an impossibly restrictive assumption were the meander region of the western boundary current under consideration. However, for examination of the main circulation features in the interior and in the regions of formation and growth of

western boundary currents, it is perhaps not essential to provide for possible bathymetric control.

At the expense of geographically realistic coastlines, assumption (F) provides mathematically tractable lateral boundary conditions at the meridional boundaries of the basin. Let $x=0$, w and $y=0$, b specify the planes which laterally bound the basin. The assertion that the northern and southern, as well as the meridional, boundaries be streamlines requires that these zonal boundaries correspond to latitudes of zero wind stress curl. At such latitudes the transport in the interior of a steady wind-driven circulation regime must be zonal (Munk, 1950).

The effects of lateral friction, neglected by assumption (G), could be significant only where large horizontal gradients of horizontal velocity occur. A scaling analysis of the horizontal momentum conservation equations (see, e.g., Fofonoff, 1962) shows that frictional effects may be quite important in such regions as the Gulf Stream. However, even if lateral friction is ignored, a steady state solution can be obtained provided that some other method of energy dissipation, such as bottom friction, is provided (see Stommel, 1957). One effect of assumption (G) is that of allowing non-zero tangential velocities at the solid meridional boundaries. This places a very severe limitation on the results of this model, if they are to be

compared with reality in the region quite close to the western boundary of the basin. In fact it can be concluded that any physically correct model which is to be used for such description must allow for zero velocities at the coasts (Stewart, 1965). It may be possible to add a frictional boundary current regime to the near shore side of the inertial currents developed in this paper and thus overcome this limitation.

With the exception of the homogeneous model, the two-layer system is the crudest approximation to an ocean in which the density varies continuously with depth. Assuming that the horizontal velocities are independent of elevation within each layer, provides for a correspondingly simple vertical structure of horizontal currents. Assumption (I) implies that the current speeds considered are, in effect, vertical averages over the layer thickness. In reality, a two-layer system evidences vertical shears of horizontal velocity; both upper and lower boundary layers may be present. However, with this two-layer system one cannot hope to obtain such fine structure. A multiple layer system is indeed a finite difference approximation to the continuous system. If more resolution of vertical structure of horizontal currents is desired, then more layers must be included.

B. Formulation of the Equations

To obtain expressions of mass and momentum conservation applicable to the two-layer model, first consider the situation of steady flow within a layer of incompressible fluid with uniform density ρ^*. Relative to the reference plane $z = 0$, let the elevations of the lower and upper streamsurfaces bounding this layer be denoted by $Z_1(x,y)$ and $Z_2(x,y)$, respectively. Let $D \equiv Z_2 - Z_1$ denote the layer thickness. At each point within the fluid let p^* denote pressure and u^* and v^* denote, respectively, the x- and y-directed components of fluid velocity.

Then, the continuity relation, valid at each point (x,y) over the horizontal extent of the fluid layer, is

$$\frac{\partial}{\partial x}(u^*D) + \frac{\partial}{\partial y}(v^*D) = 0 \ . \tag{1}$$

The conservation of horizontal momentum requires that at each point (x,y):

$$\left.\begin{aligned}
&\frac{\partial}{\partial x}\int_{Z_1}^{Z_2}(u^*)^2dz + \frac{\partial}{\partial y}\int_{Z_1}^{Z_2}u^*v^*dz \\
&-f\int_{Z_1}^{Z_2}v^*dz + \frac{1}{\rho^*}\int_{Z_1}^{Z_2}\frac{\partial p^*}{\partial x}dz = \frac{1}{\rho^*}(\tau_{x_2} - \tau_{x_1}) \ , \\
&\frac{\partial}{\partial x}\int_{Z_1}^{Z_2}u^*v^*dz + \frac{\partial}{\partial y}\int_{Z_1}^{Z_2}(v^*)^2dz \\
&+ f\int_{Z_1}^{Z_2}u^*dz + \frac{1}{\rho^*}\int_{Z_1}^{Z_2}\frac{\partial p^*}{\partial y}dz = \frac{1}{\rho^*}(\tau_{y_2} - \tau_{y_1}) \ ,
\end{aligned}\right\} \tag{2}$$

where τ_{x_j} and τ_{y_j} represent, respectively, the x- and y-directed components of horizontal stress applied by the fluid above the Z_j (j=1,2) surface on the fluid below this surface and p* is pressure. Lateral friction has been neglected, and the β-plane approximations have been made.

If u* and v* are assumed independent of elevation within the layer, equations (2) may be written

$$Du^*\frac{\partial u^*}{\partial x} + Dv^*\frac{\partial u^*}{\partial y} - fv^*D + \frac{1}{\rho^*}\int_{Z_i}^{Z_2}\frac{\partial p^*}{\partial x}dz = \frac{1}{\rho^*}(\tau_{x_2} - \tau_{x_1}) ,$$

$$Du^*\frac{\partial v^*}{\partial x} + Dv^*\frac{\partial v^*}{\partial y} + fu^*D + \frac{1}{\rho^*}\int_{Z_1}^{Z_2}\frac{\partial p^*}{\partial y}dz = \frac{1}{\rho^*}(\tau_{y_2} - \tau_{y_1}) , \qquad (3)$$

where use has been made of the continuity relation (1). If the hydrostatic relation is introduced into equation (3), and the shearing stresses are either assumed known or to be dependent on the horizontal velocity components only, then the mathematical problem comprised by equations (1) and (3) represents a system of 3 equations in the 3 unknowns u*, v* and D. (For the case of two-layers, 6 equations in 6 unknowns will be employed.) It is in the cause of obtaining a mathematically tractable system that the horizontal components of velocity have been assumed independent of elevation. In effect, this assumption implies that the horizontal velocity components of equations

(3) are to be interpreted as mean values averaged over the layer thickness.

Let u and v denote the components of velocity directed eastward and northward in the upper layer; let u' and v' denote corresponding velocity components within the lower layer. The thicknesses of the upper and lower layers are denoted by H and H', respectively.

For the two-layer system, the hydrostatic relation is

$$\frac{\partial p}{\partial z} = -\rho g, \quad \frac{\partial p'}{\partial z} = -\rho' g , \tag{4}$$

where g is the local value of earth's gravity (assumed uniform throughout the region of interest), and p and p' denote pressures within the upper and lower layers.

The density contrast may be characterized by the positive ratio

$$\gamma \equiv \frac{\rho' - \rho}{\rho} . \tag{5}$$

Following Duxbury (1963), let B represent an effective overall water depth defined by

$$\rho' B = \rho' H' + \rho H ,$$

or, using (5),

$$B = H' + (1 - \gamma)H . \tag{6}$$

Then, the hydrostatic relation may be vertically

integrated to yield the pressure fields within the two layers:

$$p = p_a + \rho g(B+\gamma H-z) \ ,$$
$$p' = p_a + \rho' g(B-z) \ , \tag{7}$$

where p_a is sea-level atmospheric pressure, assumed uniform over the horizontal extent of the basin.

Equations (3) are valid, with changes in notation, for either layer of the two-layer system. Thus, using (7), the horizontal momentum conservation relations can be written as follow:

$$Hu\frac{\partial u}{\partial x} + Hv\frac{\partial u}{\partial y} - fvH + gH\frac{\partial}{\partial x}(B+\gamma H) = \frac{1}{\rho}(\tau_x - \tau_x^I) \ ,$$
$$Hu\frac{\partial v}{\partial x} + Hv\frac{\partial v}{\partial y} + fuH + gH\frac{\partial}{\partial y}(B+\gamma H) = \frac{1}{\rho}(\tau_y - \tau_y^I) \ , \tag{8}$$

and

$$H'u'\frac{\partial u'}{\partial x} + H'v'\frac{\partial u'}{\partial y} - fv'H' + gH'\frac{\partial B}{\partial x} = \frac{1}{\rho}(\tau_x^I - \tau_x^B) \ ,$$
$$H'u'\frac{\partial v'}{\partial x} + H'v'\frac{\partial v'}{\partial y} + fu'H' + gH'\frac{\partial B}{\partial y} = \frac{1}{\rho}(\tau_y^I - \tau_y^B) \ . \tag{9}$$

If $\hat{i}$ and $\hat{j}$ are unit vectors in the positive x- and y-directions, then the vectors

$$\hat{\tau} = \hat{i}\,\hat{\tau}_x + \hat{j}\,\hat{\tau}_y ,$$

$$\hat{\tau}^I = \hat{i}\,\tau_x^I + \hat{j}\,\tau_y^I$$

and

$$\hat{\tau}^B = \hat{i}\,\tau_x^B + \hat{j}\,\tau_y^B$$

represent, respectively, the horizontal stress applied to the sea surface, the horizontal stress applied by the upper layer on the lower layer and the horizontal stress on the sea bed.

Components of volume transport through a vertical plane extending through one layer and of unit width normal to the component direction can be defined by the following relations:

$$U \equiv uH \quad , \qquad V \equiv vH \quad ,$$

$$U' \equiv u'H' \quad , \qquad V' \equiv v'H' \quad .$$

So, using equation (1), the continuity relations for the upper and lower layers can be written

$$\frac{\partial U}{\partial x} + \frac{\partial V}{\partial y} = 0 \quad , \tag{10}$$

and

$$\frac{\partial U'}{\partial x} + \frac{\partial V'}{\partial y} = 0 \quad . \tag{11}$$

Assuming the volume transport components to be single-valued and continuous, the continuity relations

(10) and (11) guarantee the existence of transport stream-functions, Ψ and Ψ', for the upper and lower layers defined by

$$U = -\frac{\partial \Psi}{\partial y}, \qquad V = \frac{\partial \Psi}{\partial x},$$
$$U' = -\frac{\partial \Psi'}{\partial y}, \qquad V' = \frac{\partial \Psi'}{\partial x}. \tag{12}$$

The horizontal velocities, pressure field, and layer thicknesses within this two-layer system are now specified by the continuity relations in the form (12) or (10) and (11), the momentum equations (8) and (9) and the pressure relations (7) together with the appropriate boundary conditions. In the next chapter the frictional model obtained by neglecting the inertial terms is considered for particular basin geometry. The analysis for inertial boundary currents, in the absence of the stress terms, is considered in Chapter V.

C. Physical Characterization

To obtain numerical results, it was necessary to select values for the basic parameters characterizing the model. In order to facilitate computations and comparisons with the studies of Stommel (1948) and Munk (1950), the latitudinal and longitudinal dimensions of the basin

were chosen to be 3400 km and 10,000 km*, respectively. The north-south center of the basin is taken at 32° N. latitude, where 1° latitude is approximately 111 km. The southern and northern boundaries of the basin are therefore located at approximately 16° and 48° N. latitude, respectively. For this latitude band the Coriolis parameter was fit to the functional form $f = f_o + \beta y$, with $y=0$ at 16° N., by the method of least squares. The resulting values of f_o and β were 4.192×10^{-5} sec^{-1} and 1.928×10^{-13} sec^{-1} cm^{-1}, respectively.

As a first approximation, the permanent pycnocline provides a natural criterion for partitioning the real ocean into two layers. Values representative of the depth to the center of the pycnocline in the North Atlantic Ocean between 15° and 45° N. latitude (Defant, 1961; Stommel, 1965) were considered. The mean upper and lower layer thicknesses, H_o and H_o' as defined by equations (21), were chosen to be 750 m and 3100 m, respectively. The mean depth of the Atlantic Ocean, excluding adjacent seas, is estimated to be 3868 m (Defant, 1961). For this incompressible model the densities can be estimated by considering the distribution of σ_t in vertical sections taken east-west through the North Atlantic (Iselin, 1936;

*Essentially, 10^4 km represents a compromise between Atlantic and Pacific zonal dimensions.

Defant, 1961). The term σ_t is defined by $\sigma_t = (\rho_{s,t,o} - 1) \times 10^3$ where $\rho_{s,t,o}$ denotes the density of a sample computed for atmospheric pressure and the temperature and salinity at which it was collected. The densities so chosen are 1.026 gm cm^{-3} and 1.028 gm cm^{-3} for the upper and lower layers. It should be noted that it is the density contrast, and not the individual values, which is of consequence in these considerations.

In summary, the values (with c.g.s. units) of the parameters chosen are presented in Table I.

TABLE I

Constants Chosen for Physical Characterization

Parameter	Value	Units	Parameter	Value	Units
b	3.4×10^8	cm	H_o	7.5×10^4	cm
w	10^9	cm	H_o'	3.1×10^5	cm
f_o	4.129×10^{-5}	sec^{-1}	ρ	1.026	gm cm^{-3}
β	1.928×10^{-13}	$sec^{-1} cm^{-1}$	ρ'	1.028	gm cm^{-3}

C H A P T E R I V

THE FRICTIONAL MODEL

A. The Equations

1. Vertically integrated equations. The nonlinear field accelerations are important only in regions of intense currents, such as the Kuroshio or Gulf Stream (Fofonoff, 1962). The neglect of such terms thus results in no significant error for the interior region. However, the resulting frictional model must be applied with caution to the region of western boundary currents. In the formation and growth region of such currents the flow is probably controlled principally by inertial effects (Morgan, 1956; Charney, 1955), except for a near shore frictional boundary layer (Stewart, 1965). In the downstream portion of such currents, the flow is certainly time dependent, evidencing meanders and eddies (Stommel, 1965). As Stommel points out, one may consider the individual eddies and meanders to be averaged out as turbulence and so interpret the mean notion as the "climatological-mean Gulf Stream."

Neglecting the terms resulting from the nonlinear field accelerations, equations (8) and (9) yield

$$-fV + \frac{g'}{2}\frac{\partial H^2}{\partial x} + gH\frac{\partial B}{\partial x} = \frac{1}{\rho}(\tau_x - \tau_x^I) \ ,$$

$$fU + \frac{g'}{2}\frac{\partial H^2}{\partial y} + gH\frac{\partial B}{\partial y} = \frac{1}{\rho}(\tau_y - \tau_y^I) \ , \tag{13}$$

and

$$-fV' + gH'\frac{\partial B}{\partial x} = \frac{1}{\rho'}(\tau_x^I - \tau_x^B) \ ,$$

$$fU' + gH'\frac{\partial B}{\partial y} = \frac{1}{\rho'}(\tau_y^I - \tau_y^B) \ , \tag{14}$$

where g' represents a reduced gravity value defined by

$$g' \equiv \gamma g \ . \tag{15}$$

2. Stress terms. For this analysis, the interlayer and bottom stresses are represented by the forms

$$\hat{\tau}^I = \rho\,\sigma\,H\,(\hat{q} - \hat{q}')$$

$$\hat{\tau}^B = \rho'\sigma'H'\hat{q}' \ , \tag{16}$$

where:

$$\hat{q} \equiv \hat{i}\,u + \hat{j}\,v \ ,$$

$$\hat{q}' \equiv \hat{i}\,u' + \hat{j}\,v'$$

and σ, σ' are frictional coefficients with c.g.s. units sec^{-1}. These stress forms are similar to that form used by Stommel (1948) for his steady, homogeneous, wind-driven

model with bottom friction only. Nevertheless, the validity of representing the stress by the functional form of equations (16) is certainly subject to question. Further discussion of these stresses is presented in section 6 of this chapter.

Now, introducing the forms specified by (16) into equations (13) and (14) yields:

$$
\begin{aligned}
-fV + \frac{g'}{2}\frac{\partial H^2}{\partial x} + gH\frac{\partial B}{\partial x} &= T_x - \sigma\left(U - \frac{H}{H'}U'\right) , \\
fU + \frac{g'}{2}\frac{\partial H^2}{\partial y} + gH\frac{\partial B}{\partial y} &= T_y - \sigma\left(V - \frac{H}{H'}V'\right) ,
\end{aligned}
\tag{17}
$$

and

$$
\begin{aligned}
-fV' + gH'\frac{\partial B}{\partial x} &= \sigma\left(U - \frac{H}{H'}U'\right) - \sigma'U' , \\
fU' + gH'\frac{\partial B}{\partial y} &= \sigma\left(V - \frac{H}{H'}V'\right) - \sigma'V' .
\end{aligned}
\tag{18}
$$

In equations (17) a kinematically expressed form of the surface stress defined by

$$\rho \hat{T} \equiv \hat{\tau}$$

(c.g.s. units $cm^2\ sec^{-2}$ of stress/density) has been introduced. The insignificant approximation $\rho/\rho' \doteq 1$ has been made in expressing the interlayer stress components in equation (18).

For simplicity and to facilitate comparison with

$$\rho \hat{T} = \hat{\tau} = - \hat{i}\, F \cos\left(\frac{\pi y}{b}\right) , \tag{19}$$

where F is a suitable dimensional constant (of the order of 1 dyne cm^{-2}) and b is the meridional dimension of the basin.

3. Approximate forms. Let $h(x,y)$ and $h'(x,y)$ denote the local variations from the mean thicknesses H_o and H_o' of upper and lower layers. Then the local layer thicknesses can be written

$$H = H_o + h , \quad H' = H_o' + h' . \tag{20}$$

The mean layer thicknesses are constants defined by

$$\begin{aligned} H_o &\equiv \frac{1}{wb} \int_o^w \int_o^b H \, dx \, dy , \\ H_o' &\equiv \frac{1}{wb} \int_o^w \int_o^b H' \, dx \, dy . \end{aligned} \tag{21}$$

Now, certainly the terms $h\frac{\partial B}{\partial x}$ and $h\frac{\partial B}{\partial y}$ are expected to be smaller than $H_o \frac{\partial B}{\partial x}$ and $H_o \frac{\partial B}{\partial y}$, respectively. If the former terms are neglected compared with the latter, the linearizing approximations,

$$H\frac{\partial B}{\partial x} \doteq \frac{\partial}{\partial x}(H_o B) , \quad H\frac{\partial B}{\partial y} \doteq \frac{\partial}{\partial y}(H_o B) ,$$

can be used to simplify equations (17). The similar approximations,

$$H'\frac{\partial B}{\partial x} \doteq \frac{\partial}{\partial x}(H_o'B) \ , \quad H'\frac{\partial B}{\partial y} \doteq \frac{\partial}{\partial y}(H_o'B) \ ,$$

serve to linearize equation (18). It should be noted that the latter approximations are less restrictive than the former, since the maximum value of h and h' are nearly equal while H_o' is approximately an order of magnitude greater than H_o.

Making the foregoing simplification and approximating H/H' in the friction terms by

$$d_o \equiv H_o/H_o' \ , \tag{22}$$

the following approximate forms of (17) and (18) obtained:

$$\begin{aligned} -fV + \frac{\partial}{\partial x}(\tfrac{g'}{2}H^2 + gH_oB) &= T_x - \sigma(U - d_oU') \ , \\ fU + \frac{\partial}{\partial y}(\tfrac{g'}{2}H^2 + gH_oB) &= T_y - \sigma(V - d_oV') \ , \end{aligned} \tag{23}$$

and

$$\begin{aligned} -fV' + \frac{\partial}{\partial x}(gH_o'B) &= \sigma(U - d_oU') - \sigma'U' \ , \\ fU' + \frac{\partial}{\partial y}(gH_o'B) &= \sigma(V - d_oV') - \sigma'V' \ . \end{aligned} \tag{24}$$

It is these forms for which analytic solutions were obtained.

The mixed linear, nonlinear form of the pressure gradient terms in equations (23) might be questioned.

Actually, the product of $\cdot H$ with the gradient of H was not approximated as was the product of H with the gradient of B for two reasons. First, the gradient of H is expected to be large compared with that of B; second, and most fortunate, it is not necessary to do so in order to solve the transport problem.

4. Lateral boundary conditions. The assumption of solid, vertical boundaries requires, of course, that these boundaries be streamsurfaces. For convenience the basin boundary was arbitrarily chosen as the streamsurface on which both transport streamfunctions assume the value zero. Thus,

$$\Psi(o,y) = \Psi'(o,y) = \Psi(w,y) = \Psi'(w,y) = 0 \quad (0 \leq y \leq b) ,$$
$$\Psi(x,o) = \Psi'(x,o) = \Psi(x,b) = \Psi'(x,b) = 0 \quad (0 \leq x \leq w) . \tag{25}$$

5. Energy relations. The momentum equations (17) and (18) can be expressed in the vector forms

$$f\, H\, \hat{k} \times \hat{q} + g' H \nabla H + g\, H \nabla B = \hat{T} - \sigma H(\hat{q} - \hat{q}') , \tag{26}$$

and

$$f\, H' \hat{k} \times \hat{q}' + g\, \hat{H}' \nabla B = \sigma H(\hat{q} - \hat{q}') - \sigma' H' \hat{q}' , \tag{27}$$

where $\hat{k}$ is the unit vector in the positive z-direction and $\nabla \equiv \hat{i} \frac{\partial}{\partial x} + \hat{j} \frac{\partial}{\partial y}$. Although somewhat simplified forms

of these equations are solved, it is of interest to form and examine the energy relations derived from these more complete forms.

Taking the dot products of $\hat{q}$ with (26) and of $\hat{q}'$ with (27) yields the energy equations based on the vertically integrated momentum equations:

$$H\,\hat{q}\cdot\nabla(gB + g'H) = \hat{q}\cdot\hat{T} - \sigma\,H(q^2 - \hat{q}\cdot\hat{q}') \,, \qquad (28)$$

and

$$H'\hat{q}'\cdot\nabla(gB) = \sigma H[\hat{q}\,\hat{q}' - (q')^2] - \sigma' H'(q')^2 \,, \qquad (29)$$

where q and q' denote the magnitudes of $\hat{q}$ and $\hat{q}'$, respectively. The terms are dependent on horizontal position coordinates only and have been normalized by the density of the appropriate layer. Each term in (28) represents a time rate of change of energy associated with a vertical column extending through the upper layer. Terms of (29) represent like changes associated with a vertical column at (x,y) extending through the lower layer.

The addition of (28) to (29) gives

$$[H\,\hat{q}\cdot\nabla(gB + g'H) + H'\hat{q}'\cdot\nabla(gB)] = [\hat{q}\cdot\hat{T}] - [\sigma H(q^2 - 2\hat{q}\cdot\hat{q}' + q'^2) + \sigma' H'(q')^2] \qquad (30)$$

The first term on the right hand side represents the net energy increase per unit time associated within a vertical

column of unit cross sectional area at (x,y) due to vertical transport of horizontal momentum to the water by the wind. The increase is seen to be positive at each position at which $(uT_x + vT_y) > 0$. For the assumed wind stress distribution given by (19), $T_y = 0$ and

$$T_x \begin{cases} > 0 & (b/2 < y \leq b) \ , \\ < 0 & (0 \leq y < b/2) \ . \end{cases}$$

As the solution shows, u has the same sign convention as does T_x. Therefore, the term, $\hat{q} \cdot \hat{T}$, is non-negative at each position within the basin. This energy input must be balanced by an equal energy dissipation from the steady flow, if a steady-state solution is to exist.

The left hand side of (30) can be written

$$\frac{1}{\rho}(\hat{q}H) \cdot \nabla p + \frac{1}{\rho}(\hat{q}'H') \cdot \nabla p' \ ,$$

or, since $\nabla \cdot (\hat{q}H) = \nabla \cdot (\hat{q}'H') = 0$ by (10) and (11) ,

$$\frac{1}{\rho}\nabla \cdot (p\hat{q}H) + \frac{1}{\rho}\nabla \cdot (p'\hat{q}'H') \ .$$

Thus, the left hand side represents the net work done per unit time against pressure forces due to cross isobaric flow in a vertical column extending through both layers. At some given point (x,y) this term may have a non-zero value. However, the net amount of such work done in the

entire system is zero provided that no discontinuity of pressure occurs in the system. This is seen by integrating the last expression over the horizontal extent of the basin, applying the divergence theorem and noting that the transport components normal to the boundaries are zero. This is as expected for a flow regime independent of time; otherwise, the strength of the total circulation would be altered in time.

The second square bracketed term on the right hand side represents the net decrease in energy per unit time associated with a vertical column extending from sea bed to sea surface. This energy transfer from the mean organized motion is due to friction at the sea bed and frictional coupling between layers. This term, which can be written

$$\sigma H(u - u')^2 + \sigma H(v - v')^2 + \sigma' H'[(u')^2 + (v')^2] ,$$

is seen to be non-negative, as expected, provided only that σ and σ' are non-negative. If a barotropic model were considered, then $u = u'$, $v = v'$ and, consequently, the total frictional dissipation of energy would be given by $\sigma' H'(q')^2$, which represents the rate of energy loss from organized motion by the process of vertically transferring horizontal momentum through the boundary layer to the bottom. The net frictional dissipation of energy in

the model, obtained by integrating the last term of (30) over the horizontal extent of the basin, must balance the net energy input over the basin by the wind stress.

Consider now the energy relations which result from the vertically integrated momentum relations (23) and (24), chosen for the frictional model. By the same procedure used to obtain (30) the following energy relation is obtained:

$$[\hat{q} \cdot \nabla(gH_oB + \tfrac{1}{2}g'H^2) + \hat{q}' \cdot \nabla(gH_o'B)] = [\hat{q} \cdot \hat{T}]$$
$$-[\sigma Hq^2 - \sigma H(1 + d_o \tfrac{H'}{H})\hat{q} \cdot \hat{q}' + (\sigma d_o + \sigma')H'(q')^2] . \quad (31)$$

Each of the terms in (31) is interpreted just as its counterpart in (30). The only difference of possible significance is in the form of the frictional term. It is therefore necessary to examine for any special criterion which must be observed in order that the sum of terms enclosed by the second square bracket set on the right hand side be non-negative.

It can be shown (Appendix A) that in order to insure that the frictional energy dissipation be positive definite, it is sufficient to require that

$$\sigma > 0, \quad \frac{\sigma'}{\sigma} \geq \frac{1}{4} \frac{(H - d_oH')^2}{H H'} . \quad (32)$$

This requirement is not very stringest for reasonably

expected local variations of H from H_o. For example, if $H_o = 750$ m, $H_o' = 3100$ m, $H = 650$ m and $H' = 3200$ m, then $\frac{\sigma'}{\sigma} \geq 1.8 \times 10^{-3}$. Even so, this added requirement, which results because of the approximations made to the momentum equations, must be satisfied for a physically correct model.

6. Estimates of frictional coefficients. One estimate of σ can be obtained from the upper layer momentum conservation relations (23), which can be expressed in the vector form,

$$f \hat{k} \times \hat{Q} + \nabla(gH_oB + \frac{g'}{2}H^2) = \hat{T} - \sigma(\hat{Q} - d_o\hat{Q}') ,$$

with

$$\hat{Q} \equiv \hat{q} H , \qquad \hat{Q}' \equiv \hat{q}'H' .$$

Forming the dot product with $\hat{Q}$ and remembering that $\nabla \cdot \hat{Q} = 0$, yields

$$\nabla \cdot [\hat{Q}(gH_oB + \frac{g'}{2}H^2)] = \hat{Q} \cdot \hat{T} - \sigma(Q^2 - d_o\hat{Q} \cdot \hat{Q}') .$$

Integrate over the horizontal extent of the basin to obtain

$$\sigma = \frac{\int_o^b \int_o^w \hat{Q} \cdot \hat{T} \, dx \, dy}{\int_o^b \int_o^w (Q^2 - d_o\hat{Q} \cdot \hat{Q}') dx \, dy} . \qquad (33)$$

Now, under the assumption that the components of vertically integrated velocity within the lower layer are not larger than the corresponding components within the upper layer, it is possible to estimate σ from (33) based on a knowledge of the wind stress over the interior and of the width and transport of the upper western boundary current. Details are presented in Appendix B. For this purpose: the representative eastward or westward wind stress over the northern or southern half of the interior region was taken as .5 dyne cm^{-2}; the representative northward transport within the upper layer boundary current was taken as 60×10^{12} cm^3 sec^{-1}*; and the width of the western boundary current was assumed to be not greater than 200 km. The resulting order of magnitude estimate for σ is between $.5 \times 10^{-6}$ and 10^{-6} sec^{-1}.

Another method of obtaining values for the frictional coefficients was suggested by R. O. Reid (personal communication, 1965) who devised the associated analysis presented in Appendix C. This method involves the comparison of implied energy dissipation rates for the present model with those derived for a free, two-layer system with very thin frictional boundary layers.

If one considers a two-layer model in each layer of

---

*This is of the order of magnitude estimated from hydrographic data (c.f. Munk, 1950).

which the velocity is assumed independent of elevation, then one is really assuming the fluid within each layer is sufficiently well mixed to be considered homogeneous and that mixing across the interface is inhibited by the density contrast through the very thin frictional boundary layers on either side of the interface. The thickness of the frictional bottom boundary layer is likewise considered small as compared with the fluid layer thickness.

The movement within such oceanic boundary layers is conceded to be disordered and turbulent. In order to obtain an expression for the vertical transfer of horizontal momentum due to turbulence, the apparent shear stress over a horizontal plane in turbulent flow is classically taken to be proportional to the derivative of the mean horizontal velocity with respect to elevation. The constant of proportionality is taken to be ρK, where K is known as the kinematic "Austausch," the kinematic coefficient of vertical eddy viscosity or simply the kinematic eddy coefficient (c.g.s. units $cm^2\ sec^{-1}$). Such a form was first introduced for turbulent flow in 1877 by Boussinesq and is analogous to Stoke's law for laminar flow (c.f. Schlichting, 1960). Values of K ranging from 1 to 10^3 $cm^2\ sec^{-1}$ have been found for the oceans (Sverdrup, et al., 1942; Defant, 1961). However, for geophysical flow models K is generally taken to be uniform.

For a model without surface stress but having horizontal pressure gradients in both layers, Reid developed expressions for the field of horizontal velocity. The flow is assumed geostrophic except within the three, thin, Ekman type boundary layers. Boussinesq forms for the stresses are assumed; the kinematic eddy coefficients, K and K' within the upper and lower layers, are assumed uniform. Expressions are derived for the implied rates of energy dissipation for vertical columns of unit cross section extending through the bottom boundary layer and through both boundary layers at the interlayer interface. These are equated to analogous expressions for the present frictional model derived from equations (28) and (29). The following approximations for σ and the ratio σ'/σ result (Appendix C):

$$\sigma \doteq \frac{1}{H}\sqrt{\frac{fK'}{2}}\,(1+\sqrt{K'/K})^{-1}\ ,$$

$$\frac{\sigma'}{\sigma} \doteq \frac{H}{H'}\,(1+\sqrt{K'/K})\ .$$

For the chosen average values of H and H' (Table I) and for $f \doteq 7.41 \times 10^{-5}$ (sec^{-1}), mean value over the meridional extent of the basin, one has (all units c.g.s.)

$$\sigma \doteq 8.1 \times 10^{-8}\sqrt{K'}\,(1+\sqrt{K'/K})^{-1}\ ,$$

and

$$\sigma'/\sigma \doteq .24\ (1 + \sqrt{K'/K})\ .$$

Now, if $K = 10^3$, $K' = 10^2$ (c.g.s.), then

$$\sigma \simeq .6 \times 10^{-6}\ (\text{sec}^{-1})\ ,$$

and

$$\sigma'/\sigma \simeq .3\ .$$

Examination of the solutions actually provides a better basis on which to choose σ and σ', since these friction coefficients can then be related to the observed width of the western boundary currents. Prior to such examination, σ' was considered to be less than or equal to σ.

B. Formal Solutions

The method of normal modes, as employed by Veronis and Stommel (1956), is used in order to solve the momentum equations (23) and (24) simultaneously for Ψ and Ψ' without increasing the order of the differential equation to be solved. The transformed boundary value problem which results consists of one linear, second order differential equation in a double-valued dependent variable and two independent variables plus four linear boundary conditions.

Cross-differentiation of the horizontal momentum equations (23) and (24) yields the following vorticity balance relations for the two layers:

$$\beta V = \left(\frac{\partial T_y}{\partial x} - \frac{\partial T_x}{\partial y}\right) - \sigma\left(\frac{\partial V}{\partial x} - \frac{\partial U}{\partial y}\right) + \sigma d_o\left(\frac{\partial V'}{\partial x} - \frac{\partial U'}{\partial y}\right) , \qquad (34)$$

and

$$\beta V' = \sigma\left(\frac{\partial V}{\partial x} - \frac{\partial U}{\partial y}\right) - \sigma d_o\left(\frac{\partial V'}{\partial x} - \frac{\partial U'}{\partial y}\right) - \sigma'\left(\frac{\partial V'}{\partial x} - \frac{\partial U'}{\partial y}\right) . \qquad (35)$$

Introducing the transport streamfunctions, defined by (12), these relations can be written as

$$\beta\frac{\partial \Psi}{\partial x} = \left(\frac{\partial T_y}{\partial x} - \frac{\partial T_x}{\partial y}\right) - \sigma\nabla^2\Psi + \sigma d_o\nabla^2\Psi' , \qquad (36)$$

and

$$\beta\frac{\partial \Psi'}{\partial x} = \sigma\nabla^2\Psi - \sigma d_o\nabla^2\Psi' - \sigma'\nabla^2\Psi' . \qquad (37)$$

Let α be an arbitrary constant and algebraically combine (36) with (37) to obtain

$$\beta\frac{\partial}{\partial x}\left(\Psi + \alpha\Psi'\right) = \left(\frac{\partial T_y}{\partial x} - \frac{\partial T_x}{\partial y}\right) - \nabla^2[(\sigma - \alpha\sigma)\Psi + (\alpha\sigma d_o + \alpha\sigma' - \sigma d_o)\Psi'] .$$

Defining a new dependent variable Φ and another undetermined constant Γ by

$$\Phi \equiv \Psi + \alpha\Psi' \equiv [(\sigma - \alpha\sigma)\Psi + (\alpha\sigma d_o + \alpha\sigma' - \sigma d_o)\Psi']\Gamma \ , \qquad (38)$$

the foregoing equation can be written

$$\frac{1}{\Gamma}\nabla^2\Phi + \beta\frac{\partial\Phi}{\partial x} = \left|\frac{\partial T_y}{\partial x} - \frac{\partial T_x}{\partial y}\right| \ . \qquad (39)$$

Now, the second identity of (38) requires that

$$1 = \sigma\Gamma(1 - \alpha) \ ,$$

and

$$\alpha = \Gamma(-d_o\sigma + \alpha d_o\sigma + \alpha\sigma') \ .$$

It is seen that the constants α and Γ represent double-valued sets, the values of which are given by

$$\alpha_1 = \frac{1}{2}(1 - \frac{\sigma'}{\sigma} - d_o) - \sqrt{\frac{1}{4}(1 - \frac{\sigma'}{\sigma} - d_o)^2 + d_o} \ ,$$

$$\alpha_2 = \frac{1}{2}(1 - \frac{\sigma'}{\sigma} - d_o) + \sqrt{\frac{1}{4}(1 - \frac{\sigma'}{\sigma} - d_o)^2 + d_o} \ , \qquad (40)$$

and

$$\Gamma_1 = \sigma^{-1}(1 - \alpha_1)^{-1} \ ,$$

$$\Gamma_2 = \sigma^{-1}(1 - \alpha_2)^{-1} \ . \qquad (41)$$

The double-valued constants α_j and Γ_j and the corresponding double-valued variable Φ_j, as defined by the

first identity of (38), will henceforth be subscripted by the letter "j", which is understood to assume the values 1 and 2.

The boundary conditions (25) can be expressed in terms of the variable Φ_j as follows:

$$\begin{aligned} \Phi_j(o,y) &= \Phi_j(w,y) = 0 \qquad (0 \leq y \leq b) , \\ \Phi_j(x,o) &= \Phi_j(x,b) = 0 \qquad (0 \leq x \leq w) . \end{aligned} \tag{42}$$

After solutions for Φ_j are obtained, Ψ and Ψ' can be recovered from

$$\begin{aligned} \Psi &= (\alpha_2 - \alpha_1)^{-1} (\alpha_2\Phi_1 - \alpha_1\Phi_2) , \\ \Psi' &= (\alpha_2 - \alpha_1)^{-1} (\Phi_2 - \Phi_1) \end{aligned} \tag{43}$$

which result from the first of identities (38).

Using the assumed wind stress distribution given by equation (19), the differential equation (39) can be written

$$\nabla^2\Phi_j + \beta\Gamma_j \frac{\partial\Phi_j}{\partial x} = -\frac{\pi F}{b\rho}\Gamma_j \sin(\frac{\pi y}{b}) . \tag{44}$$

The analysis required to solve this equation with the boundary conditions (42) is almost identical to that employed by Stommel (1948) to obtain solutions for the

one-layer model. Details are presented in Appendix D. The complete solution is given by

$$\Phi_j = -\frac{bF}{\pi\sigma}\,\Gamma_j \sin\left(\frac{\pi y}{b}\right)\left[R_j e^{a_j x} - 1 + (1 - R_j)^{c_j x}\right] \qquad (45)$$

with

$$\left.\begin{aligned} a_j &= -\frac{\beta\Gamma_j}{2} + \left[\left(\frac{\beta\Gamma_j}{2}\right)^2 + \left(\frac{\pi}{b}\right)^2\right]^{\frac{1}{2}}, \\ c_j &= -\frac{\beta\Gamma_j}{2} - \left[\left(\frac{\beta\Gamma_j}{2}\right)^2 + \left(\frac{\pi}{b}\right)^2\right]^{\frac{1}{2}}, \\ R_j &= \frac{1 - e^{c_j w}}{e^{a_j w} - e^{c_j w}}. \end{aligned}\right\} \qquad (46)$$

Using (12), the transport streamfunctions are easily recovered. Let,

$$r = \left[\frac{1}{4}\left(1 - \frac{\sigma'}{\sigma} - d_o\right)^2 + d_o\right]^{\frac{1}{2}}, \qquad (47)$$

so that

$$\alpha_2 - \alpha_1 = 2r \quad .$$

Then,

$$\Psi = M \sin(\tfrac{\pi y}{b})\{\alpha_1\Gamma_2[R_2 e^{a_2 x} - 1 + (1 - R_2)e^{c_2 x}]$$
$$- \alpha_2\Gamma_1[R_1 e^{a_1 x} - 1 + (1 - R_1)e^{c_1 x}]\} ,$$
$$\Psi' = M \sin(\tfrac{\pi y}{b})\{\Gamma_1[R_1 e^{a_1 x} - 1 + (1 - R_1)e^{c_1 x}] \qquad (48)$$
$$- \Gamma_2[R_2 e^{a_2 x} - 1 + (1 - R_2)e^{c_2 x}]\} ,$$

with

$$M \equiv \frac{bF}{2\pi\rho r} . \qquad (49)$$

Differentiation of these relations then yields the volume transports:

$$U = - \frac{F}{2\rho r} \cos(\tfrac{\pi y}{b})\{\alpha_1\Gamma_2[R_2 e^{a_2 x} - 1 + (1 - R_2)e^{c_2 x}]$$
$$-\alpha_2\Gamma_1[R_1 e^{a_1 x} - 1 + (1 - R_1)e^{c_1 x}]\} ,$$
$$U' = - \frac{F}{2\rho r} \cos(\tfrac{\pi y}{b})\{\Gamma_1[R_1 e^{a_1 x} - 1 + (1 - R_1)e^{c_1 x}]$$
$$-\Gamma_2[R_2 e^{a_2 x} - 1 + (1 - R_2)e^{c_2 x}]\} ,$$
$$V = M \sin(\tfrac{\pi y}{b})\{\alpha_1\Gamma_2[a_2 R_2 e^{a_2 x} + c_2(1 - R_2)e^{c_2 x}] \qquad (50)$$
$$-\alpha_2\Gamma_1[a_1 R_1 e^{a_1 x} + c_1(1 - R_1)e^{c_1 x}]\} ,$$
$$V' = M \sin(\tfrac{\pi y}{b})\{\Gamma_1[a_1 R_1 e^{a_1 x} + c_1(1 - R_1)e^{c_1 x}]$$
$$-\Gamma_2[a_2 R_2 e^{a_2 x} + c_2(1 - R_2)e^{c_2 x}]\} .$$

Division of these transport components by appropriate local values of layer thicknesses yields the horizontal velocity components u, u', v and v'.

The layer thicknesses, H and H', could be obtained from Ψ and Ψ' using equations (23) and (24). However, an alternate method of obtaining H and H', which requires less algebraic manipulation, has been utilized. First, a double-valued function ω_j is defined by

$$\omega_j = \frac{g'}{2}H^2 + g(H_o + \alpha_j H_o')B \ . \tag{51}$$

It can then be shown (Appendix E) that equation (39) is the necessary and sufficient condition that a finite difference between values of ω_j at two points in the xy-plane can be represented by a line integral which is independent of the path of integration in this plane. In particular,

$$\omega_j = f\Phi_j + \int_{(x_o,y_o)}^{(x,y)} [(T_x + \frac{1}{\Gamma_j}\frac{\partial \Phi_j}{\partial y})dx + (T_y - \frac{1}{\Gamma_j}\frac{\partial \Phi_j}{\partial x} - \beta\Phi_j)dy] + (\omega_j - f\Phi_j)\Big|_{(x_o,y_o)} , \tag{52}$$

where (x_o,y_o) is an arbitrary reference point in the xy-plane.

Then, the two values of ω_j, together with the corresponding α_j, can be substituted into (51) to yield

two algebraic equations in H and B. Using the definition (6) of B, these equations lead (see Appendix E) to the following functional forms for H and H′:

$$H = \{\frac{1}{g'r}[(\alpha_2 + d_o)\omega_1 - (\alpha_1 + d_o)\omega_2]\}^{\frac{1}{2}} ,$$

$$H' = [g(H_o + \alpha_1 H_o')]^{-1}[\omega_1 - \frac{g'}{2}H^2] - (1 - \gamma)H . \tag{53}$$

The following two tasks must be completed before H and H′ are completely determined by the basic parameters physically characterizing the model: (i) the integration of the line integral of (52) for particular functional forms of $\hat{T}$ and Φ_j, and (ii) the estimation of $\omega_j(x_o,y_o)$ in terms of basic parameters and known functions.

Since $\Phi_j = 0$ on the boundaries, the term $\beta\Phi_j$ contributes nothing to the line integral of (52), if one chooses $(x_o,y_o) = (w,0)$ and a path of integration consisting of the line segment $(w,0)$ to (w,y) and the line segment (w,y) to (x,y). Therefore, using the wind stress distribution, (19), equations (52) can be written

$$\omega_j(x,y) = f\Phi_j(x,y) + \omega_j(w,o) - \frac{1}{\Gamma_j}\int_o^y \frac{\partial\Phi_j(w,y)}{\partial x}dy$$

$$+ \frac{F}{\rho}(w-x)\cos(\frac{\pi y}{b}) + \frac{1}{\Gamma_j}\int_w^x \frac{\partial\Phi_j(x,y)}{\partial y}dx .$$

Introducing the functional forms of Φ_j given by equations (45) and integrating, the following lengthy relations can be obtained:

$$\begin{aligned}\omega_j(x,y) = \omega_j(w,o) &+ \frac{F}{\rho}\left(\frac{b}{\pi}\right)^2\left[a_j R_j e^{a_j w} + c_j(1 - R_j)e^{c_j w}\right] \\ &+ \frac{F}{\rho}\left[\left(\frac{1}{a_j} - a_j\frac{b^2}{\pi^2}\right)R_j e^{a_j w} + \left(\frac{1}{c} - c_j\frac{b^2}{\pi^2}\right)(1 - R_j)e^{c_j w}\right]\cos\left(\frac{\pi y}{b}\right) \\ &- \frac{F}{\rho}\left[\frac{\cos\left(\frac{\pi y}{b}\right)}{a_j} + f\frac{b}{\pi}\Gamma_j \sin\left(\frac{\pi y}{b}\right)\right]R_j e^{a_j x} + \frac{bF}{\pi\rho}f\Gamma_j \sin\left(\frac{\pi y}{b}\right) \\ &- \frac{F}{\rho}\left[\frac{\cos\left(\frac{\pi y}{b}\right)}{c_j} + f\frac{b}{\pi}\Gamma_j \sin\left(\frac{\pi y}{b}\right)\right](1 - R_j)e^{c_j x} \quad .\end{aligned} \tag{54}$$

One possible means of obtaining $\omega_j(w,o)$ is to assume values for $H(w,o)$ and $H'(w,o)$ and use the identity (51). However, these reference layer thicknesses cannot be chosen independently of the mean layer thicknesses, since definite relationships between H_o, H_o', $H(w,o)$ and $H'(w,\varrho)$ must exist. Thus, for this approach, these relationships would necessarily have to be exhibited. As an alternative, it was decided to estimate $\omega_j(w,o)$ directly as functions of the mean layer thicknesses.

Let

$$\overline{H^2} \equiv \frac{1}{wb}\int_o^b\int_o^w H^2 dx\, dy, \quad \overline{h^2} \equiv \frac{1}{wb}\int_o^b\int_o^w h^2 dx\, dy \ ,$$

$$\overline{\omega}_1 \equiv \frac{1}{wb}\int_o^b\int_o^w \omega_1 dx\, dy, \quad \overline{\omega}_2 \equiv \frac{1}{wb}\int_o^b\int_o^w \omega_2 dx\, dy \ .$$

Then, equations (54) can be averaged over the horizontal extent of the basin to obtain

$$\bar{\omega}_j = \omega_j(w,o) + W_j \ , \tag{55}$$

where

$$W_j \equiv -\frac{2bfF}{\rho\pi^2 w}\Gamma_j\left[\frac{R_j}{a_j}(e^{a_j w} - 1) + \frac{1 - R_j}{c_j}(e^{c_j w} - 1) - w\right]$$
$$+ \left(\frac{b}{\pi}\right)^2 \frac{F}{\rho}\left[a_j R_j e^{a_j w} + c_j(1 - R_j)e^{c_j w}\right] . \tag{56}$$

The definitions (51) can also be averaged to obtain

$$\bar{\omega}_j = \frac{g'}{2}\overline{H^2} + g(H_o + \alpha_j H_o')[H_o' + (1 - \gamma)H_o] \ . \tag{57}$$

So, combining (55) and (57) yields

$$\omega_j(w,o) = \frac{g'}{2}\overline{H^2} + g(H_o + \alpha_j H_o')[H_o' + (1 - \gamma)H_o] - W_j \ . \tag{58}$$

Now, if $\overline{H^2}$ can be estimated, based on values of H_o and H_o', then equations (53), (54) and (58) serve to specify H and H'. Note that

$$\overline{H^2} = H_o^2 + \overline{h^2} \ .$$

With the approximation $\overline{H^2} \doteq H_o^2$, the reference values of ω_j are given approximately by

$$\omega_j(w,o) \doteq \frac{g'}{2}H_o^2 + g(H_o + \alpha_j H_o')[H_o' + (1 - \gamma)H_o] - W_j \ . \tag{59}$$

For the purposes of this study, the effects on layer thicknesses of neglecting $\overline{h^2}$ in comparison with H_o^2 in estimating $\omega_j(w,o)$ were judged negligible on the basis of preliminary numerical calculations. However, if precise quantitative values of layer thicknesses or velocities were desired, then the complete forms (58), rather than the approximation (59), would necessarily have to be employed.

C. Approximate Forms of the Solutions

1. Approximate interior solutions. Approximate forms of the transport streamfunctions applicable to the interior region can be obtained by proceeding along either of two routes. The complete analytic solutions represented by equations (48) may be simplified for application to that region of the ocean removed by some 200 km from the western boundary. Alternatively, the differential equations (36) and (37) may be approximated for application to the interior region and the resulting forms solved. It can be shown that under the same assumptions, either approach leads to the same results.

From the vertically integrated vorticity equations (36) and (37), the approximate balance equations,

$$\beta\frac{\partial\Psi}{\partial x} = \left(\frac{\partial T_y}{\partial x} - \frac{\partial T_x}{\partial y}\right) ,$$

$$\beta\frac{\partial\Psi'}{\partial x} = \sigma\nabla^2\Psi , \tag{60}$$

can be used to predict Ψ and Ψ' within the interior region. It has been assumed that $d_o << 1$ and $\sigma' << \sigma$ in obtaining the lower layer equation. The upper layer equation represents Sverdrup's (1947) relation for the interior region. For the assumed surface stress given by (19), the upper layer approximation is

$$\frac{\partial\Psi}{\partial x} = -\frac{\pi F}{\rho b\beta}\sin(\frac{\pi y}{b}) .$$

Integration yields

$$\Psi = \frac{\pi F}{\rho b\beta}(w - x)\sin(\frac{\pi y}{b}) , \tag{61}$$

where use has been made of the boundary condition $\Psi(w,y) = 0$. Then, $\nabla^2\Psi$ can be formed and substituted into the second of (60). Integration of the ensuing equation and using the boundary condition $\Psi'(w,y) = 0$ yields

$$\Psi' = \frac{\pi^3\sigma F}{\rho b^3\beta^2}\frac{1}{2}(w - x)^2\sin(\frac{\pi y}{b}) . \tag{62}$$

The approximate forms (61) and (62) for the interior solutions can also be obtained from the complete solutions

(48) under the assumptions that d_o and σ'/σ are much less than unity.

Note that while Ψ increases linearly with the distance from the eastern meridional boundary, Ψ' increases as the second power of this distance. This indicates that the lower layer circulation pattern is more intensified to the west than is the upper layer pattern. Plots of Ψ and Ψ' have been constructed for these approximate interior solutions. The values chosen for b and w are those given in Table 1. The following values were chosen for the other required parameters:

$F = 1$ (dyne cm^{-2})

$\rho = 1$ (gm cm^{-3})

$\beta = 2 \times 10^{-13}$ (sec^{-1} cm^{-1})

$\sigma = .5 \times 10^{-6}$ (sec^{-1}) .

From (61) and (62) it is seen that along the streamsurfaces $\Psi = C$ and $\Psi' = C'$, the distance $(w - x)$ is related to y through the equations

$$(w - x) = \frac{\rho b \beta}{\pi F} \frac{C}{\sin(\frac{\pi y}{b})} ,$$

and

$$(w - x) = \left[\frac{\rho b^3 \beta^2}{\pi^3 \sigma F} \frac{2C'}{\sin(\frac{\pi y}{b})}\right]^{\frac{1}{2}} .$$

In Figures 1 and 2 are displayed the streamlines for Ψ and Ψ' as obtained from these relations.

2. Separation constants. Although the exact expressions were used in performing the numerical calculations, it is desirable to obtain approximate forms for α_j and Γ_j. The approximate forms are essential for examination of the flow directly from the analytic forms of the solution.

Note that, for the physical situation chosen, $d_o \equiv H_o/H_o' \doteq 0.24$. If the ocean were partitioned into a two-layer system based on the mean depth of the seasonal thermocline, a yet smaller value would ensue for d_o. Thus, for practical considerations, it is assumed that $d_o << 1$.

If σ'/σ is also small compared with unity, then relations (40) reduce as a first order approximation using the binomial expansion to

$$\begin{aligned} \alpha_1 &\doteq d_o \, , \\ \alpha_2 &\doteq 1 - \sigma'/\sigma \, , \end{aligned} \tag{63}$$

and from (41)

$$\begin{aligned} \Gamma_1 &\equiv \frac{1}{\sigma(1 - \alpha_1)} \doteq \frac{1}{\sigma} \, , \\ \Gamma_2 &\equiv \frac{1}{\sigma(1 - \alpha_2)} \doteq \frac{1}{\sigma'} \, . \end{aligned} \tag{64}$$

If σ'/σ approaches unity, the above approximations are altered only slightly. In the subsequent discussion, α_j and Γ_j have been approximated by (63) and (64).

3. Characteristic width scales. Examination of the solutions for Ψ and Ψ' will reveal that the parameters $1/c_j$ can be interpreted as width scales of the components comprising the western boundary currents. Approximations to the parameters c_j, as well as a_j, are presented in this section.

For

$$\sigma \leq 10^{-6}(\text{sec}^{-1}), \quad \sigma' \leq \sigma , \tag{65}$$

the approximations (64) yield

$$\Gamma_j \geq 10^{6}(\text{sec}) . \tag{66}$$

Then, since

$$\pi/b \doteq .9 \times 10^{-8}(\text{cm}^{-1}), \quad \beta/2 \doteq 10^{-13}(\text{cm}^{-1}\text{sec}^{-1}) ,$$

it is seen that

$$\left(\frac{2\pi}{b\beta\Gamma_j}\right)^2 \ll 1 .$$

The forms for a_j and c_j given by (46) can then be written

$$a_j = \frac{\beta\Gamma_j}{2}\left[\frac{1}{2}\left(\frac{2\pi}{b\beta\Gamma_j}\right)^2 - \frac{1}{8}\left(\frac{2\pi}{b\beta\Gamma_j}\right)^4 + \frac{1}{16}\left(\frac{2\pi}{b\beta\Gamma_j}\right)^6 - \ldots\right] ,$$

$$c_j = -\frac{\beta\Gamma_j}{2}\left[2 - \frac{1}{2}\left(\frac{2\pi}{b\beta\Gamma_j}\right)^2 + \frac{1}{8}\left(\frac{2\pi}{b\beta\Gamma_j}\right)^4 - \frac{1}{16}\left(\frac{2\pi}{b\beta\Gamma_j}\right)^6 + \ldots\right] . \tag{67}$$

So, as first approximations:

$$a_1 \doteq \frac{\pi^2\sigma}{b^2\beta} , \qquad a_2 \doteq \frac{\pi^2\sigma'}{b^2\beta} ,$$

$$c_1 = -\frac{\beta}{\sigma} , \qquad c_2 \doteq -\frac{\beta}{\sigma'} . \tag{68}$$

Moreover, it is seen now that

$$e^{a_j w} > 1 >> e^{c_j w} , \tag{69}$$

so that R_j are given to very good approximation by

$$R_j \doteq e^{-a_j w} . \tag{70}$$

4. Volume transports in the western boundary region. Approximating R_j by (70), the transport streamfunctions can be written

$$\Psi \doteq M \sin(\tfrac{\pi y}{b})\{\alpha_1\Gamma_2[e^{-a_2(w-x)} - 1 + (1 - e^{-a_2 w})e^{c_2 x}]$$

$$-\alpha_2\Gamma_1[e^{a_1(w-x)} - 1 + (1 - e^{-a_1 w})e^{c_1 x}]\} , \tag{71}$$

$$\Psi' \doteq M \sin(\tfrac{\pi y}{b})\{\Gamma_1[e^{-a_1(w-x)} - 1 + (1 - e^{-a_1 w})e^{c_1 x}]$$

$$-\Gamma_2[e^{-a_2(w-x)} - 1 + (1 - e^{-a_2 w})e^{c_2 x}]\} .$$

The boundary currents predicted by this model can be examined by considering the meridional volume transports for the region $x << w$, say $x \leq 200$ (km). For this region, one can approximate $(w-x)$ by w and, from (71), write the following forms applicable for V and V' near the western boundary:

$$V \doteq [A_o + A_1 e^{c_1 x} + A_2 e^{c_2 x}] \sin(\tfrac{\pi y}{b}) , \tag{72}$$

$$V' \doteq [B_o + B_1 e^{c_1 x} + B_2 e^{c_2 x}] \sin(\tfrac{\pi y}{b}) ,$$

with

$$\left.\begin{aligned}
A_o &\equiv M\alpha_1\Gamma_2 a_2 e^{-a_2 w} - M\alpha_2\Gamma_1 a_1 e^{-a_1 w} , \\
B_o &\equiv M\Gamma_1 e^{-a_1 w} - M\Gamma_2 e^{-a_2 w} , \\
A_1 &\equiv -Mc_1\alpha_2\Gamma_1(1 - e^{-a_1 w}) , \\
B_1 &\equiv Mc_1\Gamma_1(1 - e^{-a_1 w}) , \\
A_2 &\equiv Mc_2\alpha_1\Gamma_1(1 - e^{-a_2 w}) , \\
B_2 &= -Mc_2\Gamma_2(1 - e^{-a_2 w}) .
\end{aligned}\right\} \quad (73)$$

Applying the approximations (63), (64), (68), for α_j, Γ_j, a_j and c_j, respectively, and using

$$e^{-a_j w} \simeq 1 - a_j w ,$$

the constants defined by (73) can be represented by the following forms for order of magnitude considerations:

$$A_o \simeq \left(\frac{\pi}{b}\right)^2 N \frac{\sigma - (1 - d_o)\sigma'}{\beta^2} - \frac{\pi F}{b\rho\beta} ,$$

$$B_o \simeq -\left(\frac{\pi}{b}\right)^2 N \frac{(\sigma - \sigma')}{\beta^2} ,$$

$$A_1 \simeq N \frac{1}{\sigma}\left(1 - \frac{\sigma'}{\sigma}\right) ,$$

$$B_1 \simeq -N \frac{1}{\sigma} , \qquad (74)$$

$$A_2 \simeq N \frac{d_o}{\sigma'} ,$$

$$B_2 \simeq N \frac{1}{\sigma'} .$$

The constant N is defined by

$$N \equiv \frac{\pi F w}{b\rho}\left(1 - \frac{\sigma'}{\sigma} + d_o\right) . \qquad (75)$$

Then, for $\sigma = .5 \times 10^{-6}$ (sec^{-1}) and $\sigma' = \sigma/5$, equations (74) yield the following rough estimates (all with c.g.s. units $\text{cm}^2\ \text{sec}^{-1}$):

$$A_o \simeq -4 \times 10^4 , \qquad B_o \simeq -10^4 ,$$

$$A_1 \simeq 2 \times 10^7 , \qquad B_1 \simeq -2 \times 10^7 , \qquad (76)$$

$$A_2 \simeq 2 \times 10^7 , \qquad B_2 \simeq 9 \times 10^7 .$$

Using these estimates graphs of V and V′ versus x (Fig. 3) were prepared for y = b/2. These graphs were

constructed by the addition of the components comprising V and V' as given by the approximations (72) for the western boundary region.* As seen, the components A_o and B_o do not contribute significantly to the meridional transports within this region.

For the upper layer, the term $A_1 e^{c_1 w}$ decreases the westward intensification as σ increases, i.e., for increased momentum transfer to the lower layer. Since this term determines the width of the major portion of the upper current, $\lambda_1 \equiv |c_1|^{-1}$ is the effective width scale. Therefore, perhaps the best criterion for choosing σ is based on the approximation

$$\sigma \simeq \beta\lambda_1 \ . \tag{77}$$

The term $A_2 e^{c_2 x}$ allows for a feedback of energy to the upper from the lower layer in a region of effective width $\lambda_2 \equiv |c_2|^{-1}$ next to the western boundary. If the coefficient of bottom friction σ' is quite small, then the term $B_2 e^{c_2 w}$ yields a large northward transport within a region of the lower layer quite close to the boundary. In this case, momentum can be transferred upward through the interface resulting in an increase in the

*For comparison see case 4-a of Figure 4. This figure was constructed, with the aid of a computer, using the complete forms for V and V'.

northward transport of the upper layer over this same narrow boundary region. This effect can be observed in the transports for case 4-c of Figure 4, for which $\sigma' = \sigma/10 = 10^{-8}$ (sec^{-1}).

The term $B_1 e^{c_1 x}$ is negative and therefore contributes a southward transport component within the lower layer. Moreover, since the width scale of this component is the same as that for the major northward flow component in the upper layer, it can be considered as a countercurrent situated under the surface boundary flow regime.

D. Numerical Results

The graphic results presented in Figure 5 through 12 are based on computations performed with the aid of a digital computer.* While the results presented represent only a small fraction of the calculations performed for this frictional model, they are illustrative of the information which can be obtained and serve to demonstrate the salient features of the model.

Following Stommel (1948) the value chosen for F, maximum wind stress, was 1. dyne cm^{-2}, which is a reasonable approximation to wind stress computed for the North

*This is an IBM model 7094 computer located on the Texas A&M University campus.

Atlantic region (c.f. Munk, 1950). The values of other parameters selected are those presented in Table I.

Values of streamfunctions and integrated velocities were computed from the forms (71). The parameters α_j, Γ_j and M were calculated from the complete forms (40), (41) and (49); the parameters a_j and c_j were calculated using the first five terms of the series expansions (67). Since $e^{-a_j(w-x)}$ approaches unity as x approaches w, the quantities $(e^{-a_j(w-x)} - 1)$ were expressed in series forms; the quantities $(1 - e^{-a_j w})$ were expressed likewise.

Figures 5 through 8 serve to illustrate the effects on the flow in the western boundary region of the numerical values chosen for the frictional coefficients σ and σ'. The calculations for these figures were performed for $y = b/2$, i.e., $y = 1700$ (km) in the present model.

Figure 5 illustrates the effect of σ on the width of the upper boundary current based on the volume transport. The width of the Gulf Stream is some 40 to 60 km (Stommel, 1965). Thus, case 5-b, with $\sigma = .5 \times 10^{-6}$ (sec^{-1}), for which the effective width scale as given by (77) is 25 km, might illustrate the transport streamfunction for a reasonable choice of σ. Certainly a much smaller value of σ is unacceptable, for in such cases the

average meridional velocity attains unrealistically large values. This is seen from Figure 6 in which are presented, for selected values of σ, curves of the meridional current speed in the upper layer versus distance from the boundary. The maximum current speed within the Gulf Stream is probably not more than 250 to 300 cm sec^{-1}, and the maximum value of the upper layer velocity component v in the model is 288 cm sec^{-1} for $\sigma = .5 \times 10^{-6} (sec^{-1})$.

For a σ value of $.5 \times 10^{-6}$ sec^{-1}, Figure 7 presents the x-dependence of the lower transport streamfunction for selected values of σ', all of which are less than or equal to σ. Certainly, σ' can be selected so as to achieve a relatively strong southward flowing countercurrent which is located under the eastern portion of the upper current. However, this can be achieved only at the expense of predicting a high velocity, northward flowing current at the boundary in the lower layer. This is demonstrated in Figure 8, which pictures v' versus x for three of the sets of σ and σ' values used in Figure 7.

Figures 9 through 12 present transport streamlines for upper and lower layers as computed for $\sigma = .5 \times 10^{-6}$ (sec^{-1}) and $\sigma' = 10^{-7}$ (sec^{-1}). The complete solutions for the interior region appear in Figures 9 and 10. These may be compared with Figures 1 and 2 which were constructed

from the approximate solutions for the interior region. For the lower layer there is no significant difference between the approximate and the complete solutions. In the upper layer, however, it is seen that there is some difference between these solutions in the western section of the interior. The slight westward shift of the eastern side of the largest valued streamlines is of no qualitative importance. This effect would be decreased for smaller values of σ. In Figures 11 and 12 are presented the streamlines for boundary regions of the upper and lower layers, respectively.

C H A P T E R V

THE INERTIAL BOUNDARY CURRENTS

A. Basic Equations

For the development of the inertial boundary currents the stress terms can be dropped from the momentum conservation equations (8) and (9), which can then be written in the following vector forms:

$$f\,\hat{k} \times \hat{q} + \hat{q} \cdot \nabla\hat{q} + g\,\nabla(B + \gamma H) = 0 , \qquad (78)$$

$$f\,\hat{k} \times \hat{q}' + \hat{q}' \cdot \nabla q' + g\,\nabla B = 0 . \qquad (79)$$

If vertical components of local relative vorticity are defined by

$$\xi \equiv \frac{\partial v}{\partial x} - \frac{\partial u}{\partial y} , \qquad \xi' \equiv \frac{\partial v'}{\partial x} - \frac{\partial u'}{\partial y} , \qquad (80)$$

the foregoing relations can be rearranged to yield

$$\nabla J + (f + \xi)\,\hat{k} \times \hat{q} = 0 , \qquad (81)$$

and

$$\nabla J' + (f + \xi')\,\hat{k} \times \hat{q}' = 0 , \qquad (82)$$

where J and J' are mechanical energy densities and are defined by

$$J \equiv \frac{1}{2}q^2 + g(B + \gamma H) \ ,$$

$$J' \equiv \frac{1}{2}(q')^2 + g\ B \ . \tag{83}$$

Forming the dot products of $\hat{q}$ with (81) and $\hat{q}'$ with (82) yields the energy equations

$$\hat{q} \cdot \nabla J = 0 \ ,$$

$$\hat{q}' \cdot \nabla J' = 0 \ . \tag{84}$$

Thus, J and J' are conserved along streamlines. Since the flow is steady and the existence of volume transport streamfunctions, defined by (12), is assured by the continuity relations (10) and (11), the conservation of J and J' can be expressed by

$$\frac{1}{2}(u^2 + v^2) + g\ B + g'\ H = F(\Psi) \ ,$$

$$\frac{1}{2}[(u')^2 + (v')^2] + g\ B = G(\Psi') \ , \tag{85}$$

where, as shown symbolically, the functions F and G depend only on Ψ and Ψ', respectively.

Let $\hat{n}$ be a horizontal unit vector perpendicular to the velocity vector $\hat{q}$ in the upper layer. As viewed from above, $\hat{n}$ is assumed to be directed to the left of $\hat{q}$ so that $\hat{n} \cdot (\hat{k} \times \hat{q}) = q$. Then the dot product of $\hat{n}$ with (81) yields

$$\frac{\partial J}{\partial \Psi} \frac{\partial \Psi}{\partial n} - \frac{f + \xi}{H} \frac{\partial \Psi}{\partial n} = 0 ,$$

where use has been made of the relation

$$\frac{\partial \Psi}{\partial n} = - H q$$

and the fact that J is a function of Ψ only. Finally, except for the case $\frac{\partial \Psi}{\partial n} = 0$, i.e., no motion, it is seen that

$$\frac{f + \xi}{H} = \frac{\partial F}{\partial \Psi} . \tag{86}$$

This statement asserts that the quantity $(f + \xi)/H$, known as the potential vorticity, is conserved along stream-tubes. For the lower layer, the analogous relation,

$$\frac{f + \xi'}{H'} = \frac{\partial G}{\partial \Psi} , \tag{87}$$

holds, provided that the lower layer is in motion. The potential vorticity relations (86) and (87) are the basic differential equations to be solved. The formulation presented relates the potential vorticities to J and J' in a manner such that the "Bernoulli" relations (85) can be used in satisfying the conditions at lateral boundaries of the boundary current regime.

The inertial boundary current regime is assumed to be a narrow meridional strip situated along the western boundary of the basin. Within this current system it is

assumed that the cross-stream variations of the downstream velocity components are much greater than the downstream variations of the cross-stream components, i.e.,

$$\left|\frac{\partial v}{\partial x}\right| \gg \left|\frac{\partial u}{\partial y}\right| , \qquad \left|\frac{\partial v'}{\partial x}\right| \gg \left|\frac{\partial u'}{\partial y}\right| , \tag{88}$$

and that the magnitudes of the downstream velocity components can be approximated by the geostrophic relations, i.e.,

$$\begin{aligned} v &\doteq \frac{1}{f\rho}\frac{\partial p}{\partial x} = \frac{g}{f}\frac{\partial}{\partial x}(B + \gamma H) , \\ v' &\doteq \frac{1}{f\rho'}\frac{\partial p'}{\partial x} = \frac{g}{f}\frac{\partial}{\partial x}(B) . \end{aligned} \tag{89}$$

Within the Gulf Stream these assumptions are well validated by observations (Stommel, 1965).

Under these assumptions the potential vorticity relations applicable to the region can be written

$$\begin{aligned} f + \frac{g}{f}\frac{\partial^2}{\partial x^2}(B + \gamma H) &= H\frac{\partial F}{\partial \Psi} , \\ f + \frac{g}{f}\frac{\partial^2}{\partial x^2}(B) &= H'\frac{\partial G}{\partial \Psi'} . \end{aligned} \tag{90}$$

A flow regime applicable to the interior region of the basin must be assumed in order to specify conditions at the eastern edge of the boundary current region. For this purpose, the interior solution to the frictional

model was used. The southern and western boundaries of the basin are taken as the streamsurface on which both Ψ and Ψ' are zero. This condition is applied with the aid of the Bernoulli equations (85).

The assumptions (88) and (89), together with the equations (85), constitute the formulation used by Charney (1955) in his analysis of an inertial boundary current flowing above a motionless lower layer.

The functions F and G are represented by

$$F(\Psi) = F_o + F_1\Psi + F_2\Psi^2 + \dots ,$$

$$G(\Psi') = G_o + G_1\Psi' + G_2(\Psi')^2 + \dots .$$

Such an assumption certainly seems justificable for the upper layer. Suppose that F were represented by only the first two terms of this expansion. Then, from equation (86) it is seen that the potential vorticity within the interior region must be uniform, an approximation which is borne out by observations within the Central North Atlantic between 10^o and 35^o N. latitude (Stommel, 1965). Moreover, since the streamtubes within the boundary current region emmanate from the interior region and since the potential vorticity is conserved along the streamtubes, the assumption seems justified for the boundary region as well as the interior of the ocean.

It cannot be assumed, however, that the potential vorticity is uniform within each layer of this model. Such an assumption leads to the physically untenable situation for which the thickness of each layer increases linearly with distance from the southern boundary as measured along a meridional section through the interior of the basin. Therefore a second degree approximation for G in terms of Ψ' was adopted.

To allow the same degree of dependence of potential vorticity on the streamfunction within each layer, the following approximations were used:

$$F \doteq F_o + F_1\Psi + F_2\Psi^2 ,$$
$$G \doteq G_o + G_1\Psi' + G_2(\Psi)^2 . \qquad (91)$$

B. Perturbation Equations

The interior solutions for the frictional model predict that in the region just to the east of the boundary currents, say approximately 200 km from the western boundary, the streamfunctions and the layer thicknesses are, to good approximation, functions of latitude only. For the upper layer this prediction is verified observationally. Therefore, the interior layer thicknesses and streamfunctions are assumed to be functions of y only and are denoted by the subscript "I".

Let h, h′ and b denote perturbations of the layer thicknesses and effective overall depth defined by

$$H = H_I(y) + h(x,y) ,$$

$$H' = H_I'(y) + h'(x,y) , \tag{92}$$

$$B = B_I(y) + b(x,y) ,$$

where H_I, H_I' and B_I are the interior values. Thus, h, h′ and b all approach 0 at great distance from the boundary, i.e., as $x \to \infty$. Now, from the definition of the effective depth (6), the useful relations

$$\begin{aligned} B_I &= H_I' + (1 - \gamma) H_I , \\ b &= h' + (1 - \gamma) h \end{aligned} \tag{93}$$

are obtained.

If the current magnitudes are approximated by the northward velocity components within the boundary current region, then use of the geostrophic approximations (89) leads to

$$\frac{\partial \Psi}{\partial x} = Hv \doteq H\frac{g}{f}\frac{\partial (B + \gamma H)}{\partial x} = \frac{g}{f}(H_I + h)\frac{\partial (b + \gamma h)}{\partial x} ,$$

$$\frac{\partial \Psi'}{\partial x} = H'v' \doteq H'\frac{g}{f}\frac{\partial B}{\partial x} = \frac{g}{f}[B_1 + (\gamma - 1)H_I + b + (\gamma - 1)h]\frac{\partial b}{\partial x} .$$

Neglecting terms which are nonlinear in the perturbations and their derivatives and integrating yields

$$\Psi = \Psi_I + \frac{g}{f}H_I(b + \gamma h) \ ,$$

$$\Psi' = \Psi_I' + \frac{g}{f}[B_I + (\gamma - 1)H_I]b \ , \tag{94}$$

where use has been made of the fact that b, $h \to 0$ as $x \to \infty$ in order to determine the constants of integration.

Finally, using the approximate forms (91) for F and G, the potential vorticity relations (90) lead to the following linear differential equations for the perturbations b and h:

$$\frac{g}{f}\frac{\partial^2(b + \gamma h)}{\partial x^2} = (\frac{f}{H_I} + 2\gamma\frac{g}{f}F_2H_I^2)h + (2\frac{g}{f}F_2H_I^2)b \ ,$$

$$\frac{g}{f}\frac{\partial^2 b}{\partial x^2} = (\gamma - 1)\frac{f}{H_I'}h + [\frac{f}{H_I'} + 2\frac{g}{f}G_2(H_I')^2]b \ . \tag{95}$$

Use was made of the following approximations to the potential vorticities for the interior region:

$$\frac{f}{H_I} = F_1 + 2F_2\Psi_I \ ,$$

$$\frac{f}{H_I'} = G_1 + 2G_2\Psi_I' \ . \tag{96}$$

Based on a knowledge of the meridional variations of layer

thicknesses and streamfunctions in the interior, values of F_1, F_2, G_1 and G_2 can be obtained from these relations. The interior solutions then determine all of the parameters for the differential equations (95).

C. Estimates of Potential Vorticity from Frictional Model

In Figure 13 are plots of potential vorticity within the interior region of both the upper and lower layer versus values of the volume transport streamfunction within the appropriate layer. These values were calculated for a meridional section 200 km from the western boundary. The frictional model chosen is physically characterized by the constants given in Table 1 and the friction coefficients $\sigma = .5 \times 10^{-6}$ (sec^{-1}) and $\sigma' = 10^{-7}(sec^{-1})$. The resulting layer thicknesses and transport values, from which this figure was constructed, are presented in Table 2.

By inspection of Figure 13, it is seen that in the lower latitudes of the basin, the approximations (91) fit the interior solutions quite well. It is also seen that such linear approximations fit the data less well as the center of the basin is approached. Nevertheless, in order to make use of the present analysis, it was necessary to choose such linear approximations. The line segments shown in the figure correspond to the case chosen to

TABLE 2

Interior Values of Layer Thicknesses and Streamfunctions as Given by Frictional Model:
$\sigma = .5 \times 10^{-6}(sec^{-1})$, $\sigma' = 10^{-7}(sec^{-1})$.

y (km)	H_I (m)	Ψ_I ($10^6 m^3 sec^{-1}$)	H_I' (m)	Ψ_I' ($10^6 m^3 sec^{-1}$)
0	769.16	0.000	3080.88	0.000
170	787.28	6.434	3062.79	0.720
340	805.86	12.709	3044.26	1.422
510	824.33	18.671	3025.81	2.089
680	842.11	24.174	3008.08	2.704
850	858.61	29.081	2991.60	3.253
1020	873.26	33.272	2976.99	3.722
1190	885.51	36.644	2964.77	4.099
1360	894.82	39.114	2955.47	4.375
1530	900.73	40.621	2949.57	4.544
1700	902.80	41.127	2947.51	4.601

represent the data. Although this case is of primary interest, several other cases with different choices of F_2 and G_2 were investigated in order to examine the effects of such choices on the numerical calculations used in satisfying the western boundary conditions. The values of the coefficients corresponding to the line segments of Figure 13 are presented in Table 3. Comparison of equations (91) with the graph shows that for the upper layer

F_1 corresponds to the f/H_I intercept and $2F_2$ corresponds to the slope; for the lower layer analogous interpretations hold for G_1 and $2G_2$.

TABLE 3

Coefficients Characterizing Interior Potential Vorticity for Inertial Model.

F_1 $(10^{-9}cm^{-1}sec^{-1})$	F_2 $(10^{-24}cm^{-4})$	G_1 $(10^{-10}cm^{-1}sec^{-1})$	G_2 $(10^{-23}cm^{-4})$
0.5450	2.5584	1.3606	1.0089

In the present formulation, the case of an upper layer with uniform potential vorticity would correspond to $F_2 = 0$. Indeed, for the interior solution assumed, $F_2 < G_2$. However, it can be seen by inspection of Figure 13 that, for the assumed interior solution, the fractional variation of f/H_I over the lower half basin is practically as great as the fractional variation of f/H_I'. Therefore, the frictional model does not predict an interior solution for which the upper layer potential vorticity is much more nearly uniform than that for the lower layer. This is not consistent with the observed fact that within the interior the potential vorticity is nearly

uniform for upper layers bounded by isothermal surfaces. This in no way detracts from the value of this analysis for inertial currents, although it might be considered a serious weakness of the present frictional model and is perhaps worthy of future consideration.

D. Formal Solutions

The method of normal modes was again employed in order to obtain solutions for b and h. The required separation constants and new dependent variable are double-valued. The subscript "j" is again used to denote that these constants, and other quantities so subscripted, have two distinct values corresponding to j equal 1 or 2.

Multiplying the first of (95) by the separation constant ϵ_j and adding to the second gives

$$\frac{g}{f}\frac{\partial^2}{\partial x^2}[(1+\epsilon_j)b + \epsilon_j \gamma h] = [(\frac{f}{H_I} + 2\gamma\frac{g}{f}F_2 H_I^2)\epsilon_j + (\gamma-1)\frac{f}{H_I}]h$$
$$+ [2\frac{g}{f}F_2 H_I^2\epsilon_j + \frac{f}{H_I} + 2\frac{g}{f}G_2(H_I')^2]b \ . \tag{97}$$

Then, define the new double-valued variable Θ_j by

$$\Theta_j \equiv (1+\epsilon_j)b + \epsilon_j\gamma h \ , \tag{98}$$

and a second separation constant δ_j by

$$\frac{1}{\delta_j}[(1 + \epsilon_j)b + \epsilon_j \gamma h] = [(\frac{f}{H_I} + 2\gamma\frac{g}{f}F_2 H_I^2)\epsilon_j + (\gamma - 1)\frac{f}{H_I'}]h$$

$$+ [2\frac{g}{f}F_2 H_I^2 \epsilon_j + \frac{f}{H_I'} + 2\frac{g}{f}G_2(H_I')^2]b \ . \tag{99}$$

If ϵ_j and δ_j are chosen such that this last equation holds independently of the values of h and b, the differential equations (97) can be written

$$\frac{\partial^2 \Theta_j}{\partial x^2} - \frac{f}{g\delta_j}\Theta_j = 0 \ . \tag{100}$$

Equating the coefficients of h and b in equations (99) leads to two algebraic equations in δ_j and ϵ_j. Solution of this system yields the following forms:

$$\epsilon_j = -\frac{1}{2}S \pm [(\frac{S}{2})^2 + (1 - \gamma)\frac{H_I}{H_I'}]^{1/2} \ , \tag{101}$$

and

$$\delta_j = \gamma\epsilon_j[\frac{f}{H_I}\epsilon_j + 2\frac{g'}{f}F_2 H_I^2 \epsilon_j - (1 - \gamma)\frac{f}{H_I'}]^{-1} \ , \tag{102}$$

where the upper sign corresponds to the case $j = 1$, and the constant S is defined by

$$S \equiv 1 - \frac{H_I}{H_I'} - \frac{2g'}{f^2}H_I[G_2(H_I')^2 - F_2 H_I^2] \ . \tag{103}$$

The boundary conditions for the inertial regime must be restated in terms of the new dependent variable Θ_j.

By the definitions (92) of the perturbations of layer thicknesses, it is required that $h,\ b \to 0$ as $x \to \infty$. Thus, the conditions on Θ_j at the eastern edge of the region are that

$$\lim_{x \to \infty} \Theta_j = 0 \ . \tag{104}$$

It should be reiterated that, in a broader sense, it is the interior flow regime specified which serves as the eastern boundary condition for the present inertial problem; the constants F_2, G_2, F_1, etc. and the functions $H_I(y)$, $H_I'(y)$, etc. are, after all, based on the interior solutions.

The southern and western boundaries of the basin are assumed to constitute the streamsurface on which $\Psi = \Psi' = 0$. The Bernoulli relations (85) can be utilized to obtain an expression, valid along this streamsurface, for Θ_j in terms of independently determined parameters. Multiplication of the upper layer Bernoulli equation by ϵ_j and adding to the lower layer equation yields

$$\Theta_j(x,y) = \frac{\epsilon_j}{g}F_o + \frac{1}{g}G_o - \frac{1}{2g}[\epsilon_j q^2 + (q')^2]$$

$$- [(1 + \epsilon_j)B_I + \epsilon_j \gamma H_I] \ ,$$

valid along the bounding streamsurface. Evaluating on the western meridional boundary yields

$$\Theta_j(0,y) = \frac{\epsilon_j}{g}F_o + \frac{1}{g}G_o - \frac{1}{2g}[\epsilon_j q_o^2 + (q_o')^2] \tag{105}$$
$$- [(1 + \epsilon_j)B_I(y) + \epsilon_j \gamma H_I(y) ,$$

where q_o and q_o' denote magnitudes of the upper and lower fluid velocities at $x = 0$. Evaluating the same equation within the interior region on the $y = 0$ streamsurface, the interior boundary condition (104) can be used to obtain

$$0 = \frac{\epsilon_j}{g}F_o + \frac{1}{g}G_o - \frac{1}{2g}[\epsilon_j q_I^2 + (q_I')^2] \tag{106}$$
$$- (1 + \epsilon_j)B_I(0) + \epsilon_j \gamma H_I(0) .$$

Now, the current speeds should attain their maximum values along the western boundary, so that q_I^2 and $(q_I')^2$ can be neglected in comparison with q_o^2 and $(q_o')^2$, respectively. With this assumption, equation (106) can be subtracted from equation (105) to obtain the following boundary conditions for Θ_j:

$$\Theta_j(0,y) = - \frac{1}{2g}[\epsilon_j q_o^2 + (q_o')^2] - (1 + \epsilon_j)[B_I(y) - B_I(0)] \tag{107}$$
$$- \epsilon_j \gamma [H_I(y) - H_I(0)] .$$

In order to apply the western boundary conditions it is necessary to employ the geostrophic approximations (89) for the purpose of relating q_o and q_o' to $\Theta_j(0,y)$. First, note that the definitions (98) of Θ_j imply that

$$h = \frac{(1 + \epsilon_2)\Theta_1 - (1 + \epsilon_1)\Theta_2}{\gamma(\epsilon_1 - \epsilon_2)}$$
$$b = \frac{\epsilon_1\Theta_2 - \epsilon_2\Theta_1}{(\epsilon_1 - \epsilon_2)} \quad , \tag{108}$$

and, consequently,

$$h' = \frac{(1 + \epsilon_1 - \gamma)\Theta_2 - (1 + \epsilon_2 - \gamma)\Theta_1}{\gamma(\epsilon_1 - \epsilon_2)}$$
$$b + \gamma h = \frac{\Theta_1 - \Theta_2}{(\epsilon_1 - \epsilon_2)} \quad . \tag{109}$$

Then, since the flow at $z = 0$ is entirely meridional, the geostrophic relations yield

$$q_o \doteq \frac{g}{f(\epsilon_1 - \epsilon_2)} \left[\frac{\partial\Theta_1}{\partial x} - \frac{\partial\Theta_2}{\partial x}\right]\Bigg|_{x = 0} \quad ,$$
$$q_o' \doteq \frac{g}{f(\epsilon_1 - \epsilon_2)} \left[\epsilon_1 \frac{\partial\Theta_2}{\partial x} - \epsilon_2 \frac{\partial\Theta_1}{\partial x}\right]\Bigg|_{x = 0} \tag{110}$$

Equations (107) and (110) together constitute the boundary conditions at the western edge of the basin.

Returning to the differential equation (100), it is

seen that solutions to this equation, which also satisfy conditions (104), are

$$\Theta_j = E_j e^{-m_j x} , \tag{111}$$

with

$$m_j = \sqrt{\frac{f}{g\delta_j}} . \tag{112}$$

The solutions for Θ_j given by (111) represent the complete solution for the perturbations provided that E_1 and E_2 are chosen such as to satisfy (107) and (110). This requires that E_1 and E_2 be solutions for the following system of four equations:

$$\begin{aligned} q_o &= \frac{g}{f(\epsilon_1 - \epsilon_2)}[m_2 E_2 - m_1 E_1] , \\ q_o' &= \frac{g}{f(\epsilon_1 - \epsilon_2)}[\epsilon_2 m_1 E_1 - \epsilon_1 m_2 E_2] , \end{aligned} \tag{113}$$

and

$$\begin{aligned} E_j = &- \frac{1}{2g}[\epsilon_j q_o^2 + (q_o')^2] - (1 + \epsilon_j)[B_I(y) - B_I(0)] \\ &- \epsilon_j \gamma [H_I(y) - H_I(0)] . \end{aligned} \tag{114}$$

If $H_I(y)$ and $H_I'(y)$ are known, e.g., from the frictional model, the layer thicknesses H and H′ can be obtained from the solution (111) by using the definitions (92) and relations (108) and (109). The predicted thicknesses are:

$$H = H_I + \frac{1}{\gamma(\epsilon_1 - \epsilon_2)}[(1 + \epsilon_2)E_1 e^{-m_1 x} - (1 + \epsilon_1)E_2 e^{-m_2 x}] ,$$

$$H' = H_I' + \frac{1}{\gamma(\epsilon_1 - \epsilon_2)}[(1 + \epsilon_1 - \gamma)E_2 e^{-m_2 x} \tag{115}$$

$$- (1 + \epsilon_2 - \gamma)E_1 e^{-m_1 x}] .$$

The volume transport streamfunctions can be determined from equations (94), if $\Psi_1(y)$ and $\Psi_I'(y)$ are presumed known. Of course it is only necessary to select either H_I and H_I' or Ψ_I and Ψ_I', since these pairs are related by the choice of coefficients F_1, F_2, G_1 and G_2. Further mention of this point is reserved for the following section.

Elimination of q_o and q_o' from equations (113) and (114) results in a system of two quadratic equations in the two unknowns E_1 and E_2. Elimination of either of these constants leads to a quartic equation in the other. Solutions must therefore be sought by numerical procedures. This same general problem arose in Blanford's (1964) analysis of inertial currents in a multi-layer system. Blanford, dealing with non-dimensionalized variables rather than perturbations, expresses his analogous system in terms of the layer thicknesses at the western boundary. From this system a quartic equation in upper

thickness was obtained, and the roots were investigated numerically. For his model of two moving layers of uniform potential vorticity overlying a resting layer, four real roots were found. However, for only one root did both layer thicknesses and both upper and lower meridional velocities have positive values over the range of y for which the model was applicable. The other three roots represented, as expected, physically unrealistic solutions.

In the present analysis, a quartic polynomial equation can be obtained for either q_o or q_o'. The correct quartic in q_o is derived in Appendix F. This equation has not been investigated for the characteristics of its roots as a function of latitude. In fact, no attempt was made to solve this equation directly. Instead it was decided to solve the system consisting of (113) and (114) numerically, by successive approximations. Physically reasonable values were selected for q_o and q_o'; values of E_1 and E_2 were computed from (114) using these values; then, new estimates of q_o and q_o' were obtained from (113); etc. For the cases investigated, it was found that this procedure produced fairly rapid convergence, in less than 30 iterations, provided that: (i) reasonable initial estimates of q_o and q_o' were selected and (ii) the technique was usuable at all. With regard to the first restriction, the initial values of q_o and q_o'

were varied independently over the range -150 to 300 cm sec^{-1}. In every case for which convergence was obtained, i.e., for a range of q_o and q_o' including the final values, identical final values were obtained. The second restriction must be added because it was found that for certain choices of F_2, G_2, $H_I(y)$ and $H_I'(y)$ the technique would not yield a sequence of q_o' values which converged as middle latitudes were approached. Such a case will be presented in the following section. The reason for such "break-downs" in the technique have not yet been investigated.

It was first suspected that the model included some basic error. However, it was found that a somewhat different method of analysis, a variation on the same theme, would produce results which are qualitatively, and to good approximation for the upper layer quantitatively, the same. Moreover, it was found that the cases for which the analysis of this section failed at mid-latitudes could easily be extended to such latitudes using the alternate approach.

This alternate analysis, presented in Appendix G, differs from that presented in Sections B and D of Chapter V principally in that: (i) equations are developed for perturbations of the transport streamfunctions Ψ and Ψ' rather than the layer thicknesses H and H' and (ii) rather than applying the nonlinear Bernoulli relations

along the streamsurfaces $\Psi = \Psi' = 0$, the western meridional boundary conditions are linearized in a manner consistant with the linearization of the perturbation equations. This procedure leads to a completely analytic solution to the perturbation problem i.e., the necessity of employing numerical techniques in satisfying the western boundary conditions is eliminated.

The striking similarity between solutions obtained by the two methods is unexplained. It would seem that the choice of boundary conditions to be applied at the western boundary should have a rather noticable effect on the results of these perturbation models. Such does not appear to be the case, however.

E. Numerical Results

It should be stated explicitly that, pending further study, the results for this inertial model must be considered as preliminary. Further comments on this point are presented in Chapter VI. Only a limited number of numerical calculations have been performed to date. These results do, however, enable one to compare this inertial flow regime with the flow predicted by the frictional model for the same region.

This section is devoted to a discussion of some of these results as presented in Figures 14 through 19.

Basically, all of the calculations which have been performed assume the interior solutions presented in Figures 9 and 10. The boundary currents are pieced to the interior solutions 200 km from the western meridional boundary. In this section the values of layer thicknesses and volume transport streamfunctions presented in Table 2 are assumed.

In order to obtain numerical results, first, values of F_1, F_2, G_1 and G_2 are selected, based on the interior flow as explained in section C of this chapter. Then, if y-dependent forms of the interior layer thicknesses, H_I and H_I', are specified, the analysis employing layer thickness perturbations can be used to obtain the H, H', Ψ and Ψ' fields from the forms given in the preceding section. Of course, $H_I(y)$ and $H_I'(y)$ cannot be specified arbitrarily, or even independently, because within the interior region the flow must reasonably well satisfy the potential vorticity relations (96) and must be in approximate geostrophic balance.

It would seem, therefore, that the best choices for H_I and H_I' would be just the values given by the interior solution, e.g., those values presented in Table 2 in the present analysis. However, if these values are chosen, an artificial stationary wave form is introduced into the solution obtained by the analysis employing layer

thickness perturbations. It was found that this problem can be circumvented by either of two approaches: (i) employ the analysis of Section D using simple functional forms of $H_I(y)$ and $H_I'(y)$ which approximately fit the data of Table 2, or (ii) employ the analysis of Appendix G, using either simple functional forms of $H_I(y)$ and $H_I'(y)$ or exact values given in Table 2.

If the analysis employing streamfunction perturbations, i.e., that of Appendix G, is used, it is only necessary to solve the interior potential vorticity equations (96) for Ψ_I and Ψ_I' in order to obtain values of such parameters from interior values of layer thicknesses.

Numerical results have been obtained from the analysis employing thickness perturbations only for linear forms of $H_I(y)$ and $H_I'(y)$, although quadratics in y would better fit the tabulated layer thicknesses. Two distinct pairs (H_I, H_I') of linear forms have been investigated. The one corresponding best to the choices for F_1, F_2, G_1 and G_2 exactly matches the layer thicknesses at $y = 0$ and at $y = 1190$ (km). The other choice matches the layer thicknesses at $y = 0$ and at $y = 1020$ (km). The latter gives a slightly better fit to the tabulated data at lower latitudes, the latitudinal derivatives of layer thicknesses being larger in this case than in the former case.

In Figure 14 are shown the values of q_o and q_o' obtained from the analysis employing thickness perturbations. The western boundary conditions were applied numerically with the aid of an IBM 7094 computer.* Five cases are presented. Case 14-a is for the smaller values of derivatives $\frac{\partial H_I}{\partial y}$ and $\frac{\partial H_I'}{\partial y}$; cases 14-b through 14-e are for the larger valued latitudinal derivatives of layer thicknesses. In Table 4 are presented the coefficients F_2 and G_2 used in each of the five cases. In every case the values of F_1 and G_1 used were those of Table 3.

TABLE 4

Values of F_2 and G_2 Used in Cases Presented in Figure 14.

Case	F_2 $(10^{-24}cm^{-4})$	G_2 $(10^{-23}cm^{-4})$
14-a	2.5584	1.0089
14-b	1.0000	1.0089
14-c	2.0000	0.8000
14-d	2.5584	1.0089
14-e	2.5584	1.5000

*All numerical computations presented in this chapter were performed with the aid of the digital computer located on the Texas A&M University campus.

It was found that the numerical technique used in obtaining q_o and q_o' could not be used for y greater than approximately 1000 km in the case 14-a, although the derivatives $\frac{\partial H_I}{\partial y}$ and $\frac{\partial H_I'}{\partial y}$ are the only quantities whose values differ between cases 14-a and 14-d. These differences apparently affect the results a great deal, however, for not only does the case 14-d converge over the entire range of y, but also the lower layer meridional velocities are considerably smaller in case 14-d than in 14-a.

Intercomparison of data presented in Figure 14 for cases 14-b through 14-d, which are all based on the same values of $H_I(y)$ and $H_I'(y)$, enables one to ascertain the role played by F_2 and/or G_2 in determining the velocities within the boundary region. Comparing cases 14-b with 14-d, it is seen that the latitudinal rate of change of q_o, and thus of the relative vorticity in the upper layer, is greater for larger values of F_2. Moreover, the value of F_2 seems to have only very slight effect on the lower layer velocity field. Likewise, an increase in the value of G_2 appears to result in an increase of $\frac{\partial q_o'}{\partial y}$ but in no significant effect in the upper layer velocity field. This is seen by comparing case 14-e with 14-d.

Data for case 14-e was not presented for y greater

than 1020 km, since the numerical technique used to obtain E_1, E_2, q_o and q_o' failed to give results for larger y values. From available tests, whether or not this iterative numerical procedure will produce results seems to depend on the values of $H_I(y)$ and $H_I'(y)$ selected as well as the value of G_2. A real understanding of these dependencies must await the detailed investigation of the roots of the quartic polynomial equation (F-9) in q_o presented in Appendix F.

In order to obtain the solutions for the western boundary region presented in Figures 15 through 19, it was decided to utilize the analysis of Appendix G. In Figure 15, are presented the y-dependencies of q_o and q_o' in two cases for which complete numerical calculations were performed. The first, referred to as case 15-a, is for the same values of F_1, F_2, G_1, G_2 and linear forms of $H_I(y)$ and $H_I'(y)$ as case 14-a. As evidenced by comparison of upper layer thicknesses and streamfunctions and of upper layer velocities at the coast, the two analyses predict amazingly similar results for that area of the upper layer in which solutions were obtained for 14-a. For the lower layer, however, the meridional velocities seem much larger for the analysis based on perturbations of layer thicknesses. This difference may or may not be as significant as it appears from comparison of Figure 14

with Figure 15; in those cases examined for which the thickness perturbation analysis failed at mid-latitudes, a large y-increase in q_o' values was predicted for latitudes somewhat less than the latitudes of complete failure.

Figures 16 and 17 give the transport streamfunction fields, for upper and lower layers respectively, given for case 15-a by the analysis of Appendix G. It is seen that these solutions for the lower western boundary region do not exactly match the interior solutions presented in Figures 9 and 10. Some of the discrepancy is due to the linear forms assumed for $H_I(y)$ and $H_I'(y)$. However, even if the layer thicknesses match the interior solution exactly, as in the case 15-b, for which Ψ and Ψ' fields are presented in Figure 18, these differences still exist. The reason lies in the fact that the potential vorticities predicted for the interior region of the two layers by the frictional model are not simply linearly dependent on the streamfunctions. Therefore, even if exact values of H_I and H_I' are used, the assumption of such linear relations, equations (96), introduces differences between the interior streamfunctions of the frictional model and those utilized for the inertial boundary current analysis.

In addition to Ψ, the field of $(B + \gamma H)$ is represented in Figure 16. Since $(B + \gamma H)$ is equal to $(H' + H)$, this figure represents the elevation of the sea

surface relative to the sea bed. By comparing the $(B + \gamma H)$ field with the Ψ field, it is seen that the flow is toward smaller values of total depth. The B field corresponding to Ψ' was not presented in Figure 17, because isolines of these two quantities are not inclined at a large enough angle to permit them to be clearly discerned for the scale used.

In Figure 18 are presented the Ψ and Ψ' fields corresponding to case 15-b. These may be compared with data for case 15-a, presented in Figures 16 and 17. For this analysis the interior layer thicknesses tabulated in Table 2 were used. It is seen that the fit between the interior transport fields (Figs. 9 and 10) and the transport fields given for the boundary region by this case is not quite as good as is the fit between the interior transport fields and the transport fields given for the boundary region by case 15-a. However, since case 15-b is based on the exact values of layer thicknesses presented in Table 2 rather than linear functional forms, it was decided to present (Fig. 19) the horizontal distribution of meridional velocity components, v and v', as given for this case by equations (G-13).

C H A P T E R V I

DISCUSSION AND SUGGESTED FURTHER STUDIES

The principal, immediate value of Model I is that a first order approximation to the three-dimensional distribution of horizontal velocities is predicted without the necessity of requiring that vertical velocities be zero. This model therefore occupies a position intermediate between that of Stommel (1948) and the steady, wind-driven frictional model for a homogeneous ocean devised by Hassan (1964). As in the formulation of Model I, Hassan neglected nonlinear accelerations and lateral friction. However, assuming zero velocity at the sea bed, he was able to obtain series solutions for the three dimensional distribution of horizontal velocity under the provision that the vertical velocity vanish everywhere. It is felt by some, e.g., Robinson (1964), that this suppression of vertical motion is too high a price to pay in order to obtain solutions, and detracts very much from any conclusions which may be drawn from the model.

The present model, however, manifests some of the same major features predicted by the Hassan model. Hassan (1964) found that "for horizontal cross sections in any one cell, a line that passes through similar points of different cross sections will, whenever possible, incline

westward with depth." In addition, Hassan predicted that "a countercurrent will be encountered under every current." Based on the two-layer Model I, it is seen that: with increasing depth the relative westward intensification increases and a countercurrent exists beneath the western boundary current of the upper layer. One point of difference is that, within the intermediate and deep waters, Hassan's model gives several cells at a given fixed depth, but only one such cell is predicted within each layer of Model I. It seems likely that with the addition of more layers, Model I would correspond even more closely to that of Hassan.

It is interesting to note that within the lower boundary regime, regions of northward and southward velocities are separated by a distance of only a few kilometers. The direction of movement of a drogue dropped into such a flow regime would therefore depend critically upon the exact location at which it was introduced. Indeed, Swallow floats placed in deep water under the outer edge of the Gulf Stream from practically the same position have been observed to travel to the north as well as to the south.

Model I suffers from a number of shortcomings. As with all frictional models, which utilize eddy coefficients in order to express the turbulent exchange of

momentum, certain frictional coefficients must be selected in a somewhat arbitrary manner. Since lateral friction has been neglected, no countercurrent is predicted offshore from the Gulf Stream in the upper layer. In addition, non-zero velocities are predicted at the western boundary, and this boundary must therefore be considered to be the position of the core of the boundary current rather than the coast. This objection could probably be removed by providing for a boundary regime with lateral friction between the present western boundary and the coast. However, the result, of being able to predict currents to the actual coast, does not seem worth the effort required, unless the model could first be extended to include non-uniform bathymetry, since it would still be quite unrealistic to approximate the entire shelf region by depths of some 4000 m.

In fact, the first attempt at improving the present model should be an extension to include non-uniform undisturbed depth. Conceivably this would not only provide for a more realistic representation of the shelf region, but would also provide crude machinery for examining steady frictional flow in the region of the mid-Atlantic ridge system.

As based on the ocean circulation presently inferred to exist, a very real objection is that in the present models the steady velocities at great depth are not zero,

and not even necessarily very small. The addition of more layers, in particular of a resting bottom layer, would remove this liability, of course.

Model I could be formulated for a more detailed, and realistic, distribution of wind stress. Undoubtedly, this would not be worth the effort, since the resulting solutions can be envisioned from the results of the present study.

Considering the inertial model, it would seem that the greatest benefit resulting from this study is the demonstration that physically plausible results for multiple moving layers with non-uniform potential vorticity can be obtained. Moreover, it is shown that this can be done without having to resort to the numerical solution of differential equations. An almost obvious extension of this work would be the formulation for a stratified system of two moving layers overlying a resting layer and the subsequent comparison of resulting solutions with those obtained numerically for this case by Blanford (1964).

However, before any extensions of Model II are attempted, further investigation of the present solution is imperative. During the course of this study, the inertial model was considered only in the hope of providing an alternate solution for the formation region of western boundary currents. In a sense, therefore, it was considered

only for the sake of completeness. Without a knowledge of Blanford's work, the first model formulated was for a system of two moving layers with uniform potential vorticity but with non-uniform depth. Mathematical solutions were obtained before it was discovered, on the basis of numerical calculations, that the assumption of uniform potential vorticity in every layer of a layered model is most unrealistic. Such a model predicts that the layer thicknesses all increase linearly as a function of northward coordinate as evaluated along a meridional section within the oceanic interior. After being alerted by Dr. A. R. Robinson (personal communication) to the work of Blanford (1964), several other inertial models were formulated, finally resulting in Model II. This model has not yet received sufficient attention to warrant firm conclusions being drawn therefrom.

Immediate further work should include detailed investigation of: (i) the "failure" of the analysis employing layer thickness perturbations for certain values of the characterizing parameters; (ii) the roots of the quartic polynomial equation (F-9) in q_o; (iii) results predicted when observed data are used to approximate the interior solution; and (iv) the significance of the separate components of transport streamfunctions given by the analysis.

Item (iii) would presumably result in a more realistic description of the lower Gulf Stream system. In the same interest, it should be feasible to allow for the Florida Current's meridional transport along the western boundary within the framework of the present model. This might be done by removing the southern boundary for a distance of some 100 km from the western boundary and specifying that along the remainder of this boundary the transport streamfunction have the value observed for the transport of the Florida Current. However a difficulty would arise in realitically assigning a corresponding value to the lower layer streamfunction along the streamsurface formed by the southern boundary.

All presently reported models for the formation and growth region of inertial currents are devised for a horizontal sea bed. If Model II could be reformulated to provide for a non-horizontal sea bed, it might prove to be of great value in investigating the bathymetric control exercised on inertial boundary currents.

REFERENCES

Blanford, R. R.

1964. Inertial stratified flow in the Gulf Stream. California Institute of Technology Doctoral Thesis. 152 pp.

1965. Inertial flow in the Gulf Stream. Tellus, 17: 69-76.

Bryan, Kirk

1963. A numerical investigation of a nonlinear model of a wind-driven ocean. Jour. Atm. Sci., 20: 594-606.

Charney, Jule G.

1955. The Gulf Stream as an inertial boundary layer. Proc. Nat. Acad. Sci. Wash., 41: 731-740.

Defant, Albert

1961. Physical Oceanography, Vol. 1. Pergamon Press, London. 729 pp.

Duxbury, A. C.

1963. An investigation of stable waves along a velocity shear boundary in a two-layer sea with a geostrophic flow regime. Jour. Mar. Res., 21: 246-283.

Fofonoff, N. P.

1962. Dynamics of ocean currents. In The Sea. M. N. Hill, editor. Vol. 1, pp. 323-395. Interscience Publishers, N. Y.

Haltiner, G. J., and F. L. Martin

1957. Dynamical and Physical Meteorology. McGraw-Hill Book Co., Inc., N. Y. 470 pp.

Hassan, E. S. M.

1964. The general oceanic circulation; some computations, a working hypothesis, and proposed tests. Jour. Mar. Res., 22: 152-168.

Iselin, C. O'D.

1936. A study of the circulation of the western North Atlantic. Pap. Phys. Oceanogr. and Meteor., Vol. 4, No. 4. 101 pp.

Morgan, G. W.

1956. On the wind-driven ocean circulation. Tellus, 8: 301-320.

Munk, W. H.

1950. On the wind-driven ocean circulation. Jour. Meteor., 7: 79-93.

Robinson, A. R.

1964. On the arbitrary suppression of vertical motion in wind-driven models. Jour. Mar. Res., 22: 168-174.

Schlichting, Herman

1960. Boundary Layer Theory. 4th ed. McGraw-Hill Book Co., Inc., N. Y. 647 pp.

Stewart, R. W.

1965. The influence of friction on the inertial models of oceanic circulation. In Studies in Oceanography. Kozo Yoshida, editor. pp. 3-9. Univ. of Washington Press, Seattle.

Stommel, H.

1948. The westward intensification of wind-driven ocean currents. Trans. Amer. Geophys. Union, 29: 202-206.

1957. A survey of ocean current theory. Deep-Sea Res., 4: 149-184.

Stommel, H.

1965. The Gulf Stream. 2nd ed. Univ. of California Press, Berkeley. 248 pp.

Stommel, H., and A. B. Arons

1960. On the abyssal circulation of the world ocean--II; An idealized model of the circulation pattern and amplitude in oceanic basins. Deep-Sea Res., 6: 217-233.

Stommel, H., and Jaqueline Webster

1962. Some properties of thermocline equations in a subtropical gyre. Jour. Mar. Res., 20: 42-56.

Sverdrup, H. U.

1947. Wind-driven currents in a baroclinic ocean: with application to the equatorial currents of the Eastern Pacific. Proc. Nat. Acad. Sci. Wash., 33: 318-326.

Sverdrup, H. U., M. W. Johnson and R. H. Fleming

1942. The Oceans. Prentice-Hall, Inc., N. Y. 1087 pp.

Veronis, G., and H. Stommel

1956. The action of variable wind stresses on a stratified ocean. Jour. Mar. Res., 15: 43-75.

Veronis, George

1963a. On the approximations involved in transforming the equations of motion from a spherical surface to the β-plane. I. Barotropic systems. Jour. Mar. Res., 21: 110-124.

1963b. On the approximations involved in transforming the equations of motion from a spherical surface to the β-plane. II. Baroclinic systems. Jour. Mar. Res., 21: 199-204.

Wyrtki, Klaus

1961. The thermohaline circulation in relation to the general circulation in the oceans. Deep-Sea Res., 8: 39-64.

A P P E N D I X A

THE CRITERIA FOR NON-NEGATIVE ENERGY DISSIPATION

For d_o, H and H' positive, it is desired to find the restrictions on σ and σ' for which

$$\sigma H q^2 - \sigma H(1 - d_o H'/H)\hat{q} \cdot \hat{q}' + (\sigma d_o + \sigma')H'(q')^2 \geq 0 . \qquad \text{(A-1)}$$

This sum can be written

$$\sigma H(u^2 + v^2) - \sigma H(1 + d_o H'/H)(uu' + vv') + (\sigma d_o + \sigma')H'[(u')^2 + (v')^2] .$$

Then, defining constants B_1, B_2 and B_3 by the identity,

$$\sigma H u^2 - \sigma H(1 - d_o H'/H)uu' + (\sigma d_o + \sigma')H'(u')^2 \equiv B_1 u^2 + B_2(u - B_3 u')^2 , \qquad \text{(A-2)}$$

it is seen that the sum will be non-negative provided that B_1 and B_2 are non-negative, since a similar identity in v and v' can be written. Expanding the right hand side of (A-2) and equating the coefficients of u^2, uu' and

$(u')^2$, the following set of algebraic equations are obtained:

$$B_1 + B_2 = \sigma H \ ,$$

$$2B_2B_3 = \sigma H(1 + d_o H'/H) \ ,$$

$$B_2B_3^2 = (\sigma d_o + \sigma')H' \ .$$

This system has the solutions:

$$B_1 = \frac{4\sigma\sigma' HH' - \sigma^2(H - d_o H')^2}{4(\sigma d_o + \sigma')} \ ,$$

$$B_2 = \frac{(\sigma H)^2(1 - d_o H'/H)^2}{4(\sigma d_o + \sigma')H'} \ ,$$

$$B_3 = \frac{2(\sigma d_o + \sigma')H'}{\sigma H(1 + d_o H'/H)} \ .$$

Therefore, B_2 is non-negative, provided only that

$$\sigma d_o + \sigma' > 0 \ . \qquad \text{(A-3)}$$

However, if B_1 is to be non-negative, it is required also that

$$4\sigma\sigma' HH' - \sigma^2(H - d_o H')^2 \geq 0 \ . \qquad \text{(A-4)}$$

Combining the requirements (A-3) and (A-4), it is

seen that the restrictions on σ and σ' sufficient to insure condition (A-1) are that

$$\sigma > 0 \quad \text{and} \quad \frac{\sigma'}{\sigma} \geq \frac{(H - d_o H')^2}{HH'} \quad . \tag{A-5}$$

A P P E N D I X B

ESTIMATION OF σ BASED ON REPRESENTATIVE BOUNDARY CURRENT REGIME AND INTERIOR WIND STRESS

The following relation for σ results from horizontal integration of the vertically integrated momentum equations for the frictional model:

$$\sigma = \frac{\int_o^b \int_o^w \hat{Q} \cdot \hat{T} \, dx \, dy}{\int_o^b \int_o^w (Q^2 - d_o \hat{Q} \cdot \hat{Q}') \, dx \, dy} \equiv \frac{I}{II} , \qquad \text{(B-1)}$$

where I and II denote the integrals of the numerator and denominator, respectively.

Assuming that U' and V' are not larger than U and V, respectively, one can approximate

$$II \doteq \int_o^b \int_o^w Q^2 \, dx \, dy .$$

Let λ denote the width of the western boundary current; let T_o denote the representative eastward or westward wind stress over the northern or southern half of the interior region, respectively; and let Q_b and Q_I denote representative transports per unit width northward within the boundary current and eastward or westward within the interior region, respectively. Then,

$$II \simeq Q_b{}^2 \lambda b + Q_I{}^2 (w - \lambda) b \ , \qquad \text{(B-2)}$$

and

$$I \simeq Q_I T_o w b \ . \qquad \text{(B-3)}$$

Now, continuity considerations require the approximation

$$Q_b \lambda \doteq Q_I \frac{b}{2} \ .$$

Introducing this relation into the approximations (B-2) and (B-3):

$$II \simeq [b + 4(w - \lambda)\lambda/b] \lambda Q_b{}^2 \simeq (b + 4W\lambda/b) \lambda Q_b{}^2 \ ,$$

$$I \simeq 2 T_o w \lambda Q_b \ .$$

Therefore, from (A-1)

$$\sigma \simeq \frac{2 T_o w}{(b + 4w\lambda/b) Q_b} \ .$$

For the purpose of estimating σ, take:

$$\lambda \leq 200 \ (\text{km})$$

$$T_o \simeq .5 \ (\text{cm}^2 \text{sec}^{-2}) \ ,$$

$$Q_b \simeq 3 \times 10^6 (\text{cm}^2 \text{sec}^{-1}) * \ ,$$

---

*This value of Q_b yields $\lambda Q_b = 60 \times 10^{12} (\text{cm}^3 \text{sec}^{-1})$ as the transport in the upper layer boundary current.

and the values presented in Table 1 for other parameters. A rough estimate demonstrates that $4w\lambda/b$ is at most of the same order as b. Therefore, σ has been estimated using

$$\sigma \sim \frac{2T_o w}{bQ_b} \quad ,$$

which yields

$$\sigma \sim 10^{-6} \ (\text{sec}^{-1}) \ .$$

This estimate should be divided by a factor the value of which lies somewhere between 1 and 2 in order to compensate for neglecting the term $Q_b 4w\lambda/b$ in the denominator.

APPENDIX C

ESTIMATION OF σ BASED ON ENERGY DISSIPATION WITH EKMAN TYPE FRICTIONAL BOUNDARY LAYERS

Consider a free system of two layers of uniform densities with pressure gradients in both layers. Assume that there exist frictional boundary layers ① and ② above and below the interlayer interface having thicknesses small when compared with the upper and lower fluid layer thicknesses, H and H′. Also assume a bottom frictional boundary layer ③ with thickness much less than H′. Complex algebra is employed in this appendix, the horizontal velocities within the upper and lower layers being denoted by

$$q = u + i\,v \quad ,$$

and

$$q' = u' + i\,v' \quad ,$$

respectively. The shear stress on a horizontal plane in the upper, lower layer is assumed to be of the form

$$\rho K\frac{\partial q}{\partial z} \quad , \qquad \rho' K'\frac{\partial q'}{\partial z} \quad ,$$

respectively, with K and K′ independent of elevation within the appropriate layer.

The geostrophic velocities associated with the pressure gradients in upper and lower layers, respectively, are

$$q_g = -\frac{\nabla(g'H + gB)}{i f} \quad ,$$

$$q_g' = -\frac{\nabla(gB)}{i f} \quad , \tag{C-1}$$

where ∇ is the complex operator $\frac{\partial}{\partial x} + i\frac{\partial}{\partial y}$.

Assuming that the flow outside the boundary layers is vertically uniform and geostrophic, an Ekman type analysis (c.f. Haltiner and Martin, 1957) gives for the velocity in the:

upper layer near the interface,

$$q \doteq q_g + A_1 e^{-m(z-H')} \quad ; \tag{C-2}$$

lower layer near the interface,

$$q' = q_g' + A_2 e^{m'(z-H')} \quad ; \tag{C-3}$$

lower layer near the bottom,

$$q' = q_g' + A_3 e^{-m'z} \quad , \tag{C-4}$$

where

$$m = \sqrt{i\, f/K} \quad , \quad m = \sqrt{i\, f/K'} \quad .$$

It is understood that the forms (C-2), (C-3) and (C-4) apply only within the boundary layers ①, ② and ③, respectively; elsewhere within the model, velocities are given by (C-1). The complex constants A_1, A_2 and A_3 are determined from:

the bottom condition

$$q' = o \ , \quad \text{at} \quad z = o \ ;$$

the continuity of stress

$$\rho K \frac{\partial q}{\partial z} = \rho' K' \frac{\partial q'}{\partial z} \ , \quad \text{at} \quad z = H' \ ;$$

and the kinematic condition

$$q' = q \ , \quad \text{at} \quad z = H' \ .$$

Application of these conditions to the velocities given by (C-2), (C-3) and (C-4) yields:

$$A_1 = \frac{- \rho' K' m' \Delta q_g}{(\rho K m + \rho' K' m')} \ ,$$

$$A_2 = \frac{\rho K m \Delta q_g}{(\rho K m + \rho' K' m')} \ ,$$

$$A_3 = - q_g' \ ,$$

with

$$\Delta q_g \equiv q_g - q_g' \ .$$

Now, the rate of energy dissipation for a vertical column of unit cross sectional area extending through the interface boundary layers (1) and (2) is

$$G^I = \int_{H'}^{H'+H} \rho K \left|\frac{\partial q}{\partial z}\right|^2 dz + \int_{H'/2}^{H'} \rho' K' \left|\frac{\partial q'}{\partial z}\right|^2 dz \ .$$

The rate of energy dissipation in a like vertical column extending through the bottom boundary layer is

$$G^B = \int_o^{H'/2} \rho' K' \left|\frac{\partial q'}{\partial z}\right|^2 dz \ .$$

Then, using the forms of the velocities valid within the respective boundary layers and considering the boundary layer thicknesses quite small compared to fluid layer thicknesses, the energy dissipation rates can be expressed

$$G^I \doteq \int_o^\infty \rho K \left|mA_1 e^{-m\zeta}\right|^2 d\zeta + \int_o^\infty \rho' K' \left|m'A_2 e^{-m'\zeta}\right|^2 d\zeta \ , \quad \text{(C-5)}$$

and

$$G^B \doteq \int_o^\infty \rho' K' \left|m'A_3 e^{-m'\zeta}\right|^2 d\zeta \ . \quad \text{(C-6)}$$

To evaluate these integrals first note that

$$\left|mA_1 e^{-m\zeta}\right|^2 = mm^* A_1 A_1^* e^{-(m+m^*)\zeta} \ ,$$

where the superscript "*" denotes the complex conjugate. Then, some algebraic manipulation yields

$$mm^* = f/K \ , \qquad m + m^* = \sqrt{2f/K} \ ,$$

and, approximating $\rho' \doteq \rho$,

$$A_1 A_1^* \doteq \frac{K'}{\left(\sqrt{K} + \sqrt{K'}\right)^2} \left|\Delta q_g\right|^2 \ .$$

Therefore,

$$\int_o^\infty \rho K \left|mA_1 e^{-m\zeta}\right|^2 d\zeta \doteq \frac{\rho \sqrt{fK'}\ K'}{\sqrt{2}\left(\sqrt{K} + \sqrt{K'}\right)^2} \left|\Delta q_g\right|^2 \ .$$

Similarly,

$$\int \rho' K' \left|m' A_2 e^{-m'\zeta}\right|^2 d\zeta \doteq \frac{\rho \sqrt{fK'}\ K}{\sqrt{2}\left(\sqrt{K} + \sqrt{K'}\right)^2} \left|\Delta q_g\right|^2 \ .$$

So, with $\rho' \doteq \rho$,

$$G^I \doteq \rho \sqrt{f/2} \frac{\left|\sqrt{K}\ K' + \sqrt{K'}\ K\right|}{\left(\sqrt{K} + \sqrt{K'}\right)^2} \left|\Delta q_g\right|^2 \ . \qquad \text{(C-7)}$$

In like manner, from (C-6) is obtained the approximation

$$G^B \doteq \rho' \sqrt{fK'/2}\ \left|q_g'\right|^2 \ . \qquad \text{(C-8)}$$

Now, using the complex notation, the rates of energy dissipation per unit horizontal area due to interlayer

Now, using the complex notation, the rates of energy dissipation per unit horizontal area due to interlayer friction and bottom friction for the frictional model, as obtained from equations (28) and (29), can be written

$$G^I \doteq \rho\sigma H|\Delta q_g|^2 \ , \qquad \text{(C-9)}$$

and

$$G^B \doteq \rho'\sigma' H'|q_g'|^2 \ , \qquad \text{(C-10)}$$

with the approximation $\rho' \doteq \rho$ used in (C-9).

Equating the forms (C-7) with (C-9) and (C-8) with (C-10) yields

$$\sigma = \frac{1}{H}\sqrt{fK'/2}\ \left|1 + \sqrt{K'/K}\right|^{-1} \ ,$$

and

$$\sigma' = \frac{1}{H'}\sqrt{fK'/2} \ .$$

A P P E N D I X D

APPLICATION OF BOUNDARY CONDITIONS FOR FRICTIONAL MODEL

The differential equation for the frictional model can be written*

$$\nabla^2\Phi + \beta\Gamma\frac{\partial\Phi}{\partial x} = -\Gamma\frac{\pi F}{b\rho}\sin(\frac{\pi y}{b}) \quad . \qquad \text{(D-1)}$$

The general solution to (D-1) consists of a particular solution plus the general solution Φ^c to the reduced equation

$$\nabla^2\Phi^c + \beta\Gamma\frac{\partial\Phi^c}{\partial x} = 0 \quad .$$

Separation of variables leads to the following general solution for Φ^c:

$$\Phi^c = \sum_{k=1}^{\infty}(A_k e^{a_k x} + B_k e^{c_k x})(C_k \sin n_k y + D_k \cos n_k y) \quad ,$$

where (for k=1,2,...) A_k, B_k, C_k and D_k are constants of integration,

---

*In order to simplify the notation in this appendix, the subscript "j" has been dropped from the double-valued functions and parameters, Φ_j, α_j Γ_j, etc.

$$a_k = -\frac{\beta\Gamma}{2} + \left[\left(\frac{\beta\Gamma}{2}\right)^2 + n_k^2\right]^{\frac{1}{2}} ,$$

$$b_k = -\frac{\beta\Gamma}{2} - \left[\left(\frac{\beta\Gamma}{2}\right)^2 + n_k^2\right]^{\frac{1}{2}} \qquad \text{(D-2)}$$

and n_k is a positive, real constant. A particular solution to (D-1) is

$$\frac{bF}{\pi\rho}\Gamma \sin\left(\frac{\pi y}{b}\right) .$$

So,

$$\Phi = \sum_{k=1}^{\infty} (A_k e^{a_k x} + B_k e^{c_k x})(C_k \sin n_k y + D_k \cos n_k y) + \frac{bF}{\pi\rho}\Gamma \sin\left(\frac{\pi y}{b}\right)$$

is the general solution to (D-1). Applying the lateral boundary conditions leads to the complete solution.

The zonal boundary conditions,

$$\Phi(x,o) = \Phi(x,b) = 0 \qquad (0 \leq x \leq w) ,$$

can be satisfied by choosing $D_k = 0$ and $n_k = \frac{\pi k}{b}$ $(k = 1, 2, \ldots)$. Then, defining

$$R_k \equiv A_k C_k , \qquad S_k \equiv B_k C_k \qquad (k = 1, 2, \ldots) ,$$

the solution becomes

$$\Phi = \sum_{k=1}^{\infty} \left[R_k e^{a_k x} + S_k e^{c_k x}\right)\sin\left(\frac{\pi k y}{b}\right)] + \frac{bF}{\pi\rho}\Gamma \sin\left(\frac{\pi y}{b}\right) .$$

The boundary condition

$$\Phi(o,y) = 0 \qquad (0 \leq y \leq b)$$

requires

$$\begin{aligned} R_1 + S_1 &= -\frac{bF}{\pi\rho}\Gamma \ , \\ R_k &= -S_k \qquad (k = 2, 3, \ldots) \ ; \end{aligned} \tag{D-3}$$

the condition

$$\Phi(w,y) = 0 \qquad (0 \leq y \leq b)$$

requires

$$\begin{aligned} R_1 e^{a_1 w} + S_1 e^{c_1 w} &= -\frac{bF}{\pi\rho}\Gamma \ , \\ R_k e^{a_k w} &= -S_k e^{c_k w} \qquad (k = 2, 3, \ldots) \ . \end{aligned} \tag{D-4}$$

Combining requirements (D-3) and (D-4) gives

$$R_k = S_k = 0 \qquad (k = 2, 3, \ldots) \ ,$$

and

$$-\frac{bF}{\pi\rho}\Gamma = R_1 + S_1 = R_1 e^{a_1 w} + S_1 e^{c_1 w} \ .$$

Letting

$$R \equiv \frac{-R_1}{\frac{bF}{\pi\rho}\Gamma} \ , \qquad S \equiv \frac{-S_1}{\frac{bF}{\pi\rho}\Gamma} \ , \qquad a \equiv a_1 , \quad c \equiv c_1 \ ,$$

the requirements on R_1 and S_1 can be expressed

$$R = \frac{1 - e^{cw}}{e^{aw} - e^{cw}} , \qquad S = 1 - R . \tag{D-5}$$

Therefore, the complete solution for Φ is

$$\Phi = - \frac{bF}{\pi\rho}\Gamma \sin(\frac{\pi y}{b})[Re^{ax} - 1 + (1 - R)e^{cx}] ,$$

with.

$$a = - \frac{\beta\Gamma}{2} + [(\frac{\beta\Gamma}{2})^2 + (\frac{\pi}{b})^2]^{\frac{1}{2}} ,$$

$$c = - \frac{\beta\Gamma}{2} - [(\frac{\beta\Gamma}{2})^2 + (\frac{\pi}{b})^2]^{\frac{1}{2}} ,$$

$$R = \frac{1 - e^{cw}}{e^{aw} - e^{cw}} .$$

A P P E N D I X E

RELATIONS BETWEEN LAYER THICKNESSES AND TRANSPORT STREAMFUNCTIONS

In the case of the frictional model, the vertically integrated equations of momentum conservation can be written in the following vector forms:

$$-f\nabla\Psi + \nabla(\frac{g'}{2}H^2 + H_oB) = \hat{T} - \sigma[\hat{k}x\nabla\Psi - d_o\hat{k}x\nabla\Psi'] ,$$
$$-f\nabla\Psi' + \nabla(gH_o'B) = \sigma[\hat{k}x\nabla\Psi - d_o\hat{k}x\nabla\Psi'] - \sigma'\hat{k}x\nabla\Psi' \quad . \tag{E-1}$$

Let α_j and Γ_j be double-valued constants and Φ_j denote a double-valued variable defined by the identities

$$\Phi_j \equiv \Psi + \alpha_j\Psi' \tag{E-2}$$

and

$$\Psi + \alpha_j\Psi' \equiv \Gamma_j[(\sigma - \alpha_j\sigma)\Psi - (d_o\sigma - \alpha_j d_o\sigma - \alpha_j\sigma')\Psi'] \ . \tag{E-3}$$

Multiplying the second of (E-1) by α_j and adding to the first gives

$$-f\nabla(\Psi + \alpha_j\Psi') + \nabla(\frac{g'}{2}H^2 + gH_oB + \alpha_j gH_o'B) = \hat{T}$$
$$- kx\nabla[(\sigma - \alpha_j\sigma)\Psi - (d_o\sigma - \alpha_j d_o\sigma - \alpha_j\sigma')\Psi'] ,$$

or using (E-2) and (E-3),

$$-f\nabla\Phi_j + \nabla\left(\frac{g'}{2}H^2 + gH_oB + \alpha_j gH_o'B\right) = \hat{T} - \frac{1}{\Gamma_j}\hat{k}x\nabla\Phi_j \ . \qquad \text{(E-4)}$$

Now, define a double-valued function ω_j of the layer thicknesses by

$$\omega_j \triangleq \frac{g'}{2}H^2 + g(H_o + \alpha_j H_o')B \ . \qquad \text{(E-5)}$$

So, (E-4) can be written

$$-f\nabla\Phi_j + \nabla\omega_j = \hat{T} - \frac{1}{\Gamma_j}\hat{k}x\nabla\Phi_j \ . \qquad \text{(E-6)}$$

Let $ds = [(dx)^2 + (dy)^2]^{\frac{1}{2}}$ be a differential of arc length of an arbitrary curve in the horizontal plane. Let $\hat{ds}$ denote the vector,

$$\hat{i}dx + \hat{j}dy \ ,$$

originating on this curve, oriented tangent to the curve and having magnitude ds. Form the scalar product of $\hat{ds}$ with equation (E-6) to obtain

$$d\omega_j - fd\Phi_j = (T_x dx + T_y dy) + \frac{1}{\Gamma_j}\left(\frac{\partial\Phi_j}{\partial y}dx - \frac{\partial\Phi_j}{\partial x}dy\right) \ , \qquad \text{(E-7)}$$

where

$$d\omega_j \equiv \frac{\partial\omega_j}{\partial x}dx + \frac{\partial\omega_j}{\partial y}dy \ ,$$

and

$$d\Phi_j \equiv \frac{\partial\Phi_j}{\partial x}dx + \frac{\partial\Phi_j}{\partial y}dy \ .$$

Using the β-plane approximation, $f = f_o + \beta y$ with f_o and β constants,

$$f d\Phi_j = d(f\Phi_j) - \Phi_j df = d(f\Phi_j) - \beta\Phi_j dy \ .$$

Hence, (E-7) can be written

$$d(\omega_j - f\Phi_j) = (T_x + \frac{1}{\Gamma_j}\frac{\partial\Phi_j}{\partial y})dx + (T_y - \frac{1}{\Gamma_j}\frac{\partial\Phi_j}{\partial x} - \beta\Phi_j)dy \ . \qquad (E\text{-}8)$$

It is seen now that the integral

$$\int_{(x_o,y_o)}^{(x,y)} d(\omega_j - f\Phi_j)$$

is a function only of the end points (x_o,y_o) and (x,y), if, and only if,

$$\frac{\partial}{\partial y}(T_x + \frac{1}{\Gamma_j}\frac{\partial\Phi_j}{\partial y}) = \frac{\partial}{\partial x}(T_y - \frac{1}{\Gamma_j}\frac{\partial\Phi_j}{\partial x} - \beta\Phi_j) \ .$$

This requirement, however, is another statement of the differential equation,

$$\frac{1}{\Gamma_j}\nabla^2\Phi_j + \beta\frac{\partial\Phi_j}{\partial x} = \frac{\partial T_y}{\partial x} - \frac{\partial T_x}{\partial y} \ , \qquad (E\text{-}9)$$

from which Φ_j and, thus, Ψ and Ψ' are determined.

Therefore, integrating (E-8) along any arbitrary curve from (x_o,y_o) to (x,y) yields

$$\omega_j = \int_{(x_o,y_o)}^{(x,y)} \left[\left(T_x + \frac{1}{\Gamma_j}\frac{\partial \Phi_j}{\partial y}\right)dx + \left(T_y - \frac{1}{\Gamma_j}\frac{\partial \Phi_j}{\partial x} - \beta\Phi_j\right)dy\right] + f\Phi_j + (\omega_j - f\Phi_j)\Big|_{(x_o,y_o)} . \tag{E-10}$$

Using the definition of the effective overall depth, B, equations (E-5) can be written

$$\omega_1 = \frac{g'}{2}H^2 + g(H_o + \alpha_1 H_o')[H' + (1 - \gamma)H] ,$$
$$\omega_2 = \frac{g'}{2}H^2 + g(H_o + \alpha_2 H_o')[H' + (1 - \gamma)H] . \tag{E-11}$$

Multiplying these relations by $(H_o + \alpha_2 H_o')$ and $(H_o + \alpha_1 H_o')$, respectively, and subtracting gives

$$(H_o + \alpha_2 H_o')\omega_1 - (H_o + \alpha_1 H_o')\omega_2 = \frac{g'}{2}H^2(\alpha_2 - \alpha_1)H_o' .$$

Thus,

$$H = \left[\frac{2}{g'(\alpha_2 - \alpha_1)}[(\alpha_2 + d_o)\omega_1 - (\alpha_1 + d_o)\omega_2]\right]^{\frac{1}{2}} . \tag{E-12}$$

The first of (E-11) then yields H' as a function of H and ω_1,

$$H' = [g(H_o + \alpha_1 H_o')]^{-1}[\omega_1 - \frac{g'}{2}H^2] - (1 - \gamma)H . \tag{E-13}$$

A P P E N D I X F

EXPRESSION OF WESTERN BOUNDARY CONDITIONS FOR INERTIAL MODEL AS A QUARTIC POLYNOMIAL EQUATION IN q_o

From the following conditions relating q_o, q_o', E_1 and E_2 a quartic, polynomial equation in any one of these four parameters can be obtained:

$$q_o = \frac{g}{f(\epsilon_1 - \epsilon_2)}[m_2E_2 - m_1E_1] ,$$

$$q_o' = \frac{g}{f(\epsilon_1 - \epsilon_2)}[\epsilon_2 m_1E_1 - \epsilon_1 m_2E_2] , \tag{F-1}$$

and

$$E_j = -\frac{1}{2g}[\epsilon_j q_o^2 + (q_o')^2] - (1 + \epsilon_j)[B_I(y) - B_I(0)]$$

$$- \gamma\epsilon_j[H_I(y) - H_I(0)] \quad (j = 1, 2) . \tag{F-2}$$

In this appendix a polynomial equation of degree four in q_o is derived.

From the system of equations (F-1), E_j can be obtained as functions of q_o and q_o', i.e.,

$$E_j = -\frac{f}{gm_j}(\epsilon_j q_o + q_o') . \tag{F-3}$$

Then, comparing (F-2) with (F-3), it is seen that

$$J_j - \frac{2f}{m_j}(\epsilon_j q_o + q_o') + \epsilon_j q_o^2 + (q_o')^2 = 0 , \qquad \text{(F-4)}$$

with J_j, dimensional parameters having c.g.s. units $cm^2\ sec^{-2}$, defined by

$$J_j \equiv 2g\{(1+\epsilon_j)[B_I(y) - B_I(0)] + \gamma\epsilon_j[H_I(y) - H_I(0)]\} . \qquad \text{(F-5)}$$

Let

$$n_j \equiv 2fm_j/m_1m_2 \qquad (j = 1, 2) , \qquad \text{(F-6)}$$

with c.g.s. units $cm\ sec^{-1}$. Then, subtracting (F-4) for $j = 2$ from (F-4) for $j = 1$ yields an equation for q_o' as a function of q_o,

$$q_o' = \frac{J_1 - J_2}{(n_2 - n_1)} - \frac{\epsilon_2 n_1 - \epsilon_1 n_2}{(n_2 - n_1)} q_o + \frac{\epsilon_1 - \epsilon_2}{(n_2 - n_1)} q_o^2 . \qquad \text{(F-7)}$$

Adding equations (F-4) for $j = 1$ and $j = 2$, yields:

$$(J_1 + J_2) - (\epsilon_2 n_1 + \epsilon_1 n_2)q_o - (n_2 + n_1)q_o' + (\epsilon_1 + \epsilon_2)q_o^2 + 2(q_o')^2 = 0 . \qquad \text{(F-8)}$$

Equations (F-7) and (F-8) are independent. If q_o' is eliminated from (F-8) using (F-7), the following quartic equation in q_o is obtained:

$$(\epsilon_1 - \epsilon_2)^2 q_o^4 + 2(\epsilon_1 - \epsilon_2)(\epsilon_2 n_1 - \epsilon_1 n_2) q_o^3$$

$$+ [(n_2 - n_1)(\epsilon_2 n_2 - \epsilon_1 n_1) + (\epsilon_2 n_1 - \epsilon_1 n_2)^2 + 2(\epsilon_1 - \epsilon_2)(J_1 - J_2)] q_o^2$$

$$+ [2(\epsilon_2 n_1 - \epsilon_1 n_2)(J_1 - J_2) + n_1 n_2 (\epsilon_1 - \epsilon_2)(n_2 - n_1)] q_o \quad \text{(F-9)}$$

$$+ [(n_2 - n_1)(n_2 J_2 - n_1 J_1) + (J_1 - J_2)^2] = 0 \ .$$

A P P E N D I X G

ALTERNATE ANALYSIS FOR INERTIAL BOUNDARY CURRENTS

In this appendix is presented an alternate system of analysis for solving first order perturbation equations derived from the vorticity equations (90), with the approximations (91) for $F(\Psi)$ and $G(\Psi')$. In Chapter V perturbations in layer thicknesses H and H' were considered as the primary independent variables; here the equations are formulated in terms of associated perturbations in the transport streamfunctions.

Define perturbations of the transport streamfunctions by

$$\psi = \Psi - \Psi_I \,,$$
$$\psi' = \Psi' - \Psi_I' \,. \qquad \text{(G-1)}$$

Then, the linearized, integrated versions (94) of the geostrophic approximations for meridional speeds can be solved for the layer thickness perturbations h, h' and b in terms of ψ and ψ' to yield:

$$h = \frac{f}{g'}\left[\frac{\psi}{H_I} - \frac{\psi'}{H_I'}\right] ,$$

$$h' = \frac{f}{g'}\left[\frac{\psi'}{H_I'} - \frac{\rho}{\rho'}\frac{\psi}{H_I}\right] , \qquad \text{(G-2)}$$

$$b = \frac{f\psi'}{gH_I'} .$$

Using these relations and the equations

$$v = \frac{1}{(H_I + h)}\frac{\partial\psi}{\partial x} , \qquad v' = \frac{1}{(H_I' + h')}\frac{\partial\psi'}{\partial x} ,$$

the vorticity relations (90) can be expressed in terms of ψ and ψ'. The resulting equations can be linearized to yield

$$\frac{\partial^2\psi}{\partial x^2}\left[2F_2H_I^2 + \frac{f^2}{g'H_I}\right]\psi - \frac{f^2}{g'H_I'}\psi' ,$$

$$\frac{\partial^2\psi'}{\partial x^2} = \left[2G_2(H_I')^2 + \frac{f^2}{g'H_I'}\right]\psi' - \frac{\rho f^2}{\rho' g'H_I}\psi . \qquad \text{(G-3)}$$

In deriving (G-3), use has been made of the following approximate forms of the vorticity relations valid in the interior region:

$$f = H_I(F_1 + 2F_2\psi_I) , \qquad f = H_I'(G_1 + 2G_2\psi_I') . \qquad \text{(G-4)}$$

Using the method of normal modes, the boundary value problem can be formulated in terms of the double-valued variable Θ_j, defined by

$$\Theta_j \equiv \psi\epsilon_j + \psi' , \tag{G-5}$$

with double-valued separation constants ϵ_j and m_j defined by

$$\begin{aligned} m_j^2(\psi\epsilon_j + \psi') \equiv & [2F_2H_I^2\epsilon_j + \frac{f}{g'H_I}\epsilon_j - \frac{\rho f^2}{\rho' g' H_I}]\psi \\ & + [2G_2(H_I')^2 + \frac{f^2}{g'H_I'} - \frac{f^2}{g'H_I}\epsilon_j]\psi' . \end{aligned} \tag{G-6}$$

The resulting differential equation is

$$\frac{\partial^2\Theta_j}{\partial x^2} - m_j^2\Theta_j = 0 . \tag{G-7}$$

The interior condition is

$$\lim_{x \to \infty} \Theta_j = 0 . \tag{G-8}$$

The western meridional boundary condition is

$$\Theta_j\Big|_{x=0} = -\Psi_I\epsilon_j - \Psi_I' . \tag{G-9}$$

This latter boundary condition seems the most important feature distinguishing this analysis from that presented in sections B and D of Chapter V. Since this boundary condition is linear in the perturbations ψ and ψ', it can be applied analytically so that no numerical techniques are involved. Moreover, such a linearized boundary

condition seems more consistent with the linearized differential equation than does the application of the nonlinear Bernoulli relations employed in section D of Chapter V.

The solution for Θ_j, satisfying (G-7, 8, 9) is

$$\Theta_j = -(\Psi_I \epsilon_j + \Psi_I')e^{-m_j x}, \qquad \text{(G-10)}$$

with:

$$\left.\begin{aligned} m_j &= \left[2G_2(H_I')^2 + \frac{f^2}{g'H_I'}(1 - \epsilon_j)\right]^{1/2}, \\ S &\equiv H_I''/H_I - 1 - 2g'H_I'[G_2(H_I')^2 - F_2H_I^2]/f^2, \\ \epsilon_j &= -S/2 \pm [(S/2)^2 + (\rho H_I')/(\rho' H_I)]^{1/2}, \end{aligned}\right\} \qquad \text{(G-11)}$$

with the + or - sign corresponding to $j = 1$ or 2, respectively. In obtaining equations (G-11) the defining relations (G-6) were employed, of course.

Finally, the definitions (G-5) can be employed to separate the solution and recover the anomalies of transport streamfunctions. The complete transport streamfunctions are then:

$$\Psi = \Psi_I + \psi$$

$$= \Psi_I + \frac{1}{(\epsilon_1 - \epsilon_2)}[\Psi_I\epsilon_2 + \Psi_I')e^{-m_2x} - (\Psi_I\epsilon_1 + \Psi_I')e^{-m_1x}] ,$$

$$\Psi' = \Psi_I' + \psi' \qquad \text{(G-12)}$$

$$= \Psi_I' + \frac{1}{(\epsilon_1 - \epsilon_2)}[\epsilon_2(\Psi_I\epsilon_1 + \Psi_I')e^{-m_1x} - \epsilon_1(\Psi_I\epsilon_2 + \Psi_I')e^{-m_2x}] .$$

The use of equations (G-2) yields, to the same approximations, the layer thicknesses. The meridional speeds within the boundary layers can be obtained from the geostrophic approximations (89). Alternatively, the meridional speeds can be obtained from (G-12), using the definitions of the transport streamfunctions. This latter approach yields

$$\left.\begin{aligned} v &\doteq [H(\epsilon_1 - \epsilon_2)]^{-1}[m_1(\Psi_I\epsilon_1 + \Psi_I')e^{-m_1x} \\ &\qquad - m_2(\Psi_I\epsilon_2 + \Psi_I')e^{-m_2x}] \\ v' &\doteq [H'(\epsilon_1 - \epsilon_2)]^{-1}[m_2\epsilon_1(\Psi_I\epsilon_2 + \Psi_I')e^{-m_2x} \\ &\qquad - m_1\epsilon_2(\Psi_I\epsilon_1 + \Psi_I')e^{-m_1x}] . \end{aligned}\right\} \text{(G-13)}$$

FIGURE 1

Volume transport streamlines in upper layer as computed from approximate solutions for the interior region ($x > 200$ km) of the ocean basin.

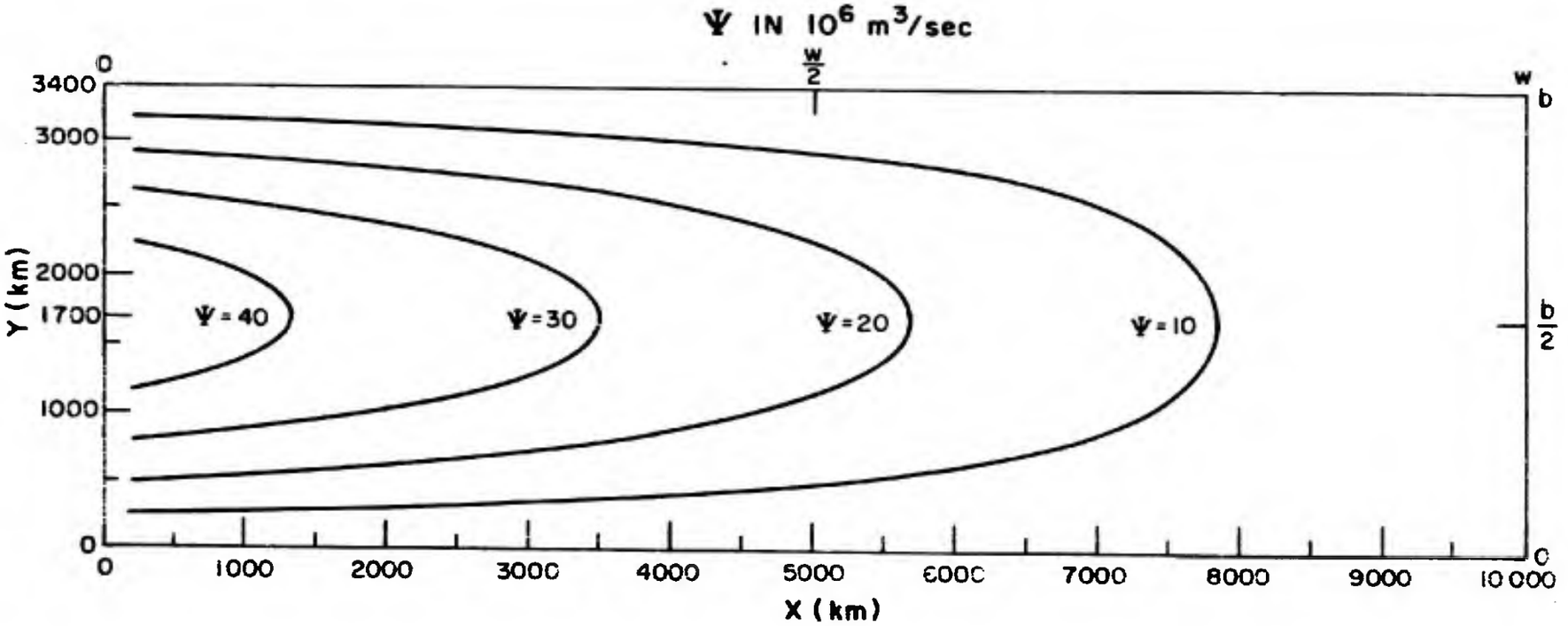
Ψ IN 10^6 m^3/sec
0
W/2
W
3400
3000
2000
1700
1000
0
Y (km)
Ψ = 40
Ψ = 30
Ψ = 20
Ψ = 10
b
b/2
0
0
1000
2000
3000
4000
5000
6000
7000
8000
9000
10 000
X (km)

FIGURE 2

Volume transport streamlines in lower layer as computed from approximate solutions for the interior region ($x > 200$ km) of the ocean basin.

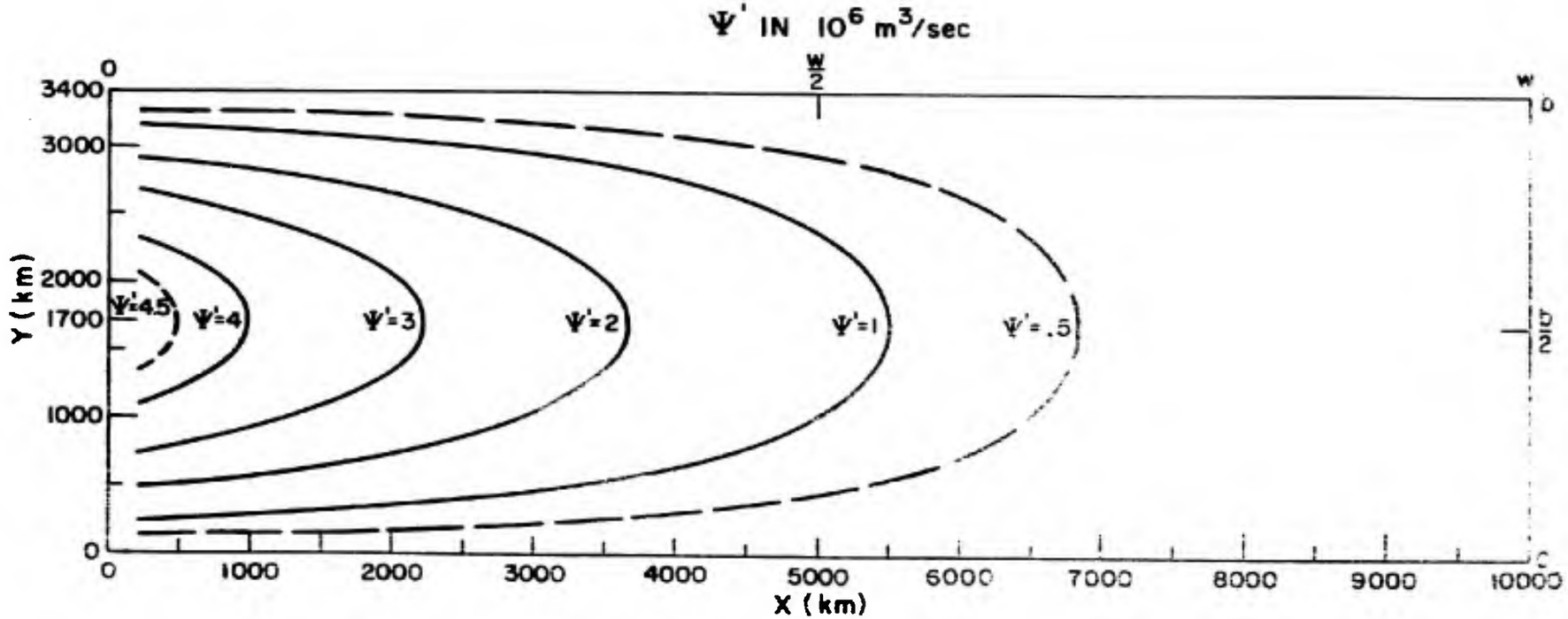
Ψ' IN 10^6 m^3/sec
0
W/2
W
3400
3000
2000
1700
1000
0
Y (km)
Ψ'=4.5
Ψ'=4
Ψ'=3
Ψ'=2
Ψ'=1
Ψ'=.5
W/2
0
1000
2000
3000
4000
5000
6000
7000
8000
9000
10000
X (km)

FIGURE 3

Curves of $V(x,b/2)$ and $V'(x,b/2)$ versus distance from western boundary as constructed graphically from approximate solutions for the western boundary region.

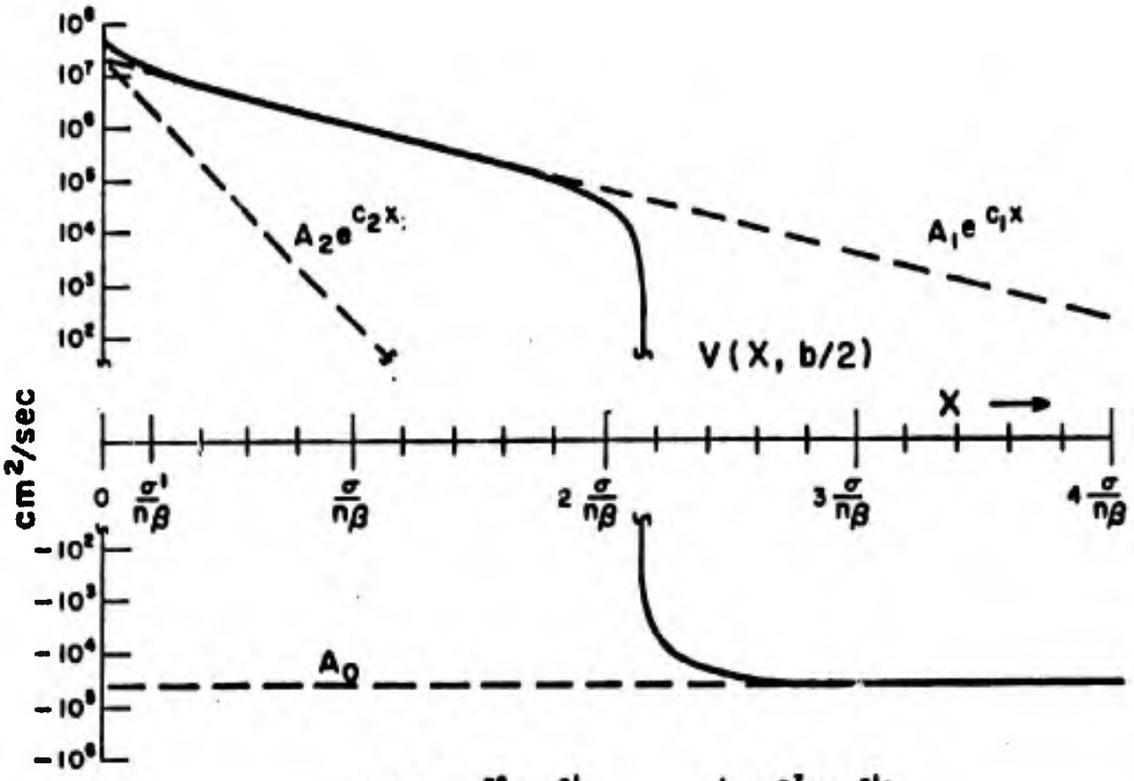

$\sigma = .5 \times 10^6\ (sec^{-1})$ $\sigma' = 10^{-7}\ (sec^{-1})$

$n = 1/\ln 10$

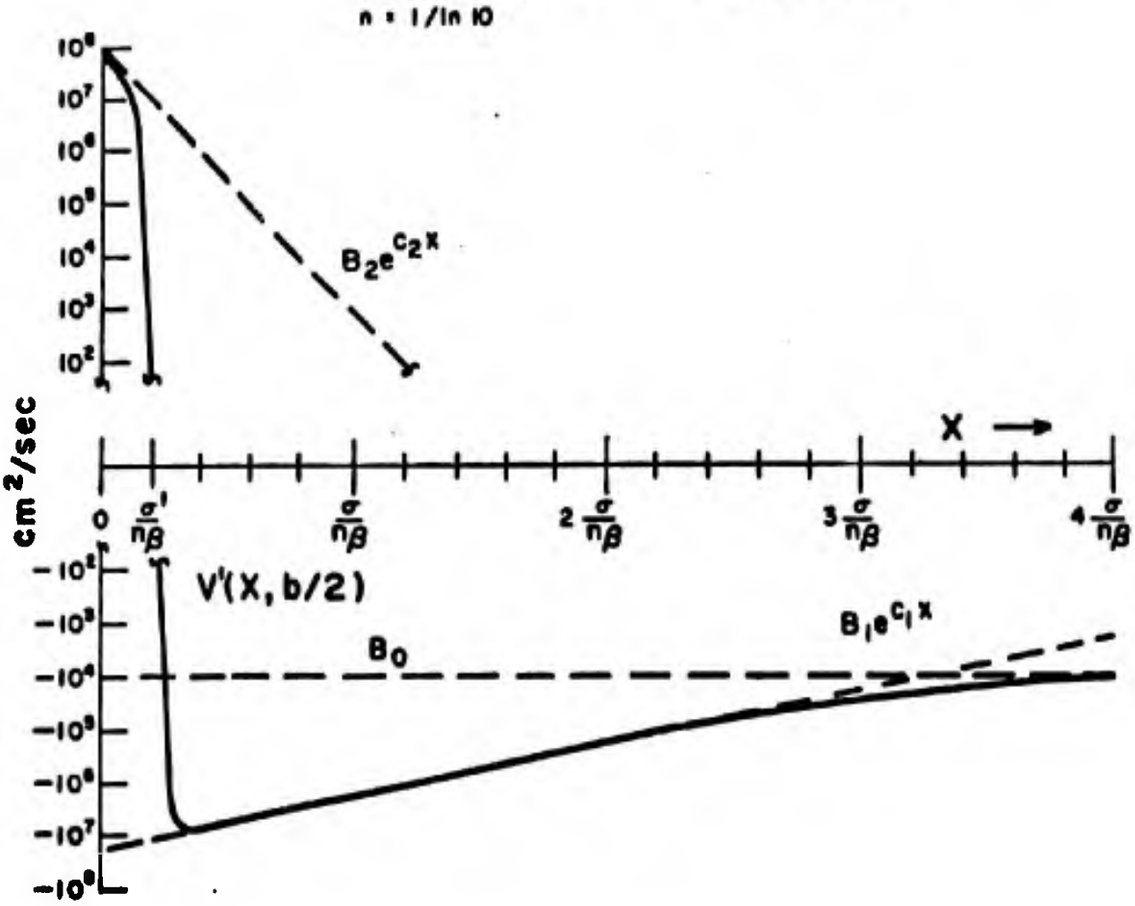

FIGURE 4

Curves of $V(x,b/2)$ and $V'(x,b/2)$ versus distance from western boundary as functions of σ and σ'. Calculated from complete solutions.

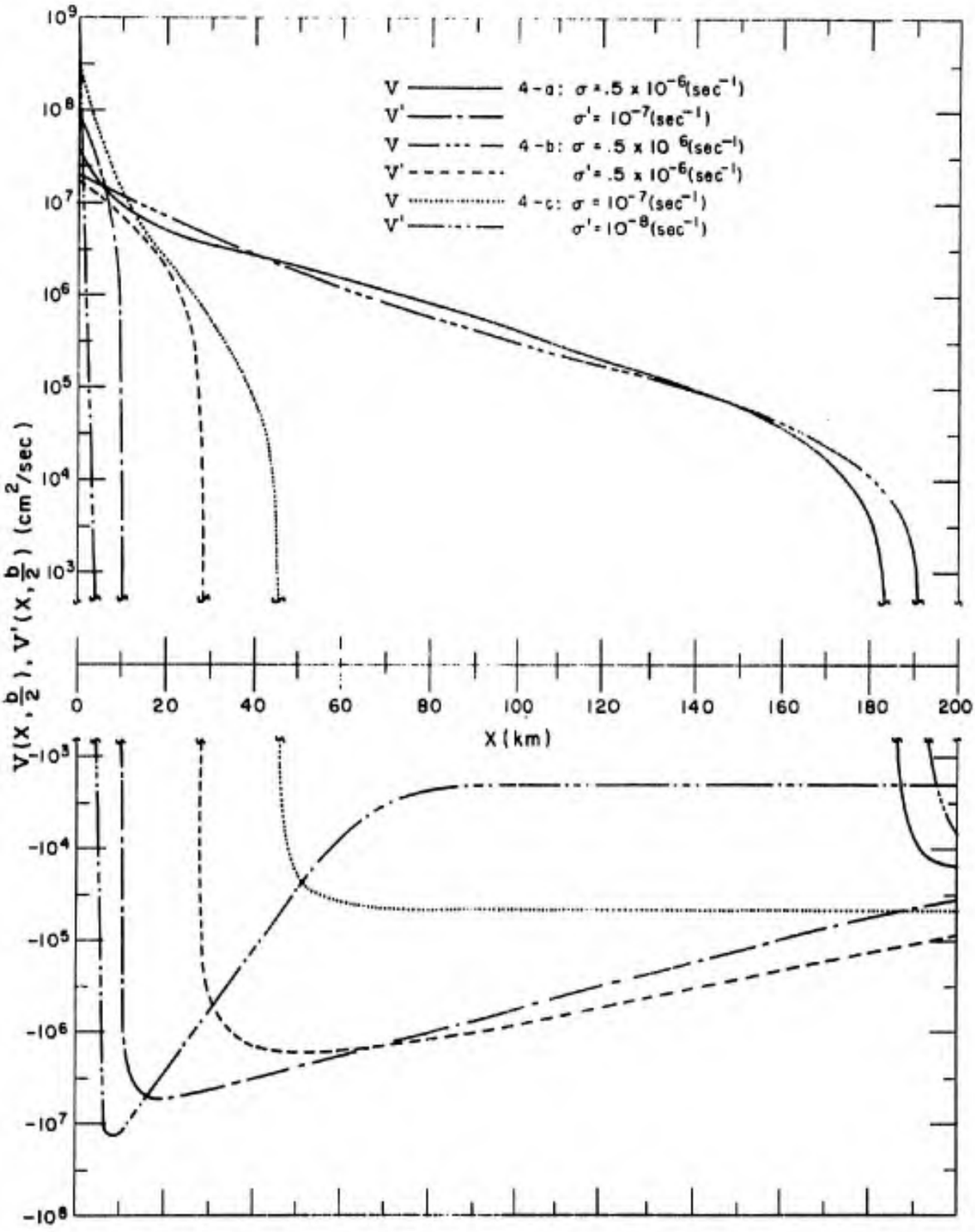
V —— 4-a: σ = .5 x 10⁻⁶(sec⁻¹)
V' —·— σ' = 10⁻⁷(sec⁻¹)
V —··— 4-b: σ = .5 x 10⁻⁶(sec⁻¹)
V' - - - σ' = .5 x 10⁻⁶(sec⁻¹)
V ····· 4-c: σ = 10⁻⁷(sec⁻¹)
V' —··— σ' = 10⁻⁸(sec⁻¹)
V(X, b/2), V'(X, b/2) (cm²/sec)
X (km)
0
20
40
60
80
100
120
140
160
180
200
10⁹
10⁸
10⁷
10⁶
10⁵
10⁴
10³
-10³
-10⁴
-10⁵
-10⁶
-10⁷
-10⁸

FIGURE 5

Curves of $\Psi(x,b/2)$ for western boundary region as functions of σ, with $\sigma' = \sigma$.

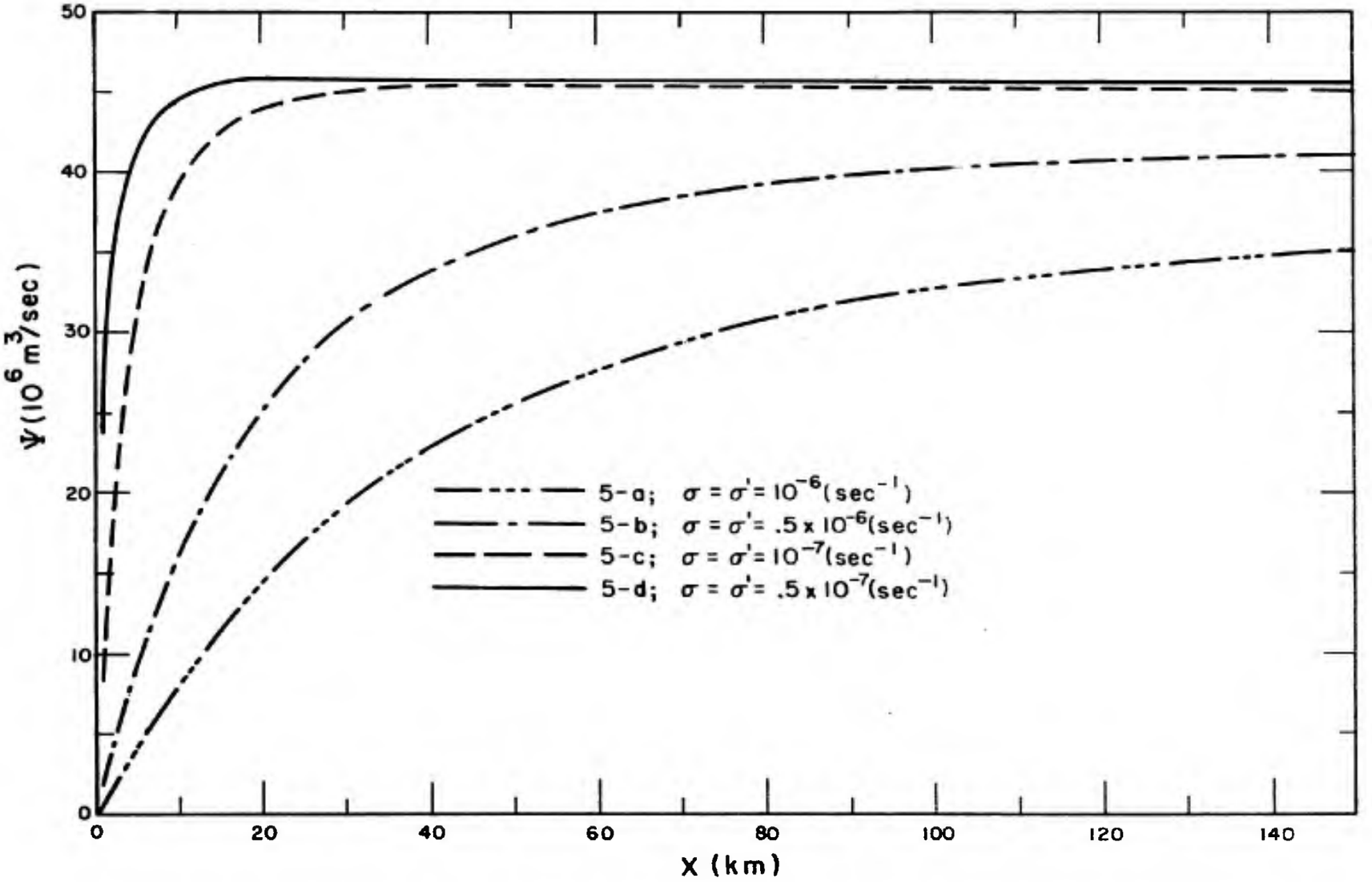
50
40
30
20
10
0
0
20
40
60
80
100
120
140
Ψ(10^6 m^3/sec)
X (km)
5-a; σ = σ' = 10^-6 (sec^-1)
5-b; σ = σ' = .5 x 10^-6 (sec^-1)
5-c; σ = σ' = 10^-7 (sec^-1)
5-d; σ = σ' = .5 x 10^-7 (sec^-1)

FIGURE 6

Meridional velocity component, at $y = b/2$ within upper layer, versus distance from western boundary as function of σ, with $\sigma' = \sigma$.

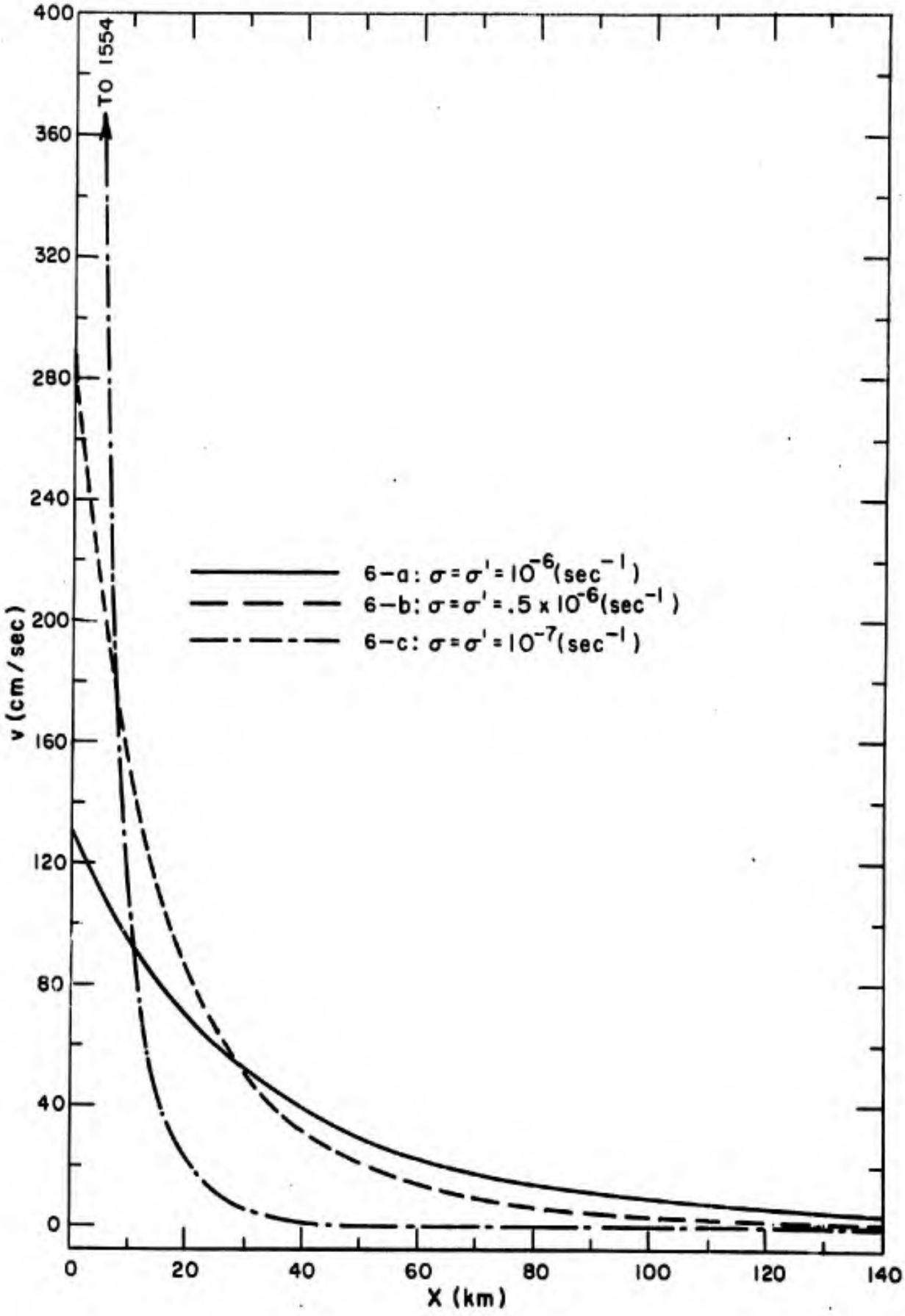
400
360
320
280
240
200
160
120
80
40
0
TO 1554
v (cm/sec)
6-a: σ = σ' = 10^-6 (sec^-1)
6-b: σ = σ' = .5 x 10^-6 (sec^-1)
6-c: σ = σ' = 10^-7 (sec^-1)
0
20
40
60
80
100
120
140
X (km)

FIGURE 7

Curves of $\Psi'(x,b/2)$ for western boundary region as functions of σ', with $\sigma = .5 \times 10^{-6}(sec^{-1})$.

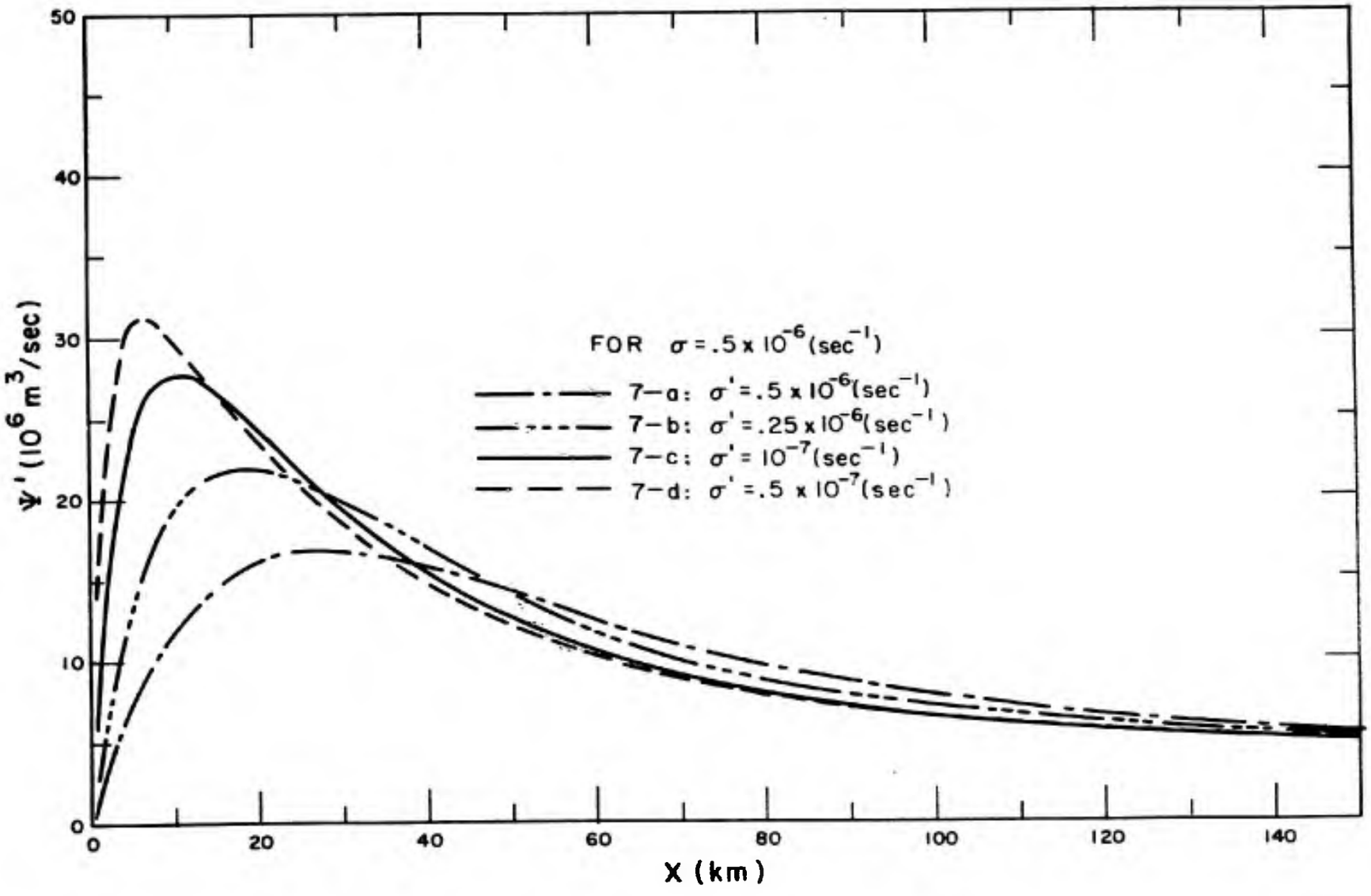
50
40
30
20
10
0
0
20
40
60
80
100
120
140
Ψ' (10^6 m^3/sec)
X (km)
FOR σ = .5 x 10^-6 (sec^-1)
7-a: σ' = .5 x 10^-6 (sec^-1)
7-b: σ' = .25 x 10^-6 (sec^-1)
7-c: σ' = 10^-7 (sec^-1)
7-d: σ' = .5 x 10^-7 (sec^-1)

FIGURE 8

Meridional velocity component, at y = b/2 within lower layer, versus distance from western boundary as function of σ', with $\sigma = .5 \times 10^{-6}(sec^{-1})$.

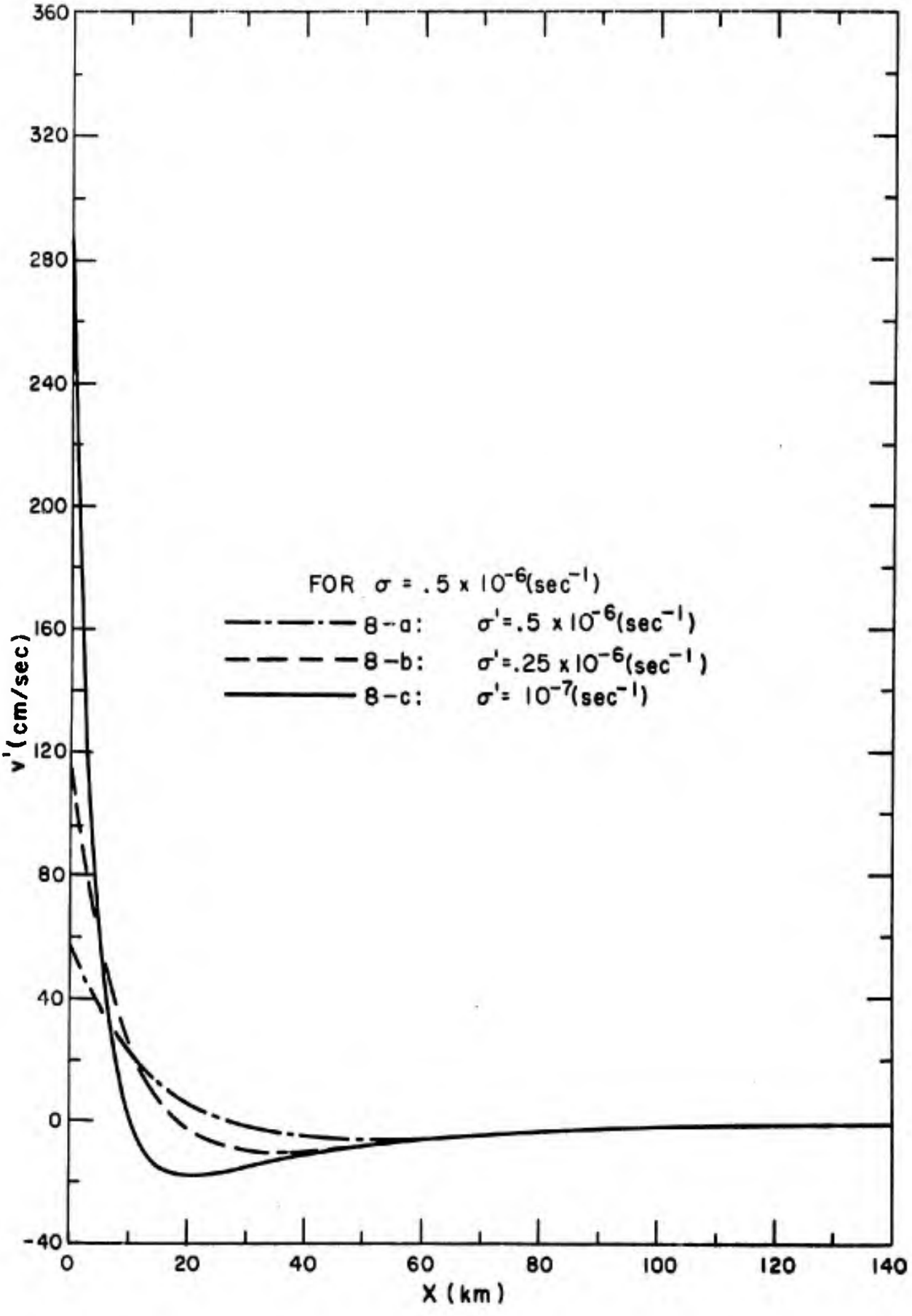
360
320
280
240
200
160
120
80
40
0
-40
0
20
40
60
80
100
120
140
X (km)
v' (cm/sec)
FOR σ = .5 x 10⁻⁶(sec⁻¹)
8-a: σ'=.5 x 10⁻⁶(sec⁻¹)
8-b: σ'=.25 x 10⁻⁶(sec⁻¹)
8-c: σ'= 10⁻⁷(sec⁻¹)

FIGURE 9

Volume transport streamlines in interior region ($x > 200$ km) of upper layer as computed from complete solutions with $\sigma = .5 \times 10^{-6}(\text{sec}^{-1})$ and $\sigma' = 10^{-7}(\text{sec}^{-1})$.

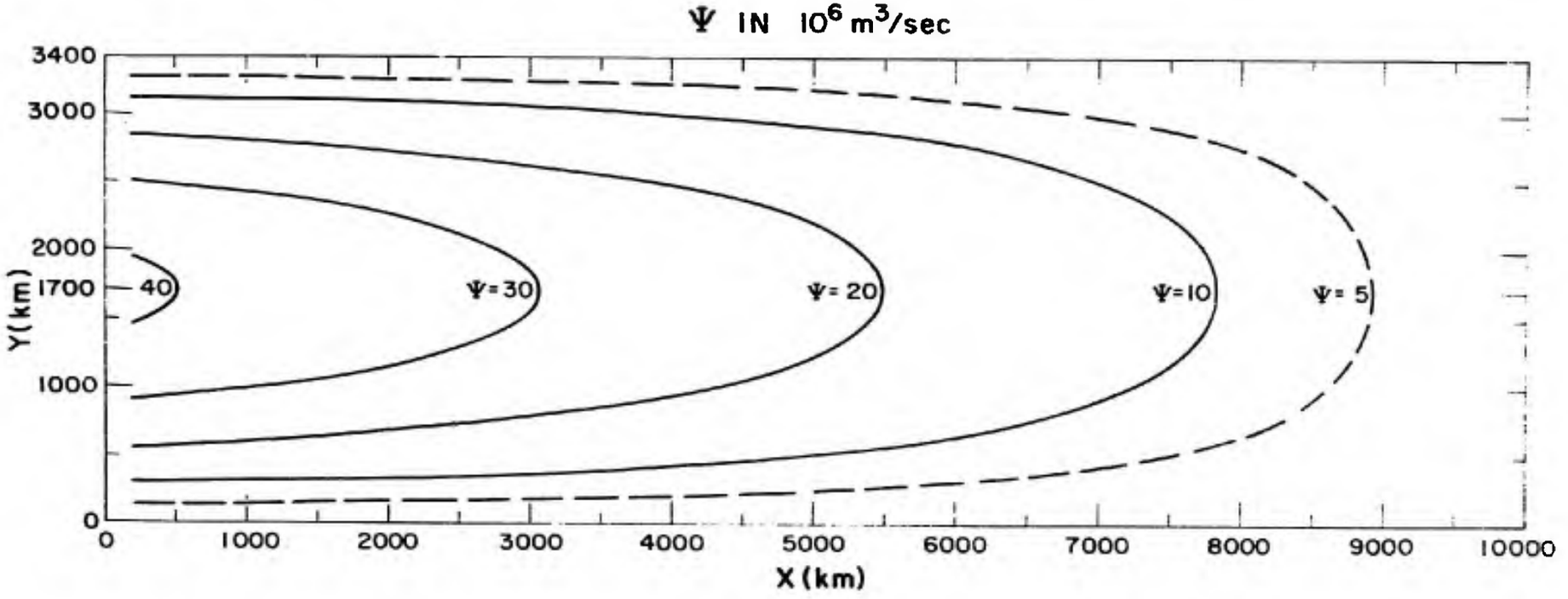
Ψ IN 10^6 m^3/sec
3400
3000
2000
1700
1000
0
Y(km)
40
Ψ=30
Ψ=20
Ψ=10
Ψ=5
0
1000
2000
3000
4000
5000
6000
7000
8000
9000
10000
X (km)

FIGURE 10

Volume transport streamlines in interior region ($x > 200$ km) of lower layer as computed from complete solutions with $\sigma = .5 \times 10^{-6}(\text{sec}^{-1})$ and $\sigma' = 10^{-7}(\text{sec}^{-1})$.

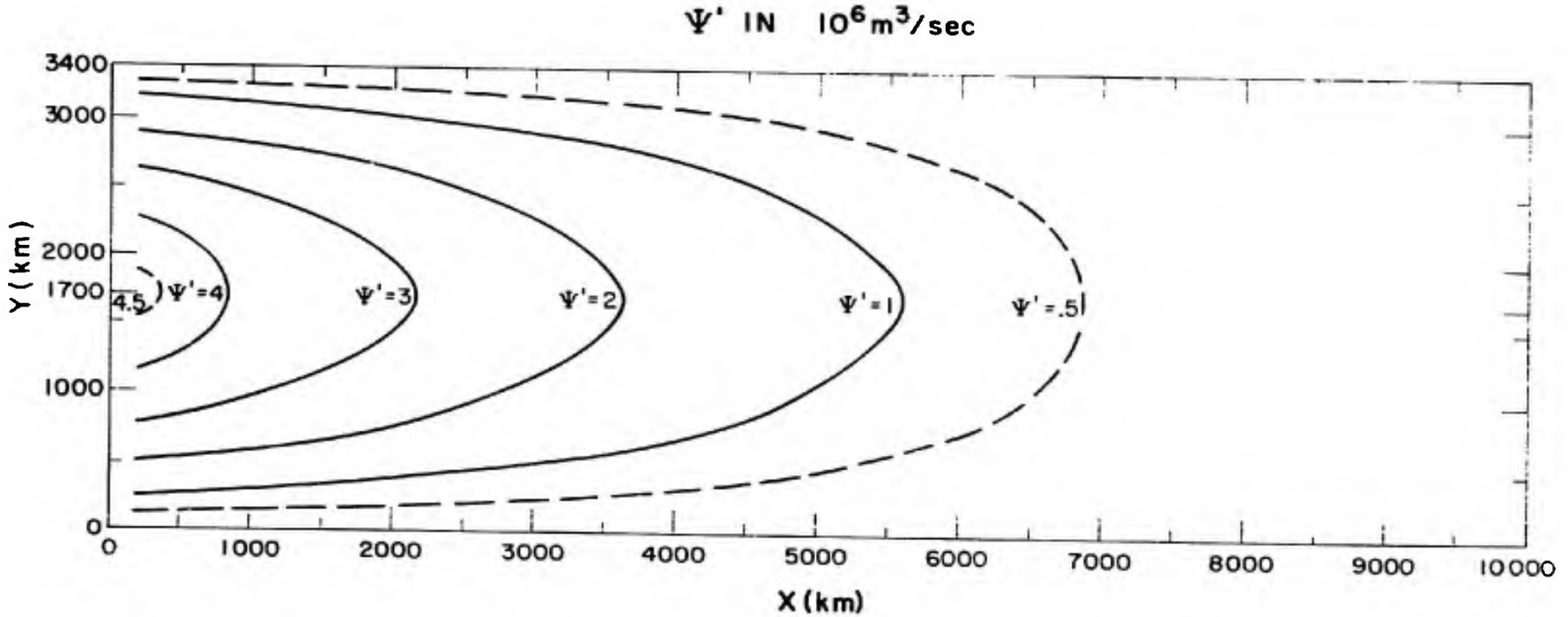
Ψ' IN 10^6 m^3/sec
3400
3000
2000
1700
1000
0
Y (km)
4.5
Ψ'=4
Ψ'=3
Ψ'=2
Ψ'=1
Ψ'=.5
0
1000
2000
3000
4000
5000
6000
7000
8000
9000
10000
X (km)

FIGURE 11

Volume transport streamlines within the western boundary region of the upper layer for $\sigma = .5 \times 10^{-6}(sec^{-1})$ and $\sigma' = 10^{-7}(sec^{-1})$.

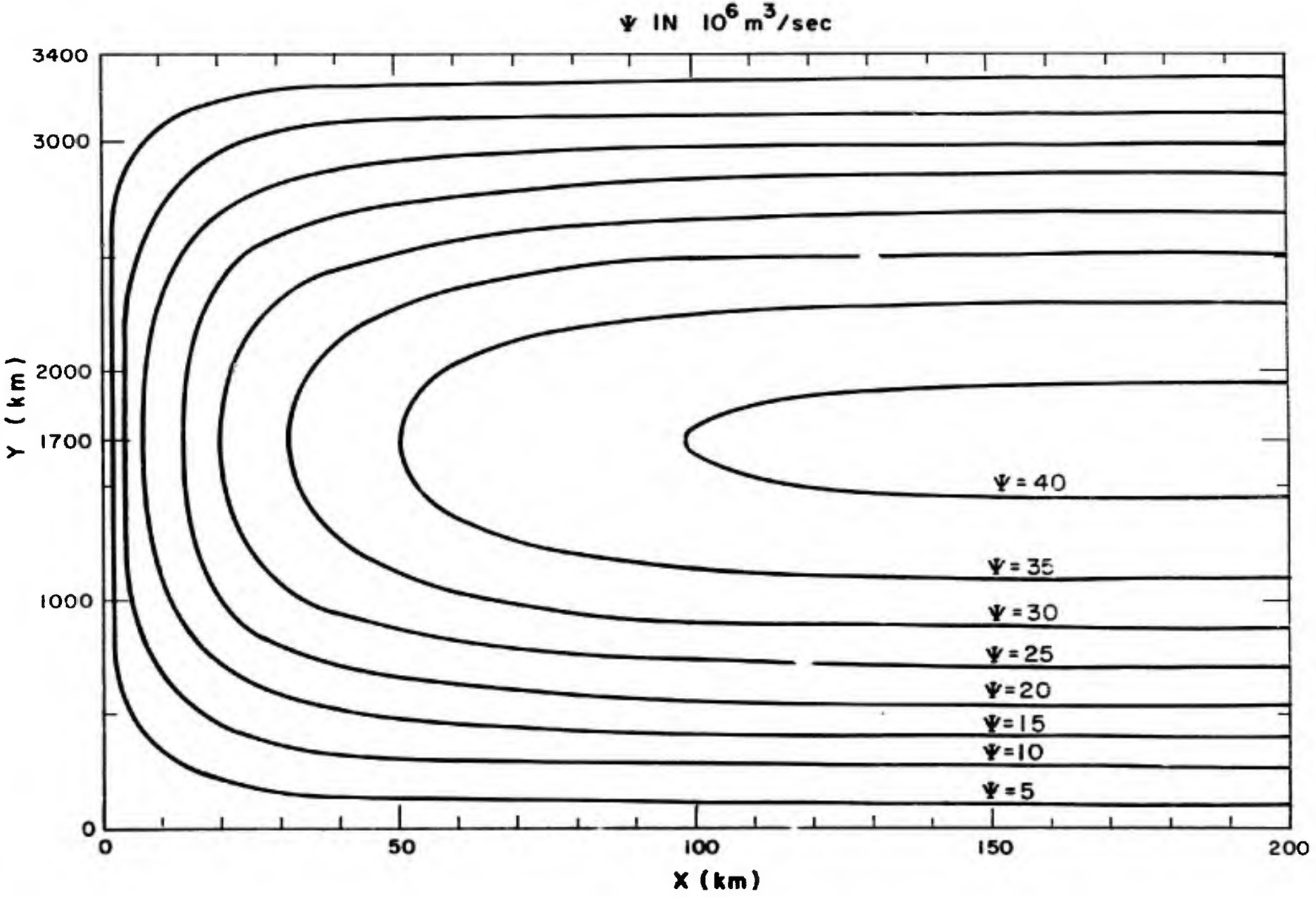
Ψ IN 10^6 m^3/sec
3400
3000
2000
1700
1000
0
Y (km)
Ψ = 40
Ψ = 35
Ψ = 30
Ψ = 25
Ψ = 20
Ψ = 15
Ψ = 10
Ψ = 5
0
50
100
150
200
X (km)

FIGURE 12

Volume transport streamlines within the western boundary region of the lower layer for $\sigma = .5 \times 10^{-6}(sec^{-1})$ and $\sigma' = 10^{-7}(sec^{-1})$.

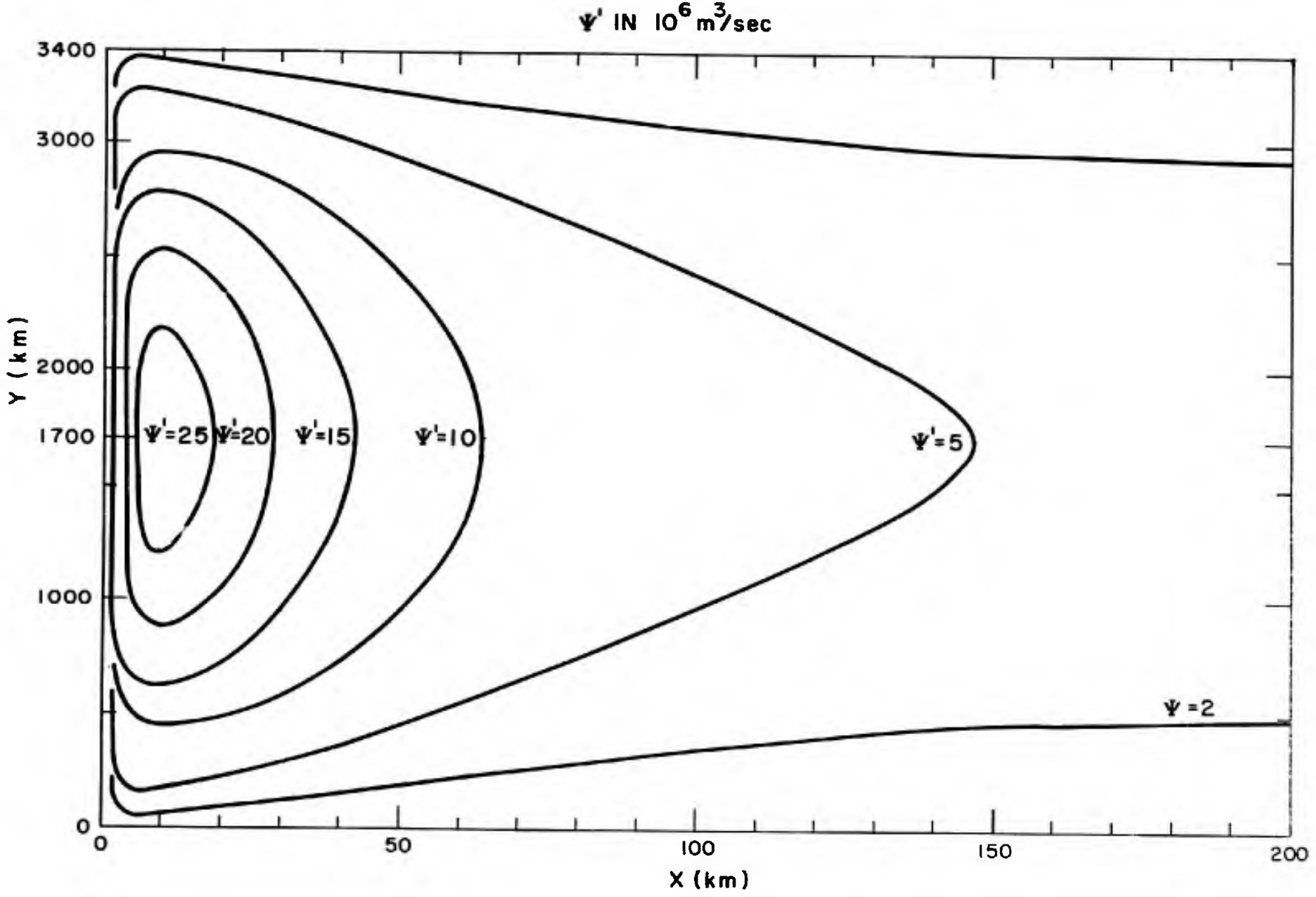
Ψ' IN 10^6 m^3/sec
3400
3000
2000
1700
1000
0
Y (km)
Ψ'=25
Ψ'=20
Ψ'=15
Ψ'=10
Ψ'=5
Ψ=2
0
50
100
150
200
X (km)

FIGURE 13

Approximate potential vorticity versus values of transport streamfunction at eastern edge of western boundary current region. Dots indicate points computed at x = 200 (km) from frictional model with $\sigma = .5 \times 10^{-6}(sec^{-1})$, $\sigma' = 10^{-7}$ (sec^{-1}) and other parameters as presented in Table 1. Solid lines indicate the relationships chosen to specify the interior flow for the inertial boundary model.

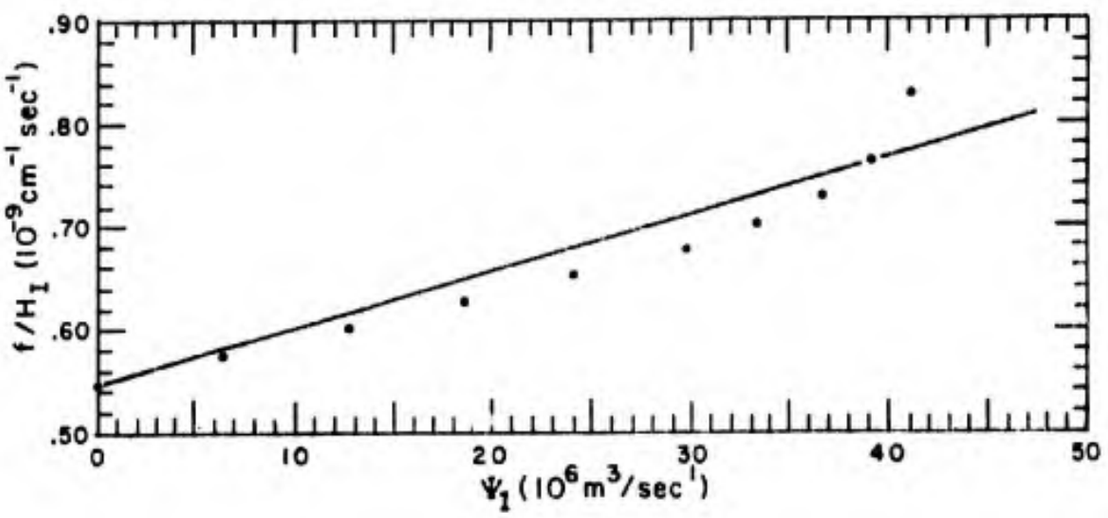
.90
.80
.70
.60
.50
f/H_I (10^-9 cm^-1 sec^-1)
0
10
20
30
40
50
Ψ_I (10^6 m^3/sec^1)

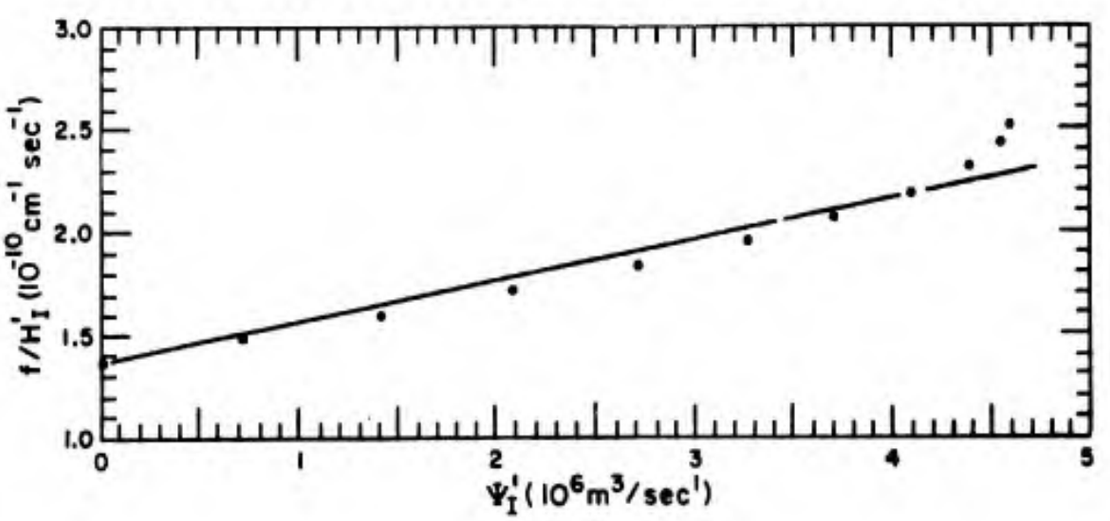
3.0
2.5
2.0
1.5
1.0
f/H'_I (10^-10 cm^-1 sec^-1)
0
1
2
3
4
5
Ψ'_I (10^6 m^3/sec^1)

FIGURE 14

Upper and lower layer meridional fluid velocity components at western boundary, q_o and q_o' respectively, as obtained for the analysis employing perturbations of layer thicknesses. The values of F_1 and G_1 used are given in Table 3; the values of F_2 and G_2 used are given in Table 4. Linear forms of H_I and H_I' versus y were assumed for all cases. For case 14-a, these forms are based on thicknesses at y = 0 and 1190 km (Table 2); for the other cases, H_I and H_I' are based on the tabulated thicknesses at y = 0 and 1020 km.

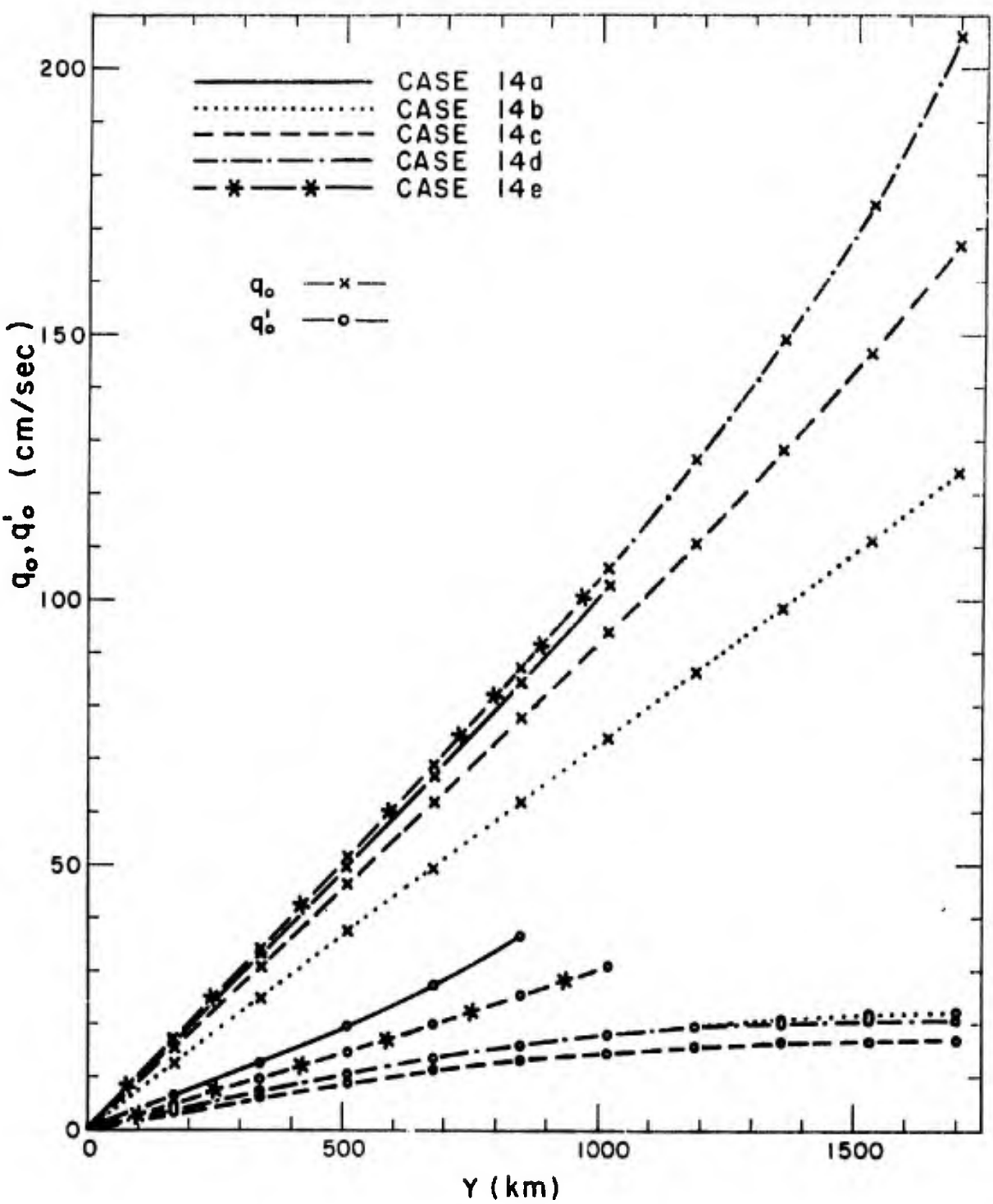
CASE 14a
CASE 14b
CASE 14c
CASE 14d
CASE 14e
q_o
q_o'
200
150
100
50
0
0
500
1000
1500
q_o, q_o' (cm/sec)
Y (km)

FIGURE 15

Meridional velocity components in upper and lower layers at western boundary, q_o and q_o' respectively, as computed using the analysis employing perturbations of streamfunctions (Appendix G). Values of F_1, G_1, F_2 and G_2 used are those given in Table 3. For case 15-a, the interior layer thicknesses were assumed to be linear functions of y and were based on the thickness values given in Table 2 for y = 0 and 1190 km. For case 15-b, the interior layer thicknesses tabulated in Table 2 were used.

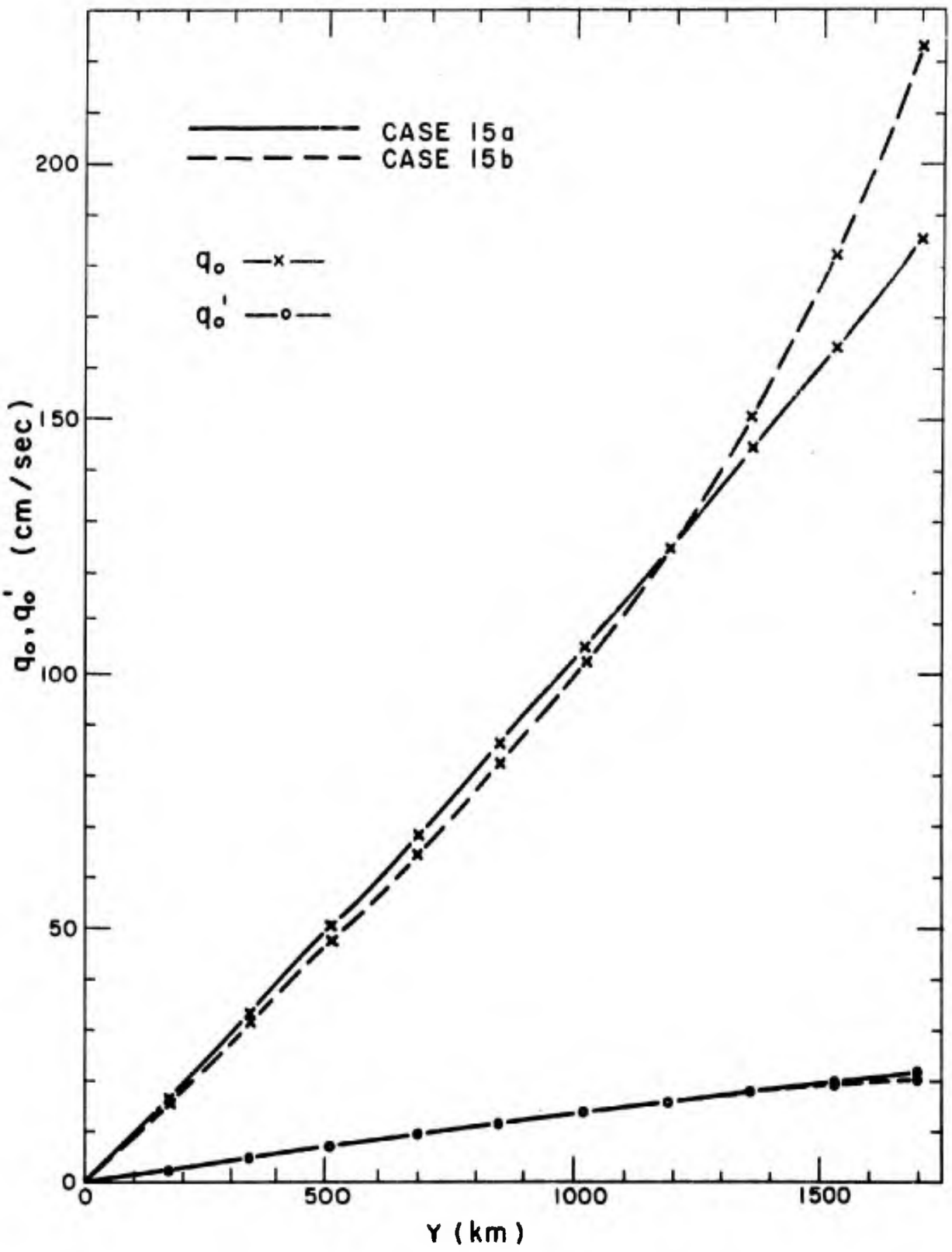
CASE 15a
CASE 15b
q_o
q_o'
200
150
100
50
0
0
500
1000
1500
q_o, q_o' (cm/sec)
Y (km)

FIGURE 16

Volume transport streamlines for the upper layer and contours of sea surface elevation, relative to sea bed, for case 15-a.

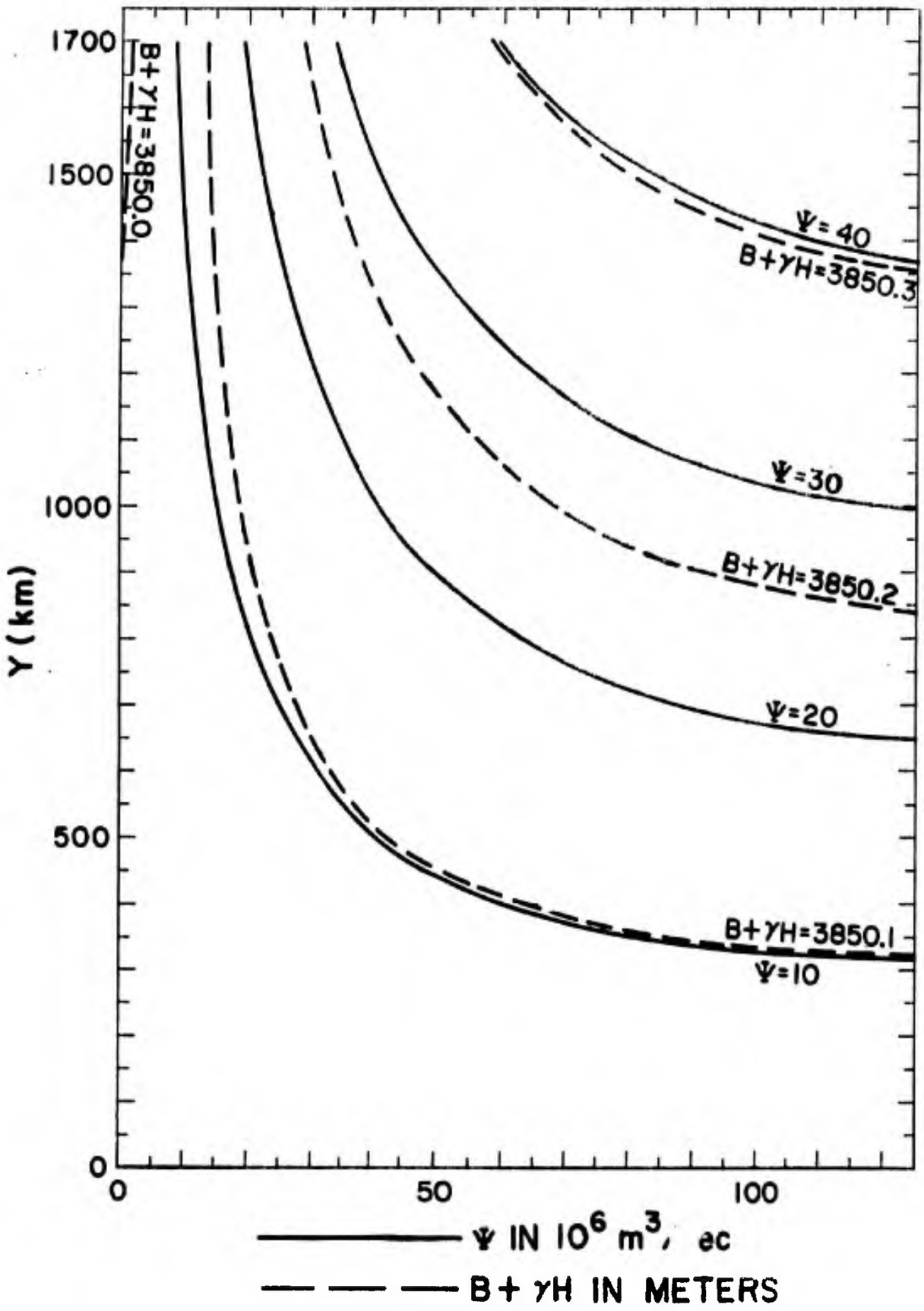
1700
1500
1000
500
0
0
50
100
Y (km)
B+γH=3850.0
Ψ=40
B+γH=3850.3
Ψ=30
B+γH=3850.2
Ψ=20
B+γH=3850.1
Ψ=10
Ψ IN 10^6 m^3, ec
B + γH IN METERS

FIGURE 17

Volume transport streamlines in lower layer for case 15-a.

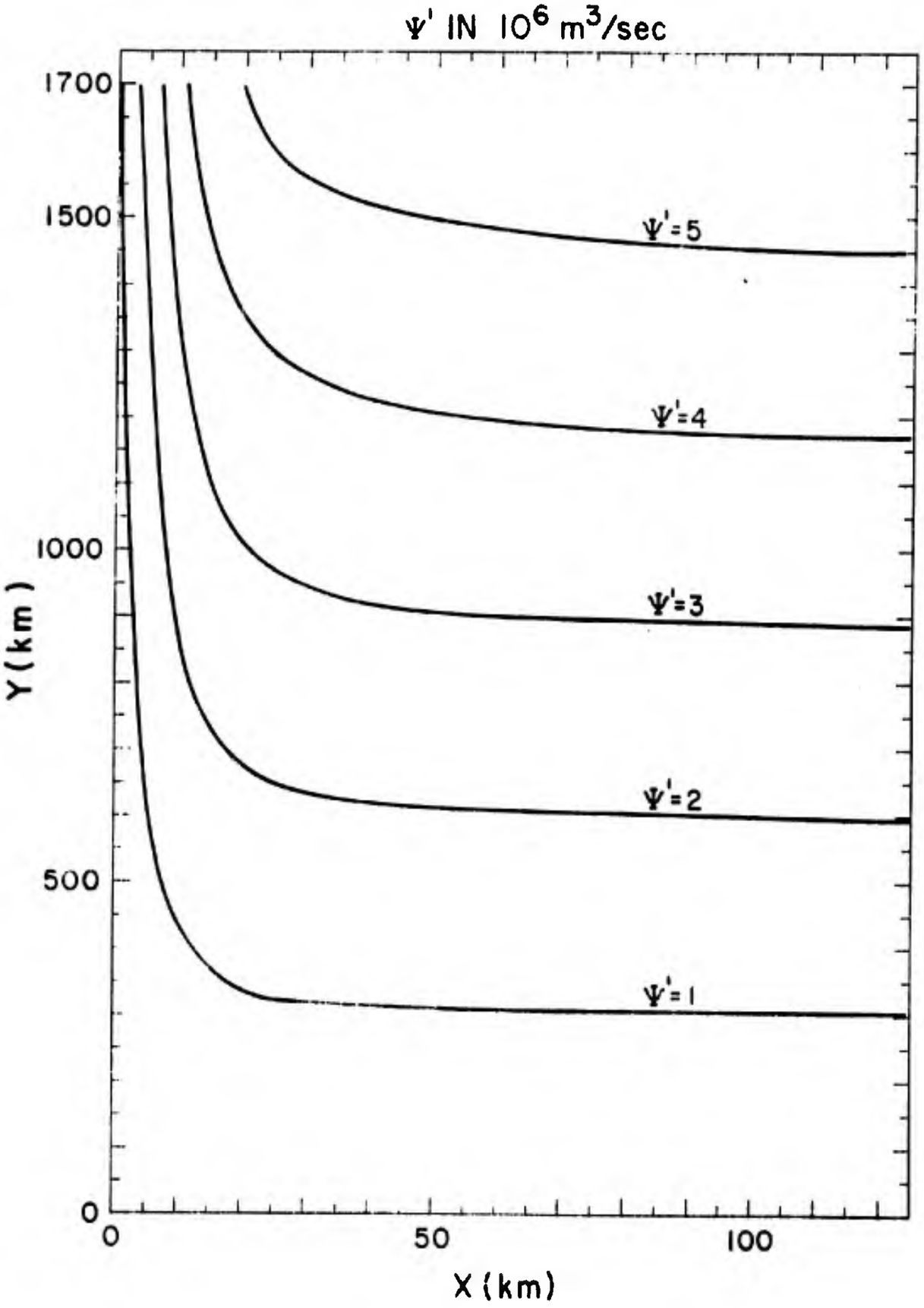
Ψ' IN 10^6 m^3/sec
1700
1500
1000
500
0
Y (km)
Ψ'=5
Ψ'=4
Ψ'=3
Ψ'=2
Ψ'=1
0
50
100
X (km)

FIGURE 18

Volume transport streamlines within upper and lower layers as computed for case 15-b.

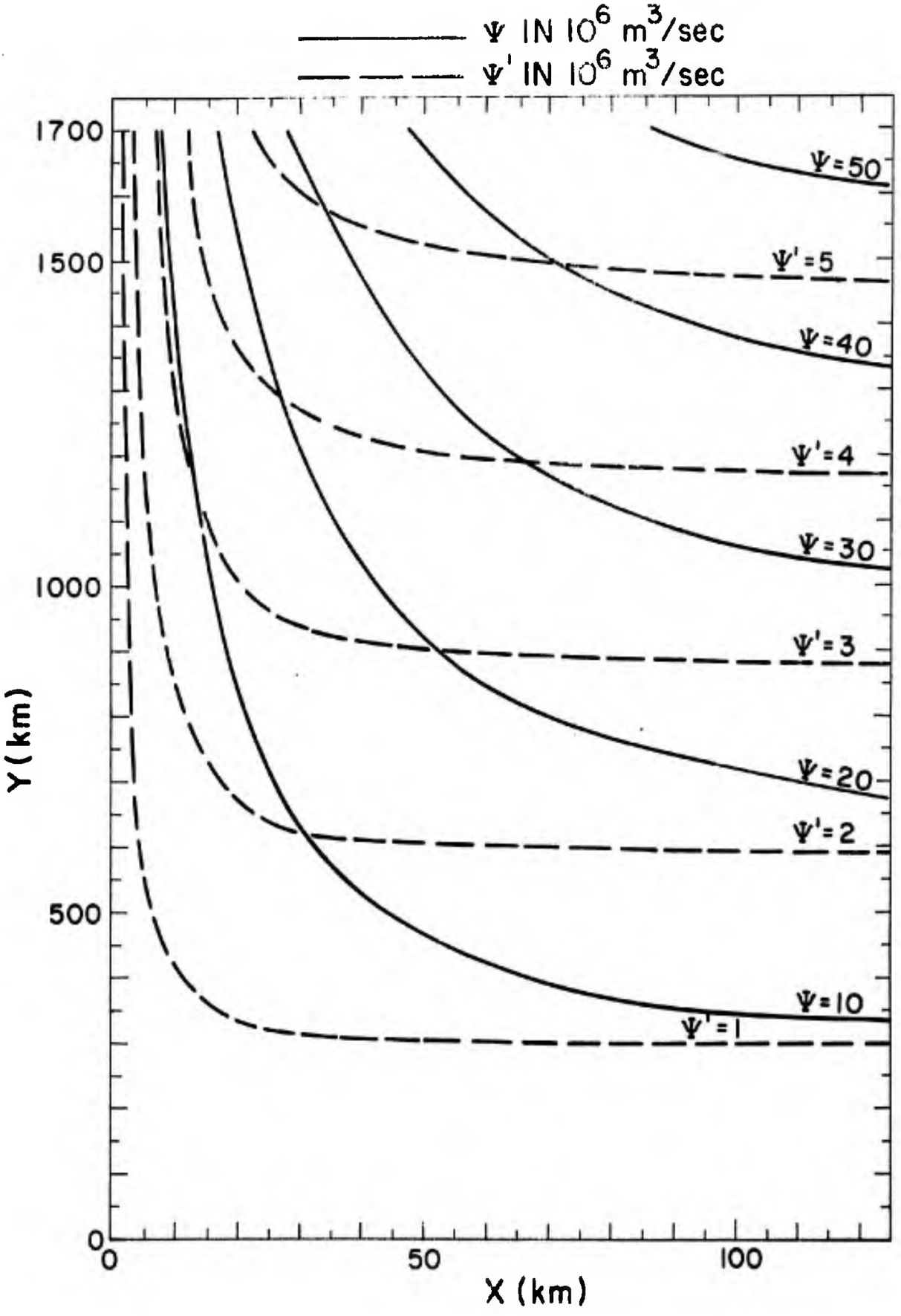
Ψ IN 10^6 m^3/sec
Ψ' IN 10^6 m^3/sec
Ψ=50
Ψ'=5
Ψ=40
Ψ'=4
Ψ=30
Ψ'=3
Ψ=20
Ψ'=2
Ψ=10
Ψ'=1
1700
1500
1000
500
0
0
50
100
Y (km)
X (km)

FIGURE 19

Horizontal distribution of meridional components of velocities within the upper and lower layers, v and v′ respectively, as computed for case 15-b.

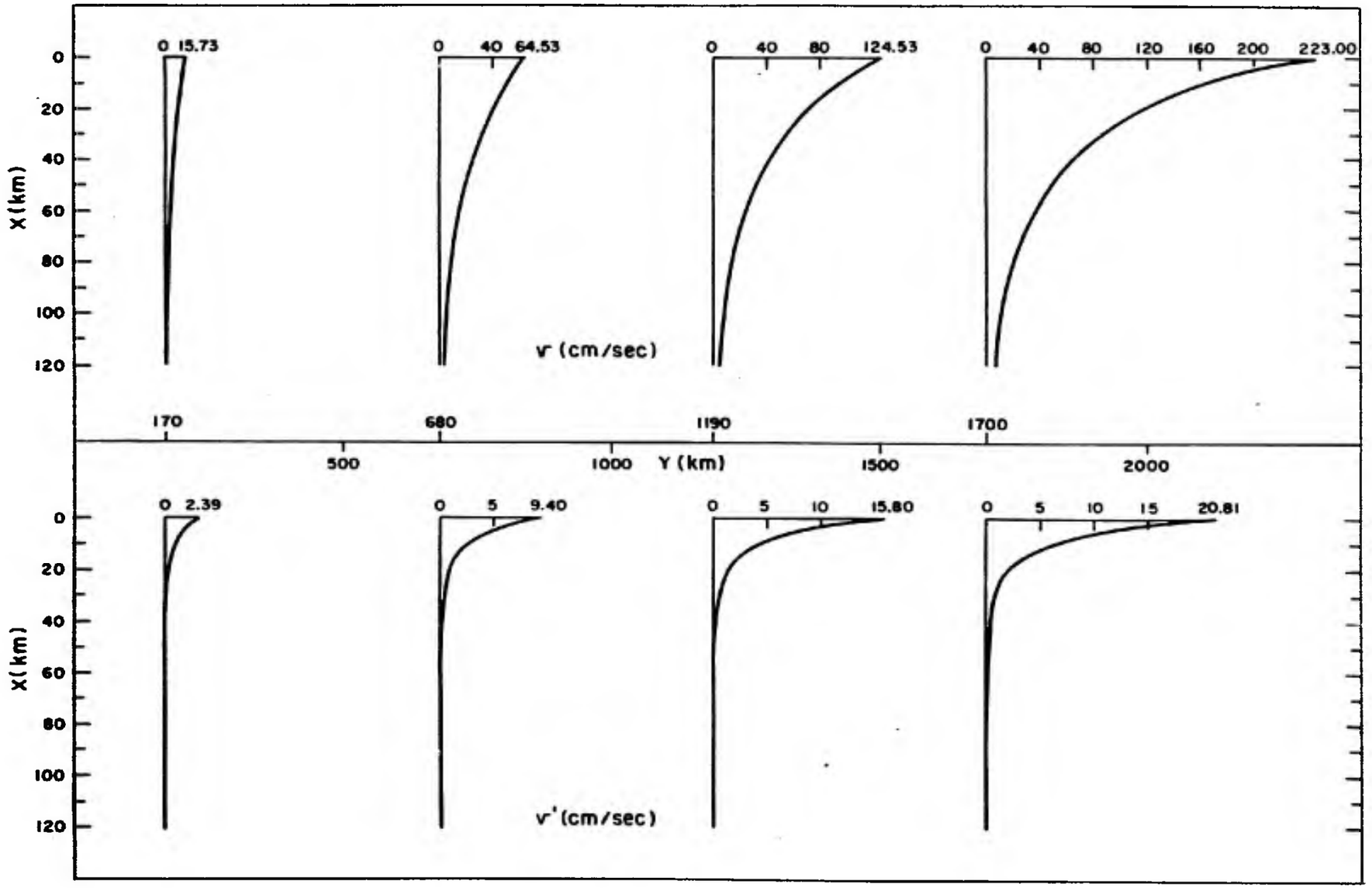
0 15.73
0 40 64.53
0 40 80 124.53
0 40 80 120 160 200 223.00
X (km)
0
20
40
60
80
100
120
v' (cm/sec)
170
680
1190
1700
500
1000
Y (km)
1500
2000
0 2.39
0 5 9.40
0 5 10 15.80
0 5 10 15 20.81
v''(cm/sec)

Security Classification

DOCUMENT CONTROL DATA - R&D

(Security classification of title, body of abstract and indexing annotation must be entered when the overall report is classified)

1. ORIGINATING ACTIVITY *(Corporate author)*
Department of Oceanography
Texas A&M University, College Station, Texas
(Texas A&M Research Foundation)

2a. REPORT SECURITY CLASSIFICATION
Unclassified

2b GROUP
Unclassified

3. REPORT TITLE
On Steady, Wind-Driven Ocean Currents in a Stratified Model of Two Moving Layers.

4. DESCRIPTIVE NOTES *(Type of report and inclusive dates)*
Technical report (a theoretical study executed during period 15 Dec. 1964 - 30 Sept. 1965)

5. AUTHOR(S) *(Last name, first name, initial)*
Nowlin, Worth D., Jr.

6. REPORT DATE	7a. TOTAL NO. OF PAGES	7b. NO. OF REFS
November 1965	94 sheets	26

8a. CONTRACT OR GRANT NO.	9a. ORIGINATOR'S REPORT NUMBER(S)
Nonr 2119(04)	65-32T
b. PROJECT NO. Texas A&M Project 286	
c.	9b. OTHER REPORT NO(S) *(Any other numbers that may be assigned this report)* None
d.	

10. AVAILABILITY/LIMITATION NOTICES
No limitations, Price: Cost of reproduction.

11. SUPPLEMENTARY NOTES	12. SPONSORING MILITARY ACTIVITY
None	Office of Naval Research Geophysics Branch, Washington, D.C.

13. ABSTRACT Considered are steady, wind-driven currents in a rectangular basin with horizontal sea bed. Horizontal velocities are assumed independent of elevation within each of two stably stratified layers. A frictional model without lateral friction is envisaged. Turbulent exchange of horizontal momentum between layers and to the sea bed is provided by assuming interlayer and bottom stresses proportional to the vertical contrast of horizontal velocity across the interfaces. The constants of proportionality, estimated from independent considerations, are decisive in controlling the flow patterns and energy dissipation from the steady organized flow. The solution, for a zonal wind stress which varies latitudinally as a cosine, depicts a more intensified anticyclonic gyre in the lower than in the upper layer. This differential intensification produces a relatively strong, narrow countercurrent underlying the eastern portion of the upper boundary current. An alternate solution for the formation region of western boundary currents, a system of steady inertial currents in two moving layers is presented. Potential vorticity in each layer is expressed as a linear function of the appropriate transport streamfunction. Approximate solutions are obtained by employing perturbations on the basic state given at the eastern edge of the boundary region by interior solutions to the frictional model. Two methods of analysis yield solutions: one employs layer thickness perturbations and uses numerical methods to satisfy nonlinear western boundary conditions; the other employs perturbations of the streamfunctions and linearized boundary conditions without using numerical methods.

DD FORM 1 JAN 64 1473

Security Classification